8.18 The Biological Pump in the Past

MP Hain and DM Sigman, Princeton University, Princeton, NJ, USA
GH Haug, Geologisches Institut, Zürich, Switzerland

This article is a revision of the previous edition article by D. M. Sigman and G. H. Haug, volume 6, pp. 491–528, © 2003, Elsevier Ltd.

8.18.1 Introduction

Almost all organisms on Earth either harvest energy and produce organic matter through photosynthesis, or feed on organic matter that was ultimately produced by these 'photoautotrophs.' In addition to light as their source of energy, photoautotrophs require nutrients and inorganic carbon, which they extract from the environment. On land, newly produced biomass is rapidly recycled by plant respiration or heterotrophy, but a small fraction survives for a longer time before decomposition, either as long-lived tissue (e.g., wood), soil organic matter, peat, or organic matter buried in sediments. This leads to the accumulation of terrestrial organic carbon, at the expense of the environmental inorganic carbon reservoir, including atmospheric carbon dioxide (CO_2). An increase in the quantity of terrestrial organic carbon driven by a temporary excess in organic carbon production relative to its oxidation thus lowers atmospheric CO_2.

In the ocean, there are no aggregations of biomass comparable to the forests on land. Yet biological productivity in the ocean plays a central role in the sequestration of carbon away from the atmosphere, overshadowing the effects of terrestrial biospheric carbon storage on timescales longer than a few centuries. In an effort to communicate the ocean's role in the regulation of atmospheric CO_2, marine scientists frequently refer to the ocean's biologically driven sequestration of carbon as the 'biological pump.' Every year, a fraction of the biomass produced in the sunlit surface ocean sinks into the dark ocean interior before being decomposed, thereby 'pumping' both nutrients and organic carbon (C_{org}) into the deep ocean, where the carbon is sequestered away from the atmosphere and the nutrients cannot be immediately used to fuel new production of biomass. The original strict definition of the 'biological pump' (Volk and Hoffert, 1985) emphasizes the importance of the biological sinking flux on the distribution of carbon in the ocean; the surface ocean is depleted in carbon relative to the ocean interior (**Figure 1**). As only the surface ocean can exchange carbon with the atmosphere, the sequestration of carbon at depth results in a lower partial pressure of CO_2 (pCO_2) of the surface water, thus also lowering atmospheric CO_2. Soon after the discovery of much lower than modern atmospheric CO_2 concentration during the last ice age (Berner et al., 1978; Delmas et al., 1980; Neftel et al., 1982), it was argued that a stronger biological pump must have been the cause of this CO_2 drawdown (Broecker, 1982a,b). The main focus of this review is to provide an overview of the concepts, tools, and observations that have been developed since then to reconstruct the efficiency of the biological pump in the past and to quantify the impact it has had on atmospheric CO_2 levels. As we see later, this body of work speaks to the three major topics of modern oceanography: the ocean's physical circulation, chemical composition, and biological activity.

The place of the biological pump in the global carbon cycle is illustrated in **Figure 2**. The atmosphere exchanges carbon

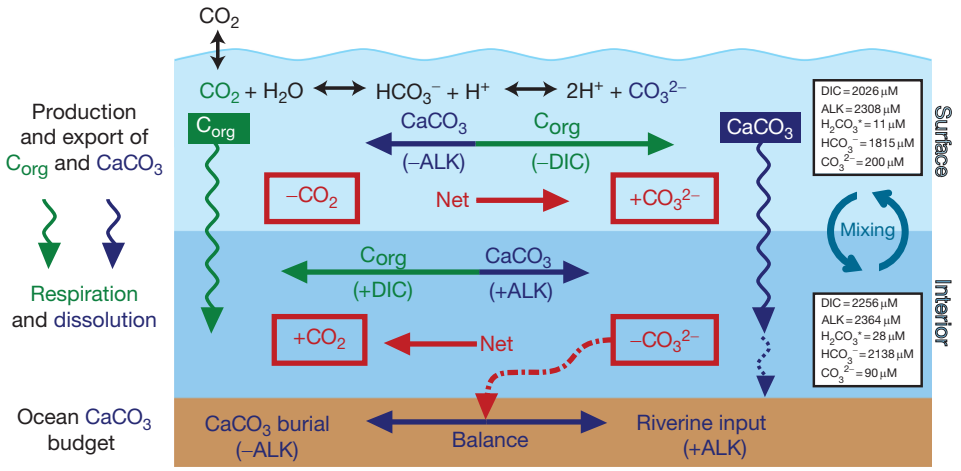

Figure 1 A schematic of the ocean's 'biological pump,' the sequestration of carbon and alkalinity from the surface ocean (light blue) into the ocean interior (dark blue), and their effects on the ocean's carbon chemistry. The net production of biomass (photosynthesis minus respiration) in the sunlit surface ocean does not accumulate in the surface but is instead exported (green wavy arrow) to the ocean interior, thereby sequestering organic carbon (C_{org}) and nutrients (not shown; see **Figure 6(a)–(c)**). Some organisms construct inorganic hard parts from $CaCO_3$ (ALK:DIC = 2:1). Unlike organic matter, almost all of which is respired during its downward passage through the water column, much of the $CaCO_3$ rain (blue wavy arrow) sinks all the way to the seafloor, and then a significant fraction of it (~25%) is preserved and buried in the sediments (see **Section 8.18.2.2**). The biological pump therefore consists of a 'soft-tissue' and a 'carbonate' component that have opposing effects on ocean chemistry and atmospheric CO_2: the net removal of dissolved inorganic carbon (DIC) via C_{org} export raises the pH and the carbonate ion concentration (CO_3^{2-}) and lowers the CO_2 concentration of surface water and the atmosphere, whereas the removal of ALK via $CaCO_3$ export lowers pH and CO_3^{2-} and raises CO_2 (see **Section 8.18.2.1** for details). The respiration of C_{org} and the dissolution of $CaCO_3$ in the interior release DIC and ALK so as to cause the opposite chemical changes at depth; however, the rise in CO_2 at depth does not increase atmospheric CO_2. The 'pumping' of DIC, ALK, and nutrients maintains vertical chemical gradients in the face of ocean circulation that continuously mixes surface and interior water. The white boxes on the right show DIC and ALK as well as calculated carbon speciation for the average global surface and the deep ocean, respectively. This schematic omits other processes that contribute to carbon and alkalinity differences between ocean surface and interior, such as the 'solubility pump' (e.g., Toggweiler et al., 2003a).

with essentially three reservoirs: the ocean, the terrestrial biosphere, and the geosphere. The ocean holds roughly fifty times as much carbon as does the atmosphere and almost twenty times as much as the terrestrial biosphere. At any given time, only ~10% of the carbon in the ocean can be said to be sequestered by the action of the biological pump. However, given the much greater size of the ocean carbon reservoir, even a small change in the amount of deeply sequestered carbon can have a substantial impact on the atmospheric CO_2 inventory.

The effect of the biological pump is not permanent because ocean overturning continuously acts to erase the gradient in carbon concentration that is driven by the sinking of carbon-bearing biogenic material, thereby exposing once sequestered carbon to the atmosphere and reversing the drawdown of atmospheric CO_2 that was caused by its sequestration (e.g., DeVries et al., 2012). Thus, the biological pump exerts its control on atmospheric CO_2 only on the timescale that it takes ocean overturning to bring the water of the ocean interior to the surface (between 500 and 1500 years depending on the ocean basin; e.g., DeVries and Primeau, 2011). For its carbon sequestration to persist, its component processes (e.g., the downward flux of organic matter) must be maintained.

The dynamics of marine C_{org} can be described as a set of three nested cycles in which the biological pump is the cycle with flux and reservoir of intermediate magnitude (**Figure 3**). The cycle with the shortest timescale, which operates within the surface ocean, is composed of net primary production by phytoplankton (their photosynthesis less their respiration) and heterotrophic respiration by zooplankton and bacteria that oxidize most of the primary production back to CO_2. This cycle is by far the greatest in terms of the flux of carbon, but the reservoir of C_{org} that accumulates in surface waters (phytoplankton biomass, dead organic particles, and dissolved organic carbon) is small relative to the atmospheric reservoir of CO_2, and it has a short residence time (less than a year). However, 10–50% of the organic matter produced by net primary production escapes immediate heterotrophic respiration within the surface and instead sinks (or is mixed) to depth before it is decomposed (e.g., Henson et al., 2012 and references therein). This 'export production' drives the biological pump (**Figure 3**).

At the long timescale extreme of the global carbon cycle, a tiny fraction of the organic matter exported from the surface ocean survives its passage through the water column and sediment/water interface and is buried in the accumulating sediments, thereby removing carbon from the ocean/atmosphere system (**Figure 3**). On the timescale of geologic processes, this carbon removal is balanced by the oxidation of the organic matter when it is exposed at the Earth surface by uplift and weathering or when it is released by metamorphism and volcanism. While the fluxes involved in this cycle are small, the organic carbon reservoir of the solid Earth is large, so that the importance of these fluxes increases with timescale, becoming clearly relevant on the timescale of millions of years. Neither

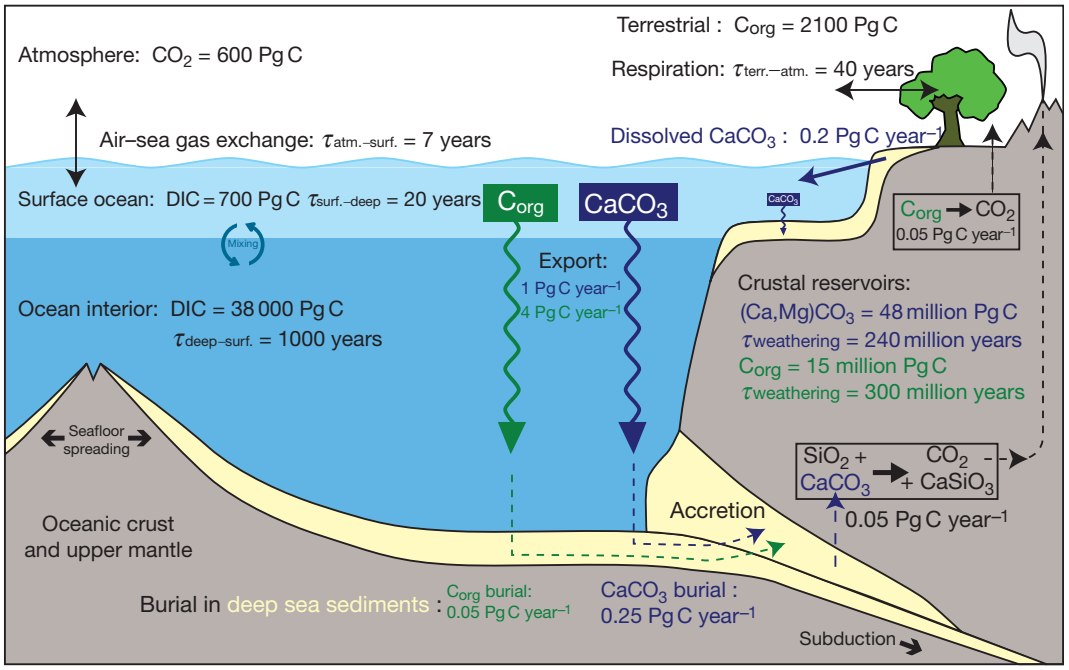

Figure 2 A simplified view of the Holocene (preindustrial) carbon cycle (largely based on Holmen, 1992). Units of carbon are petagrams (Pg, 10^{15} g). Exchanges of the atmosphere with the surface ocean and terrestrial biosphere are relatively rapid, such that changes in the fluxes alter atmospheric CO_2 on the timescale of years to decades. Exchange between the surface ocean and the deep ocean is such that centuries to millennia are required for a change to yield a new steady state. Because the deep-ocean carbon reservoir is large relative to the surface ocean, terrestrial biosphere, and atmosphere, its interactions with the surface ocean, given thousands of years, determine the total amount of carbon to be partitioned among these three reservoirs. In a lifeless ocean, the only cause for gradients in CO_2 between the deep ocean and the surface ocean would be temperature (i.e., the 'solubility pump' (Toggweiler et al., 2003a; Volk and Hoffert, 1985)) – deep waters are formed from especially cold surface waters, and carbon dioxide is more soluble in cold water. The rain of organic matter ('C_{org}') out of the surface ocean, represented by the green wavy downward arrow, greatly enhances the surface-to-deep CO_2 gradient, being the driver of the 'soft-tissue' component of the biological pump. The downward rain of calcium carbonate microfossils out of the surface ocean, represented by the purple wavy downward arrow, drives the 'carbonate pump.' Its effect is to raise the pCO_2 of the surface ocean and atmosphere (see **Figure 1**); this involves the alkalinity of seawater, as is discussed in **Sections 8.18.2.1–8.18.2.2**. Almost all of the organic matter raining out of the surface ocean is degraded back to CO_2 and inorganic nutrients as it rains to the seafloor or once it is incorporated into the surficial sediments; only ~1% (~0.05 Pg out of ~4 Pg) is removed from the ocean/atmosphere system by burial (the dashed green arrow), which is balanced by slow C_{org} weathering on land. This is in contrast to the calcium carbonate rain out of the surface (the dashed purple arrow), roughly 25% of which is buried. In parallel, the weathering rate of calcium carbonate on land is significant on millennial timescales (the left-pointing purple arrow). Some of the $CaCO_3$ buried on the deep-ocean seafloor is subducted, leading eventually to the release of CO_2 from the metamorphism of calcium carbonate to silicate minerals. The residence time of carbon in reservoir A with respect to the exchange flux to reservoir B is shown as τ_{A-B}.

the C_{org} burial flux nor the release of carbon from the solid Earth helps to maintain the gradient of carbon concentration between the ocean's surface and its interior and thus, by definition, these aspects of the carbon cycle are not part of the biological pump. While these processes are clearly of interest in Earth history, for the sake of brevity, they are not discussed further below.

Additionally, also for the sake of brevity, we presume below a set quantity of the 'major nutrients' nitrogen and phosphorus in the ocean; that is, we do not consider the possibility or implications of ocean nutrient reservoir changes. In so doing, we are skipping an extremely rich topic that is almost certainly relevant to past events in Earth history. Further, the first hypotheses regarding glacial/interglacial CO_2 change focused on nutrient reservoir changes (Broecker, 1982a,b). We avoid this topic here because we think there are strong arguments against a role for such changes in glacial/interglacial change (e.g., Ren et al., 2012), which we have discussed in previous reviews (e.g., Sigman and Boyle, 2000; Sigman and Haug, 2003).

So far, we have discussed biogenic material in terms of organic matter, but many marine organisms also extract carbon from surface waters to produce inorganic carbon compounds, chiefly calcium carbonate ($CaCO_3$). As discussed in detail in **Section 8.18.2.1**, the rain of $CaCO_3$ from the surface to depth acts to raise atmospheric CO_2 despite driving carbon sequestration akin to the sinking of organic matter. For this reason, it is important to distinguish these two components of the biological pump: the 'soft-tissue pump' and the 'carbonate pump' (**Figure 1**). As with the respiration of C_{org} rain, the majority of the $CaCO_3$ rain from the surface dissolves while sinking or once it reaches the seafloor. However, relative to organic matter, a greater fraction of the $CaCO_3$ rain is preserved and buried, so that $CaCO_3$ production by organisms in the surface is a major contributor to open ocean sedimentation, and this burial flux constitutes the largest sink of carbon from the ocean/atmosphere system. On the timescale of a few thousand years, this sizable loss of $CaCO_3$ from the ocean is balanced primarily by input through rivers that carry dissolved $CaCO_3$

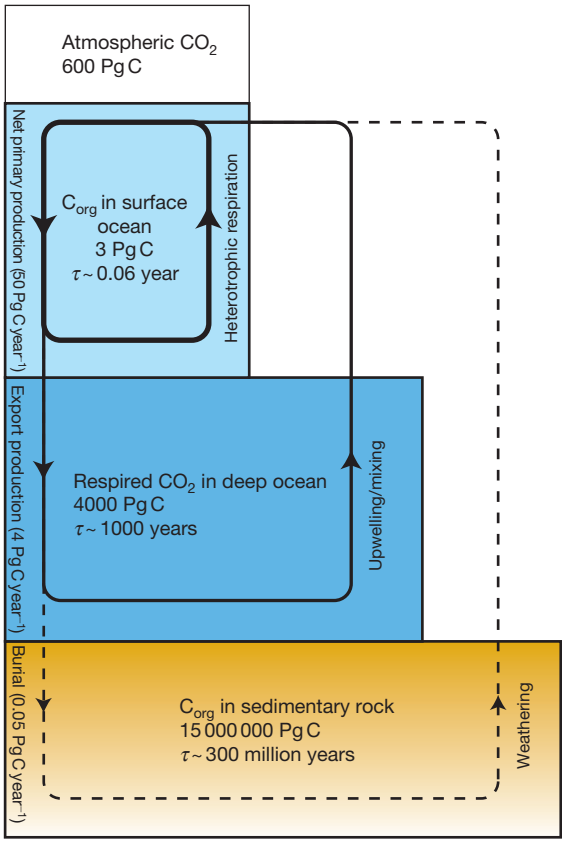

Figure 3 The nested cycles of marine organic carbon (C_{org}), including (1) net primary production and heterotrophic respiration in the surface ocean, (2) export production from the surface ocean and respiration in the deep sea followed by upwelling or mixing of the respired CO_2 back to the surface ocean (the soft-tissue component of the biological pump; the focus of this chapter), and (3) burial of sedimentary organic carbon and its release to the atmosphere by weathering or other geologic processes. The slight imbalance of each cycle fuels the longer timescale cycles. The carbon reservoirs shown refer solely to the fraction affected by organic carbon cycling; for instance, the deep-ocean value shown is of carbon dioxide produced by respiration, not the carbon released from $CaCO_3$ dissolution or the DIC in deep water that derives from air/sea CO_2 equilibration at the ocean surface followed by surface water sinking.

derived from weathering of sediments and rocks on land (**Figure 2**). As was true for the soft-tissue pump, only the component of $CaCO_3$ rain from the surface that does dissolve at depth contributes to the surface-to-deep carbon concentration gradient, thereby constituting the carbonate pump.

Besides the soft-tissue and carbonate pumps, the temperature-dependent solubility of CO_2 also results in a surface-to-deep gradient in ocean carbon concentration. Cold deep waters form near the poles and fill the abyssal depths of all major ocean basins, while the warm surface waters of the low- and mid-latitudes are too buoyant to sink and are thus confined to the uppermost water column. As CO_2 is more soluble at low temperatures, the thermal structure of the ocean imposes a carbon gradient in the same direction as the biological pump. This effect has been named the 'solubility pump' (Toggweiler et al., 2003a; Volk and Hoffert, 1983); unlike the other pumps, it is maintained, not erased, by ocean circulation.

Once techniques were developed to measure the CO_2 concentration of air bubbles trapped in ice cores, it was discovered that atmospheric CO_2 levels were low during the last ice age (Berner et al., 1978; Delmas et al., 1980; Neftel et al., 1982). Since that time, major international research efforts have provided a transformative account of atmospheric CO_2 variations that mirror the waxing and waning of ice ages – over the last glacial cycle (Barnola et al., 1987), the last two glacial cycles (Jouzel et al., 1993), the last four glacial cycles (Petit et al., 1999), and the last eight glacial cycles (Lüthi et al., 2008; Siegenthaler et al., 2005; see also EPICA Community Members, 2004; **Figure 4**). During interglacial times, such as the Holocene (roughly the past 10 000 years), the atmospheric partial pCO_2 was typically near 280 parts per million by volume (ppmv). During peak glacial times, such as the Last Glacial Maximum (LGM) about 22 000 years ago, atmospheric CO_2 was 180–200 ppmv or roughly 80–100 ppmv lower. Overall, the decline from high interglacial to low glacial levels proceeds over tens of thousands of years, punctuated by rapid fluctuations (e.g., Indermühle et al., 2000; Neftel et al., 1988) and episodes of rapid decline (e.g., Ahn and Brook, 2008), whereas the rise of CO_2 at the abrupt termination of ice ages takes only a few thousand years (e.g., Monnin et al., 2001; Neftel et al., 1982). The rapidity of major rises and falls in CO_2 is strong evidence that much of the CO_2 change was driven by carbon redistributions within the atmosphere/ocean/terrestrial biosphere system. Thus, changes in the efficiency of the biological pump – and their impacts on the ocean's $CaCO_3$ cycle – have emerged as a prime contender to explain the overall pattern of reconstructed CO_2 variations. Moreover, for the last glacial cycle and especially, the last deglaciation, temporal resolution, dating, and correlation to other climate records have improved (e.g., Ahn and Brook, 2007, 2008; Bender, 2002; Bender et al., 1994; Bereiter et al., 2012; Blunier and Brook, 2001; Kawamura et al., 2007; Lemieux-Dudon et al., 2010; Monnin et al., 2001; Neftel et al., 1988; Severinghaus et al., 1998; Sowers and Bender, 1995; Sowers et al., 1989, 1993). The improving ice core records and their correlation to marine observations reveal temporal coincidence between millennial-scale variations of CO_2 and changes in the ocean's circulation and biological productivity (e.g., Anderson et al., 2009a; Barker et al., 2009, 2011; Burke and Robinson, 2012; Fischer et al., 2010; Gherardi et al., 2009; McManus et al., 2004; Robinson et al., 2005a; Sigman et al., 2010; Skinner et al., 2010; Thornalley et al., 2011a,b; Waelbroeck et al., 2011).

Release and sequestration of carbon by the ocean imply a significant role of the greenhouse gas CO_2 in the energetics of glacial/interglacial climate change (e.g., Cai and Cowan, 2007; Pepin et al., 2001; Weaver et al., 1998; Webb et al., 1997). However, the ultimate pacing of glacial cycles is statistically linked to 'Milankovitch cycles' in the orbital parameters of the Earth, with characteristic frequencies of roughly 100, 41, and 23 thousand years (Berger, 1978a,b, 1988; Hays et al., 1976; Huybers, 2007, 2011; Huybers and Wunsch, 2005). Thus, the radiative forcing of variable CO_2 levels is best viewed as an amplifying feedback in the climate system. Conversely, it appears that, even on short timescales, the biological pump and the carbon cycle are sensitive to changes in the climate system (e.g., Le Quere et al., 2007; Russell et al., 2006; Sarmiento et al.,

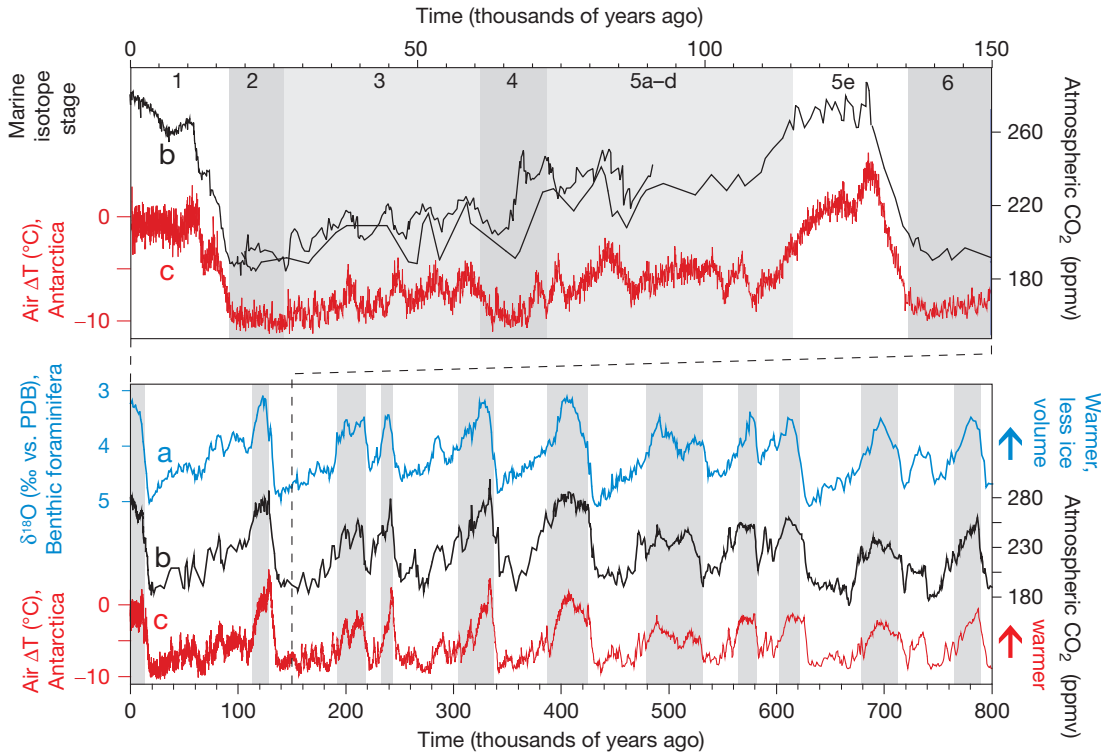

Figure 4 The history of ice age cycles, atmospheric CO_2, and Antarctic temperature. The $^{18}O/^{16}O$ ratio (expressed as $\delta^{18}O$) measured in the shells of deep seafloor-dwelling benthic foraminifera recovered from ocean sediment cores (blue curve; Lisiecki and Raymo, 2005, and references therein) reflects both the extraction of ^{16}O-rich ocean water to form massive continental ice sheets and the cooling of the deep sea during glacial cycles (i.e., cooling and glaciation cause higher $\delta^{18}O$). Atmospheric CO_2 – as recorded by the gas content in ice cores from Antarctica (black curves; Ahn and Brook, 2007, 2008; Indermühle et al., 2000; Lüthi et al., 2008; Monnin et al., 2001; Petit et al., 1999; Raynaud et al., 2005; Siegenthaler et al., 2005) – was the highest during interglacial periods (gray vertical shading in lower panel) and declined in a punctuated pattern after the glacial inceptions. During peak glacial periods, atmospheric CO_2 was 80–100 ppmv lower than during peak interglacial periods, with upper and lower limits that are reproduced in each of the 100 000 year cycles. The change in Antarctic temperature (red curve; as recorded in the ratio of deuterium to hydrogen of the ice; Jouzel et al., 2007) covaries with the changes in ice volume and deep ocean temperature but exhibits much more pronounced change upon glacial inceptions than the other two records. Ice cores records indicate that atmospheric CO_2 was among the first parameters to change at the termination of glacial maxima, roughly in step with southern hemisphere warming and preceding the decline in northern hemisphere ice volume.

1998). In the age of man-made climate change, it is a high priority to understand this coupling on a mechanistic level.

8.18.2 Concepts

Reconstructions of oceanic, atmospheric, and terrestrial conditions during the ice ages are required to identify the mechanisms that caused the drawdown of atmospheric CO_2 during the ice ages and at what point in time they were activated. However, the reconstruction of environmental parameters is not easily translated into the effect of a given change on atmospheric CO_2; both conceptual and numerical models are required for this purpose. Here, we describe a hierarchy of concepts, from alkalinity to ocean ventilation, that form a theoretical basis for the interpretation of environmental reconstructions in terms of CO_2 impact.

8.18.2.1 Aqueous Carbon Chemistry

CO_2 gas has a low solubility in seawater, but it forms carbonic acid (H_2CO_3) that can deprotonate to hydrogencarbonate ion (HCO_3^-) and carbonate ion (CO_3^{2-}) which together greatly increase the concentration of dissolved inorganic carbon (DIC) (eqn [1] and **Figure 1**):

$$CO_2(g) + H_2O \leftrightharpoons H_2CO_3^* \leftrightharpoons H^+ + HCO_3^- \leftrightharpoons 2H^+ + CO_3^{2-} \quad [1]$$

In eqn [1], $H_2CO_3^*$ refers to both dissolved CO_2(aq) and H_2CO_3. Formally, the concentration of DIC equates to the sum of the individual concentrations of all the DIC species.

When water is in contact with the atmosphere, CO_2 can either evade to the atmosphere or invade the water, depending on the difference between the partial pressure of CO_2 of the atmosphere (pCO_2^{atm}) and that of the water (pCO_2^{aq}), which depends solely on the concentration of $H_2CO_3^*$ and the thermodynamic solubility constant K_{sol} (eqn [2a]):

$$pCO_2(aq) = K_{sol} \cdot H_2CO_3^* \quad [2a]$$

The expression relative to DIC is more complicated because of the deprotonated components of DIC (eqn [2b]):

$$pCO_2(aq) = K_{sol} \cdot DIC \cdot \frac{1}{1 + \frac{K_1}{H^+} + \frac{K_1 \cdot K_2}{H^+ \cdot H^+}} \quad [2b]$$

The thermodynamic constants, especially K_{sol}, are temperature and salinity dependent such that the net effect of reconstructed bulk ocean cooling (~2.7 °C; Headly and Severinghaus, 2007) and elevated salinity (>1.15 practical salinity units; Adkins et al., 2002) should have combined to drive ~20 ppm of the 80–100 ppm glacial CO_2 drawdown (the cooling causing an atmospheric CO_2 decline and the increased salinity causing a CO_2 rise). To explain the rest of the CO_2 decline, $H_2CO_3^*$ must have been lower (in the sense of eqn [2a]) due to some combination of low DIC and low H^+ (in the sense of eqn [2b]). It is simplest to describe the effect of the biological pump on CO_2 as stemming from sequestration of DIC at depth, which lowers the DIC and thus pCO_2 in surface waters that must then equilibrate with the atmosphere. However, the larger part of the surface ocean pCO_2 reduction by the biological pump operates through the pH effect of lowering surface ocean DIC ($pH = -\log_{10}(H^+)$); it is specifically the weak acid $H_2CO_3^*$ that is removed in the production and export of soft-tissue organic matter, which raises the pH of surface waters and repartitions DIC away from $H_2CO_3^*$ and toward hydrogencarbonate and carbonate (Figure 1).

As a result of the pH dynamic, an adequate description of the biological pump must include its simultaneous effect on DIC and 'alkalinity,' the latter referring to the excess of base over acid in ocean waters. The alkalinity (ALK) of a seawater sample roughly corresponds to the amount of strong acid that needs to be added to fully protonate HCO_3^- and CO_3^{2-}. As we explore in more detail in Section 8.18.2.2, the soft-tissue pump exports DIC (in the form of organic carbon, C_{org}) from surface waters but does not greatly affect its ALK, whereas the export of $CaCO_3$ associated with the carbonate pump depletes surface water ALK and DIC in exactly a 2:1 ratio.

The following approximate relationships (Broecker and Peng, 1982) are helpful in understanding the chemical underpinnings of the biological pump by illustrating the opposing effects of changes in DIC and ALK (eqn [3a]–[3d]):

$$HCO_3^- \approx 2DIC - ALK \quad [3a]$$

$$CO_3^{2-} \approx ALK - DIC \quad [3b]$$

$$H^+ \propto \frac{HCO_3^-}{CO_3^{2-}} \approx \frac{2DIC - ALK}{ALK - DIC} \quad [3c]$$

$$pCO_2 \propto H^+ \cdot HCO_3^- \approx \frac{(2DIC - ALK)^2}{ALK - DIC} \quad [3d]$$

Referring to these approximations, the biological pump affects seawater chemistry in two independent ways. First, when organisms extract DIC from surface water (the soft-tissue pump, green in Figure 1), HCO_3^- declines (eqn [3a]) and CO_3^{2-} rises (eqn [3b]). That is to say, in addition to the simple removal of DIC, the remaining carbon is shifted from $H_2CO_3^*$ and HCO_3^- toward CO_3^{2-} (from left to right in eqn [1]). This shift is manifested in a decline in H^+ (eqn [3c]), which, along with the reduction in HCO_3^-, causes the reduction of pCO_2 (eqn [3d]). Second, when organisms extract ALK from surface water (the greatest effect of the carbonate pump, purple in Figure 1), HCO_3^- rises (eqn [3a]) and CO_3^{2-} declines (eqn [3b]). That is, the removal of ALK shifts the carbon species from CO_3^{2-} toward HCO_3^- and $H_2CO_3^*$ (from right to left in eqn [1]). Thus, ALK removal manifests itself as a rise in both HCO_3^- (eqn [3a]) and H^+ (eqn [3c]), which combine to cause an increase in pCO_2 (eqn [3d]). Remineralization of biogenic material at depth, after it was exported from the surface, releases DIC and ALK, thereby causing chemical changes in deep water in the reverse direction as their removal causes in surface waters (Figure 1). As was outlined earlier, the biological pump is defined through the DIC gradient it maintains in the ocean, with lower DIC at the surface than at depth. The effect on atmospheric CO_2 of the biological pump, however, operates through the combined depth gradients in DIC and ALK and their net effect on surface water pH and pCO_2.

The final aspect of ocean carbon chemistry that is important to review in the context of glacial/interglacial CO_2 variations involves the dissolution of $CaCO_3$. Since the concentration of calcium (Ca^{2+}) is almost uniform in the ocean, the expression for the $CaCO_3$ saturation state (Ω) can be usefully simplified (eqn [4]):

$$\Omega \approx \frac{CO_3^{2-}}{CO_3^{2-}(sat)} \approx \frac{ALK - DIC}{CO_3^{2-}(sat)} \quad [4]$$

In principle, $CaCO_3$ is precipitated from solution when supersaturated ($\Omega > 1$), and it dissolves when undersaturated ($\Omega < 1$). In the modern ocean, the kinetics of abiotic $CaCO_3$ precipitation render this process unimportant, and almost all $CaCO_3$ precipitation is mediated or controlled by organisms growing in highly supersaturated waters near the surface (Stumm and Morgan, 1981). Indeed, the removal of DIC from surface waters by the biological pump is one reason for this $CaCO_3$ supersaturation (see eqn [3b]; Figure 1). For every mole of $CaCO_3$ burial on the seafloor, two moles of ALK and one mole of DIC are permanently removed from the ocean, thereby raising CO_2 in the atmosphere (eqn [3d]; Figure 1). However, for three reasons, most of the $CaCO_3$ rain from the surface dissolves rather than being buried in deep-sea sediments. First, the solubility of $CaCO_3$ (i.e., $CO_3^{2-}(sat)$ in eqn [4]) increases with pressure, and pressure increases with water depth so as to reduce Ω. Second, as a consequence of the sequestration of DIC by the biological pump, CO_3^{2-} is much lower in the ocean interior than at the surface (see eqn [3b]; Figure 1). Third, the respiration of C_{org} in seafloor sediments reduces the CO_3^{2-} in the sediment pore water so as to allow for sedimentary $CaCO_3$ dissolution even if the overlying bottom water is supersaturated ($\Omega > 1$), and it enhances dissolution where the bottom water is undersaturated (Emerson and Bender, 1981). Overall, a substantial fraction of the $CaCO_3$ rain is preserved and buried when it is intercepted by shallow seafloor (Figure 2), but it dissolves essentially completely if it rains onto deeper seafloor. The carbonate compensation depth, above which $CaCO_3$ accumulates in seafloor sediments and below which it does not (because it dissolves at the same rate that it is delivered), and the lysocline, the depth interval in the water column over which the rate of $CaCO_3$ dissolution increases dramatically, are both correlated with the depth horizon at which $CaCO_3$ is at saturation (e.g., Archer, 1991).

8.18.2.2 Soft-Tissue versus Carbonate Pump

As described earlier, the soft-tissue and carbonate components of the biological pump affect the DIC and ALK of surface water in different ways so as to cause opposing effects on

atmospheric CO_2 (eqn [3b] and Figure 1). However, the carbonate pump only partially cancels the soft-tissue pump's CO_2 drawdown because its effect on CO_2 is typically weaker. Further, there are two major sources of decoupling between these opposing pumps: (1) not all organic matter that sinks is associated with $CaCO_3$ and (2) there are distinct fates for soft-tissue versus carbonate material that sink into the ocean interior. In this section, we describe how the two pumps are decoupled in the modern ocean and how this may relate to ocean changes during the ice ages.

One cornerstone of modern oceanography is the discovery that the concentration of nutrients, oxygen, and DIC are correlated in the ocean interior and that these correlations correspond to the respiration products of organic matter produced in surface waters (Redfield, 1934). The soft tissue of planktonic organisms of the open ocean is characterized by relatively conserved proportions of carbon, the amount of oxygen consumed during respiration, and the nutrients nitrogen (N) and phosphorus (P, as PO_4^{3-}), which became known as the canonical 'Redfield ratios' – C:N:P:O_2 of 106:16:1:−276 (Anderson and Sarmiento, 1994; Redfield, 1958; Takahashi et al., 1985; but for evidence of variability, see Deutsch and Weber, 2012; Mills and Arrigo, 2010; Weber and Deutsch, 2010). The detailed comparison of ocean interior distributions of nutrients with apparent oxygen consumption by respiration reveals that only roughly half of the major nutrients, N and P, in the ocean interior are derived from organic matter respiration ('regenerated nutrients'), whereas the other half ('preformed nutrients') must have been emplaced by ocean circulation. Since regenerated nutrients were used in the surface to produce C_{org}, their appearance at depth signals the sinking and subsequent sequestration of carbon in the deep ocean, while the preformed nutrients were not utilized at the surface and thus do not contribute to carbon sequestration (i.e., they represent a 'missed opportunity' for carbon sequestration). The ocean average concentration of regenerated nutrients thus tracks the overall strength of the soft-tissue pump, and the fraction of all P that is regenerated can be referred to as the 'efficiency' of the soft-tissue pump (if all P is regenerated, the soft-tissue pump is working at maximum efficiency). Based on these considerations and the carbon chemistry outlined in Section 8.18.2.1, the impact on CO_2 of changes in the concentration/fraction of regenerated nutrients can be calculated (Ito and Follows, 2005). Depending mainly on the assumed stoichiometry (i.e., the C:P ratio) of the organic matter, the sensitivity of atmospheric CO_2 to the soft-tissue pump in isolation ranges between 13 and 20 ppm CO_2 drawdown for every 0.1 μM ocean average increase in regenerated P (Hain et al., 2010; Ito and Follows, 2005; Kwon et al., 2011; Marinov et al., 2006).

The ratio of $CaCO_3$ to soft tissue varies greatly among organisms. Thus, there is no globally valid relationship between the export rates of C_{org} and $CaCO_3$. Moreover, sinking C_{org} is rapidly respired in the shallow water column (Berelson, 2001 and references therein; Martin et al., 1987) along with the release of regenerated nutrients, whereas the dissolution of sinking $CaCO_3$ proceeds much more slowly, and so most of the rain dissolves only once it has reached the deep seafloor. For these reasons, the regenerated nutrient metric (and oxygen depletion) cannot be used to infer the strength of the carbonate pump. Techniques have been developed to deconvolve from ocean data the concentration of alkalinity that can be attributed to the dissolution of $CaCO_3$ (Chung et al., 2003; Feely et al., 2002; Sabine et al., 2002), and changes in this globally averaged metric can be used to calculate the CO_2 effect of changes in the strength of the carbonate pump (Hain et al., 2010). The sensitivity of atmospheric CO_2 to the carbonate pump is ~5 ppm CO_2 increase for every 10 μM ocean average increase in alkalinity from $CaCO_3$ dissolution at depth (Hain et al., 2010; Kwon et al., 2011).

For the biological pump to drive a change in atmospheric CO_2, either regenerated nutrient or regenerated alkalinity has to change. This can be achieved by changing either the rate of the pumps (remineralization/dissolution rates of the biogenic rain) or the rate at which ocean circulation works against the pumps (the rate at which ocean interior water is brought to the surface). Specifically, greater export of organic matter and/or a greater residence time of the products of respiration in the interior result in a decline of unused nutrients in the surface and act to transform preformed P to regenerated P, thereby causing a drawdown of atmospheric CO_2. Likewise, an increase of the $CaCO_3$ rain and/or an increase of the residence time of its dissolution products at depth act to increase the concentration of sequestered alkalinity, which causes atmospheric CO_2 to rise. Therefore, reconstructions of ice age export production, $CaCO_3$ rain, and the rate of exchange between the surface and the deep ocean are important constraints on the role of the biological pump in driving the observed CO_2 variations (Sections 8.18.3.1–8.18.3.2). Additionally, reconstructions of a few environmental parameters, such as the oxygen concentration of the ocean interior or the distribution of stable carbon isotopes, speak relatively directly to the concentration of carbon sequestered by the soft-tissue pump (Section 8.18.3.3).

Despite the formal correctness of the flux-based view of the soft-tissue and carbonate pumps phrased above, it has often led to incorrect inferences. For example, many workers think of carbon storage in the interior as necessarily being correlated with the age of the deep ocean. This is violated in many cases, largely because there is typically coupling (and variable coupling) between the rate at which deep water is brought to the surface (causing nutrient supply) and the rate at which C_{org} is produced and sinks out of the surface ocean. For example, increasing the surface/deep communication in a region where all the surface nutrients are consumed (such as the low-latitude ocean) causes the increased upward transport of deeply sequestered CO_2 to be countered by increased C_{org} export, with no net effect in the soft-tissue pump (e.g., in the context of a conceptualized two-box ocean; Figure 5(a)). Despite the deep ocean becoming more recently ventilated ('younger') in this situation, the strength and efficiency of the soft-tissue pump are unchanged. In contrast, if surface/deep communication increases in a region of incomplete surface nutrient consumption, then the upwelling of sequestered carbon may increase more than the countering downward flux of sinking C_{org}. In this case, increased ocean ventilation (i.e., a younger deep ocean) will indeed translate to a weaker soft-tissue pump. Finally, we must note that the carbonate pump has very different (and typically much weaker) coupling to the rate at which water cycles between the surface and the deep ocean. The $CaCO_3$ flux is not as strongly correlated with nutrient supply

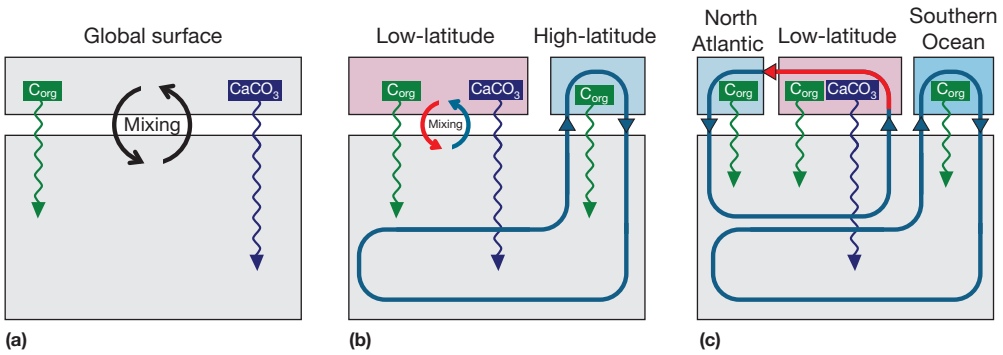

Figure 5 The general historical sequence of conceptual views of the ocean that have been formalized into 'box models' used to quantitatively investigate the biological pump and glacial/interglacial CO_2 change. The ocean is best understood as (a) separate surface and interior reservoirs (two 'boxes'), with ocean overturning simplified as mixing (see **Section 8.18.2.2**) and the biological pump driving DIC (and a smaller amount of alkalinity) out of the surface ocean box and into the deep box (Broecker, 1982a,b). In greater detail, the surface ocean includes at least two distinct domains: (b) The warm, strongly density stratified, nutrient-poor low-latitude surface and the less well stratified and nutrient-rich high-latitude surface, the latter ventilating most of the ocean interior (Knox and McElroy, 1984; Sarmiento and Toggweiler, 1984; Siegenthaler and Wenk, 1984; see also **Figure 6** and **Section 8.18.2.3**); (c) It is still more accurate to recognize that the ocean interior is ventilated by two high-latitude regions with distinct conditions, the nutrient-rich Southern Ocean and the nutrient-poor North Atlantic, the latter representing a region that allows nutrient-poor low-latitude surface waters back into the ocean interior (Toggweiler, 1999; see **Section 8.18.2.4**). Even in the current age of spatially resolved ocean models with thousands of boxes, these simple conceptualizations remain highly relevant (e.g., Marinov et al., 2008).

to the surface ocean, so that changes in the rate of deep-ocean ventilation translate more directly to changes in the carbonate pump. Because the increased upwelling of regenerated alkalinity is unlikely to be matched perfectly by increasing $CaCO_3$ rain, an increased surface/deep communication will likely yield a decrease in the proportion of total alkalinity in the ocean interior that is regenerated (i.e., an increase in preformed alkalinity). That is, unlike for the soft-tissue pump, it is relatively safe to assume that an 'older' deep ocean is one with a stronger carbonate pump while a 'younger' deep ocean has a weaker carbonate pump.

These caveats speak to the limitations of thinking of the ocean as two reservoirs – surface and interior (**Figure 5(a)**). Specifically, the two-box ocean view does not speak to the fact that low- and high-latitude ocean regions show different degrees of coupling between nutrient supply from the interior and C_{org} (and $CaCO_3$) production in surface waters. Moreover, it does not address the fact that most of the communication between the ocean interior and the surface ocean occurs in polar regions. Next, we turn to this low- versus high-latitude distinction (**Figure 5(b)**).

8.18.2.3 Low- versus High-Latitude Ocean

As outlined earlier, only roughly half of the total ocean inventory of the major nutrients, N and P, is regenerated from soft-tissue rain and thus only this half contributes to biological carbon sequestration at depth and atmospheric CO_2 drawdown. The origin of the other half of the ocean's nutrient inventory, preformed nutrients, must be surface water where biological productivity does not utilize all nutrients. Shipboard sampling efforts have been interpolated to yield the average concentration of various nutrients in surface waters (**Figure 6(a)–6(c)**), and the ocean's color as observed from space can be used to deduce the concentration of chlorophyll – the pigment used by phytoplankton to harvest the sun's energy during photosynthesis – which may be taken as a crude representation of the distribution of ocean productivity (**Figure 6(d)**). Based on these data, the surface ocean may be usefully separated into two domains: (1) the high-latitude surface with high nutrient concentrations and high productivity and (2) the low-latitude surface with low nutrient concentrations and low productivity (**Figure 5(b)**). Shortly after Broecker (1982a,b) described the potential of changes in the biological pump to explain glacial/interglacial CO_2 change, three research groups pointed out the significance of this three-box (two surface, one deep) view of the ocean for ice age CO_2 changes (Knox and McElroy, 1984; Sarmiento and Toggweiler, 1984; Siegenthaler and Wenk, 1984). In this section, we separately discuss the soft-tissue and carbonate pumps in this context.

The CO_2 record recovered from ice cores (**Figure 4**) is punctuated by episodes of rapid CO_2 decline and CO_2 rise. Indeed, these CO_2 changes appear too rapid and have the wrong timing to be explained by changes in the ocean's phosphate (P) inventory (Broecker and Henderson, 1998; Sigman and Boyle, 2000), and we subscribe to the view that the nitrogen inventory could not have changed independently of it (Deutsch et al., 2007; Haug et al., 1998; Ren et al., 2009; Tyrrell, 1999). Despite these constraints, the soft-tissue pump can still be the cause of the CO_2 drawdown: less of ocean's P may have been preformed (without carbon sequestration) and thus more regenerated (driving carbon sequestration). In the modern low-latitude ocean, biology is already able to make use of almost all nutrients brought to the surface, and thus only more efficient utilization of nutrients in the high-latitude ocean can increase the global efficiency of the soft-tissue pump. Moreover, surface water at high latitude is cold and dense while low-latitude surface water is warm and buoyant. Therefore, the voluminous ocean interior is filled with water rich in preformed nutrients originating from the high-latitude surface – this is the reason that half of the ocean's nutrient inventory is preformed today. There are two ways to reduce surface nutrient concentrations at high latitudes: (1) greater productivity leading to a greater rate of organic matter export

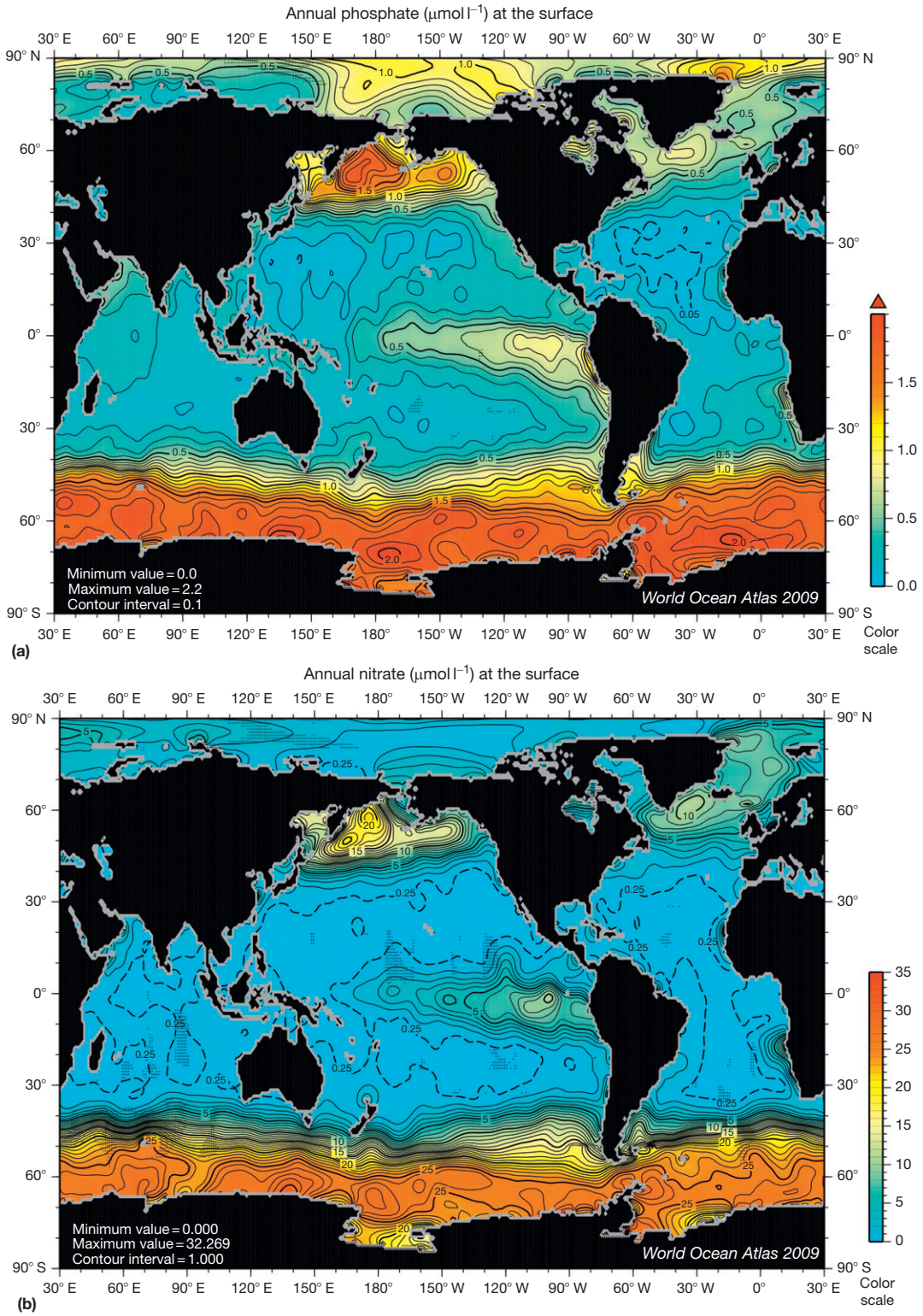

Figure 6 Surface ocean parameters fundamental to productivity in the surface ocean: the surface concentrations of the 'major nutrients' (a) phosphate (P-bearing PO_4^{3-}) and (b) nitrate (N-bearing NO_3^-), and of (c) the nutrient silicate (SiO_4^{4-}), which is required mostly by diatoms, a group of phytoplankton that build opal tests; and the concentrations of (d) chlorophyll, a qualitative index of phytoplankton abundance and thus net primary productivity.

(Continued)

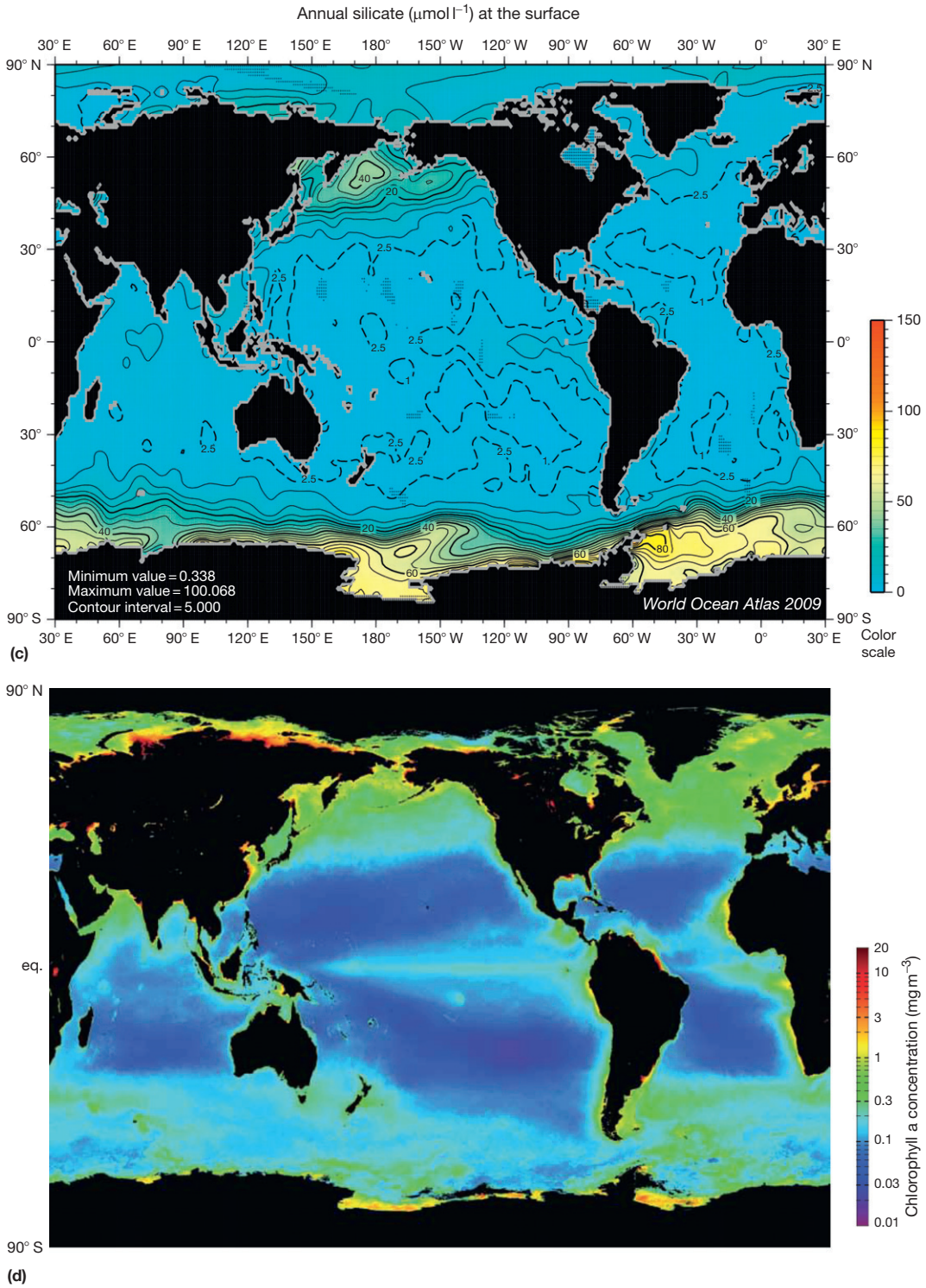

Figure 6—Cont'd Comparison of (d) with (a), (b), and (c) demonstrates that phytoplankton abundance, at the coarsest scale, is driven by the availability of these nutrients, and these nutrients are generally most available in the polar ocean, where nutrient-rich deep water mixes more easily to the surface. However, among the nutrient-bearing high-latitude regions, there is not a good correlation between nutrient concentration and chlorophyll, indicating that other parameters (i.e., iron and light) come to limit productivity in these regions. The high-latitude ocean of the southern hemisphere, which has the highest nutrient concentrations, is known as the Southern Ocean. It is composed of the more polar Antarctic Zone, where the silicate concentration is high and diatom productivity is extensive, and more equatorward Subantarctic Zone, where nitrate and phosphate remain high but silicate is scarce. The strong global correlation between phosphate and nitrate, originally recognized by Redfield (1934), allows us to group the two major nutrients (N and P) together when considering their internal cycling within the ocean, as they are exhausted in more or less the same regions (see **Section 8.18.2.2**). The nutrient data in (a), (b), and (c) are from the 2009 World Ocean Atlas (Garcia et al., 2009). The surface chlorophyll map in (d) is from composite data from the NASA SeaWiFs satellite project collected between September 1997 and August 2000 (http://oceancolor.gsfc.nasa.gov/).

(i.e., stronger pumping) and (2) slower supply of nutrients to the surface, such that, without increasing productivity, a greater fraction of the gross nutrient supply is converted to soft-tissue rain. Today, there is only a small density difference between the high-latitude surface and the ocean interior, which leads to rapid exchange and a high rate of nutrient supply to the surface. A reduction of gross nutrient supply thus demands a decrease of the exchange flux with the nutrient-rich ocean interior. Even in the face of lower productivity, surface nutrient status can decline if nutrient supply declines more than productivity does – the efficiency of the soft-tissue pump and its CO_2 drawdown can increase even if the 'pumping rate' of organic matter declines. Overall, to reconstruct the contribution of the soft-tissue pump to ice age CO_2 drawdown, it is important to reconstruct the high-latitude surface nutrient concentration, which will set the concentration of 'unused' (i.e., preformed) nutrients in the global ocean (see **Section 8.18.3.1.1**). To distinguish between the possible causes for an increase of nutrient drawdown – more 'pumping' (i.e., more soft-tissue rain) or less 'leaking' (i.e., less gross nutrient supply from depth) – it is important to reconstruct past high-latitude productivity (see **Section 8.18.3.1.2**).

Among the planktonic organisms that dwell in the open ocean surface, only some produce $CaCO_3$ shells (e.g., coccolithophores and foraminifera), while others use silica (SiO_2; e.g., diatoms and radiolarians) or produce no hard parts at all (e.g., green algae). Regardless of which material, the ballast of hard parts appears to help particles to sink (Armstrong et al., 2002), such that foraminifera, coccolithophores, and diatoms are more important in the biogenic rain than they are in total productivity (Armstrong et al., 2002). Of the different forms of hard parts, only the rain of $CaCO_3$ sequesters alkalinity via the carbonate pump.

Diatoms can grow and reproduce rapidly relative to other autotrophic phytoplankton (Egge and Aksnes, 1992). However, diatoms and other organisms with siliceous hard parts require dissolved silica as an additional nutrient while the rest of the organisms do not (Officer and Ryther, 1980), and they are less well suited to nutrient-poor waters than open ocean cyanobacteria and other small phytoplanktonic forms (Morel, 1987). SiO_2 is a scarce commodity in surface waters, with the exception of the high-latitude Southern Ocean and North Pacific (**Figure 6(c)**). Therefore, diatoms dominate productivity and particle export in these two regions, whereas the vast majority of $CaCO_3$ rain occurs in the remainder of the ocean including the low-latitude surface and the North Atlantic. To reconstruct changes in the carbonate pump and to infer its impact on atmospheric CO_2, it is thus critical to reconstruct the rate of low-latitude $CaCO_3$ rain (see **Section 8.18.3.1.2**) as well as the average time it takes for the sequestered (i.e., regenerated) alkalinity to return to the surface (see **Section 8.18.3.2.2**). As pointed out earlier, much of the $CaCO_3$ rain reaches the cold deep ocean, and thus the rate of water exchange between the high-latitude surface and the ocean interior is the critical parameter that determines the residence time of regenerated alkalinity at depth (Hain et al., 2010). Moreover, a greater supply of dissolved SiO_2 to the low-latitude surface is expected to increase the fraction of export production by diatoms, such that even at constant low-latitude export production, the rate of $CaCO_3$ rain may have declined in the past (Matsumoto and Sarmiento, 2008).

Deep-ocean ventilation works to counter the gradient driven by fluxes of both C_{org} and $CaCO_3$ associated with the soft-tissue and carbonate pumps, respectively. As the soft-tissue and carbonate pumps have opposing effects on atmospheric CO_2, the net effect of the rate of deep-ocean ventilation requires careful consideration. For example, a reduction in exchange between the ocean interior and a high-nutrient region of the high-latitude surface may promote more complete nutrient utilization in the surface or, as described below, may cause other regions with more complete nutrient utilization to become more important in the ventilation of the ocean interior. Either of these changes would make the global soft-tissue pump more efficient, leading to a lower steady-state atmospheric CO_2 concentration. However, the decrease in high-latitude ventilation also allows for more regenerated alkalinity to be sequestered in the interior by the carbonate pump, which works to raise CO_2. While the effect on CO_2 of the soft-tissue pump typically dominates when high-latitude ventilation is changed in geochemical models, the CO_2 effect of the carbonate pump can be equal or even greater in some model scenarios (Hain et al., 2010, 2011).

8.18.2.4 Southern Ocean versus North Atlantic

The deep ocean is filled with cold and dense waters that originate from the high-latitude ocean surface, and these waters carry a large burden of preformed nutrients that represent a missed opportunity for biological carbon sequestration. The Three-box view described earlier (**Figure 5(b)**) captures this fundamental aspect of the ocean, but it cannot account for the differences among the distinct high-latitude regions. Today, most of the ocean's volume is filled from the Southern Ocean surface ($\geq$50%) and the northern North Atlantic ($\sim$25%), whereas the volumetric importance of water derived from the northern North Pacific and the low-latitude surface is minute (DeVries and Primeau, 2011; Gebbie and Huybers, 2010). Low-latitude surface waters in the real ocean are too warm and buoyant to fill the ocean interior, and therefore the low-latitude surface ocean cannot directly raise the global efficiency of the soft-tissue pump despite near complete nutrient drawdown. In this regard, the three-box view of the ocean violates reality (**Figure 5(b)**; see **Section 8.18.2.3**). However, much of the deep water that is formed in the North Atlantic (North Atlantic Deep Water – NADW) derives from the low-latitude nutrient-poor surface ocean, causing NADW to have a low concentration of preformed nutrients. Thus, it is through the North Atlantic that low-latitude biogeochemical conditions impose their effect on the efficiency of the soft-tissue pump. As a result, more recent model studies have recast the high-latitude/low-latitude competition of the three-box models into a competition between the Southern Ocean and the North Atlantic (**Figure 5(c)**; e.g., Hain et al., 2010; Ito and Follows, 2005; Marinov et al., 2008; Sigman and Haug, 2003; Sigman et al., 2010; Toggweiler, 1999; Toggweiler et al., 2003b). In these models, a shift in ventilation of the ocean interior from the Southern Ocean to the North Atlantic works to lower CO_2. Of course, this is true only as long as the surface nutrient concentration of the northern North Atlantic is low compared with that of the Southern Ocean.

The circumstances of deep-water formation in the Southern Ocean and the North Atlantic are distinct. In the Polar Antarctic

Zone of the Southern Ocean, near the coast of Antarctica, deep-water formation is closely related to the winter-time cooling of surface waters, sea ice formation, and the interaction of subsurface waters with ice shelves (e.g., Iudicone et al., 2008; Orsi et al., 1999; Price and Baringer, 1994), leading to deep waters that are the densest of the modern ocean, mainly because they are extremely cold (Antarctic Bottom Water – AABW). Due to the small density difference between the deep ocean and the Antarctic surface, vertical exchange of water and nutrient supply to the surface is rapid, leading to very high surface nutrient concentrations and a large burden of preformed nutrients carried by AABW (**Figure 7(a)**; Southern Ocean loop). In the North Atlantic, however, the Gulf Stream and its extension (the North Atlantic Drift) carry very warm and salty low-latitude surface water to high latitude. In the Greenland and Labrador seas, these very saline surface waters cool to become sufficiently dense to sink, leading to more saline but less cold deep waters (NADW) than AABW (e.g., Kuhlbrodt et al., 2007). As

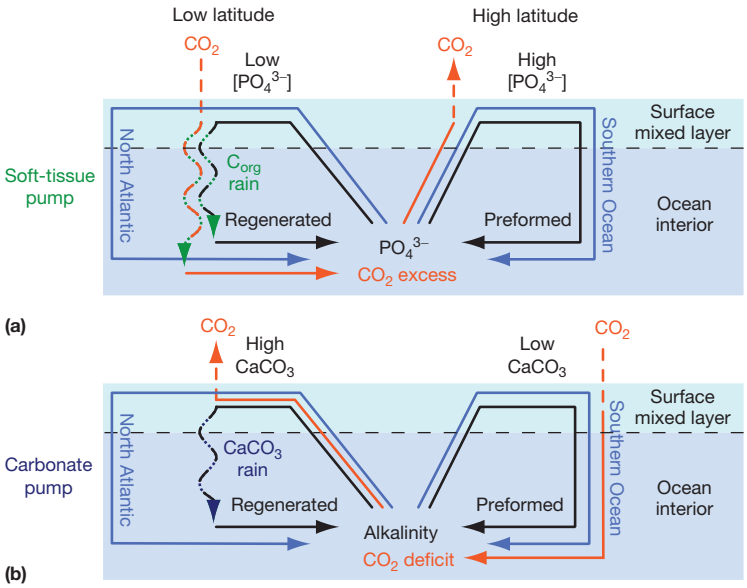

Figure 7 Schematic view of the roles of different ocean regions in (a) the soft-tissue pump and (b) the carbonate pump. In both panels, the blue and orange lines show the transport of water and CO_2, respectively. In (a), the black lines show the transport of major nutrients (represented by phosphate); in (b), the black lines show the transport of alkalinity. The solid, wavy, and dashed lines indicate transport by water flow, sinking organic matter, and air–sea exchange, respectively. The deep ocean interior is filled with cold, dense waters originating from polar ocean regions, either the northern North Atlantic (left-hand side) or the Southern Ocean (right-hand side). We first consider the implications of this bipolar deep-ocean ventilation for the soft-tissue pump. In (a), the loop on the left shows the high efficiency imparted to the pump by the low-latitude, low-nutrient surface regions. Nutrient-bearing subsurface water, after being upwelled or mixed to the surface, is warmed by the sun, making it buoyant, and the growth of phytoplankton completely extracts its dissolved nutrients. The particulate organic matter from this growth sinks into the ocean interior, where it is decomposed to 'regenerated' nutrient and excess CO_2 (CO_2 added by regeneration of C_{org}), sequestering CO_2 away from the atmosphere and into the deep ocean. Under steady ocean circulation, the continuous upwelling and warming of water in the low latitudes must be balanced by an equivalent rate of densification and sinking and deep-water formation. The nutrient-poor low-latitude surface waters cannot return immediately into the interior but must first become dense by cooling; today, this occurs dominantly in the high-latitude North Atlantic, included on the left side of the diagram. The loop on the right shows the low efficiency imparted by the high-latitude, high-nutrient surface regions, currently dominated by the Southern Ocean, especially its Polar Antarctic Zone near the margin of Antarctica. Because of vigorous vertical circulation, rapid nutrient supply, and poor light and iron conditions in the Antarctic, nutrient-rich and excess CO_2-rich water comes into the surface and descends again with most of its dissolved nutrient remaining (now referred to as 'preformed'). Soft-tissue organic matter consists of assimilated carbon and nutrients, such that preformed nutrients in the ocean interior record a 'missed opportunity' for deep-ocean carbon sequestration by the soft-tissue pump. Put another way, the Southern Ocean loop releases to the atmosphere CO_2 that had been sequestered by the regenerated nutrient loop involving the low latitudes and North Atlantic. Therefore, reducing the volume of the ocean interior ventilated by the Southern Ocean loop (i.e., increasing the volume ventilated by the North Atlantic loop) represents one mechanism for increasing the efficiency of the soft-tissue pump. There is a similar effect of the two regions of ventilation on the carbonate pump (b), but this translates to an opposing effect on atmospheric CO_2 (see orange arrows). Biogenic $CaCO_3$ rain is prominent in the low-latitude ocean. Therefore, when nutrient-bearing water is cycled through the North Atlantic loop of ocean overturning, the rain of $CaCO_3$ sequesters alkalinity in the deep ocean (as 'regenerated alkalinity'), which raises the concentration of CO_2 in surface waters and pushes CO_2 into the atmosphere. In contrast, the Southern Ocean is dominated by Si-bearing biogenic opal (see **Section 8.18.2.2**), such that Southern Ocean overturning brings regenerated alkalinity to the surface, allows it to take up CO_2, and then sends it back into the interior as 'preformed alkalinity.' As a result, if more of the ocean is ventilated by the North Atlantic, the carbonate pump is also made more efficient, which cancels part of the CO_2 decline driven by the increased efficiency of the soft-tissue pump. Two processes decouple the carbonate pump from the soft-tissue pump and its preformed nutrient metric: (1) at the surface, the production ratio of $CaCO_3$ to organic matter varies greatly among regions and conditions and (2) at depth, sinking organic matter is rapidly respired during its passage through the water column (releasing sequestered carbon and regenerated nutrients) while most $CaCO_3$ sinks to the seabed before dissolving. One consequence of this decoupling is that slower deep-ocean ventilation more reliably strengthens the carbonate pump than it does the soft-tissue pump, the latter being more sensitive to the surface ocean conditions during that ventilation process.

outlined earlier, the nutrient-depleted low-latitude surface water also imposes relatively low nutrient concentrations on the entire North Atlantic, such that NADW carries a relatively small burden of preformed nutrients (**Figure 7(a)**; North Atlantic loop).

As discussed in **Section 8.18.2.3**, simply reducing the nutrient concentration in the high-latitude surface translates directly to a more efficient soft-tissue pump and thus reduces atmospheric CO_2. However, since the North Atlantic and the Southern Ocean carry greatly different concentrations of preformed nutrients, the soft-tissue pump can also become more efficient if more of the ocean volume is filled by NADW at the expense of AABW – without any change in surface nutrient status (Hain et al., 2010; Marinov et al., 2008; Sigman and Haug, 2003; Toggweiler et al., 2003b). Indeed, atmospheric CO_2 is extremely sensitive to this 'ventilation volume' mechanism: given the $\sim$1 μM difference in preformed phosphate between AABW and NADW, if only 10% ocean volume now filled by AABW is replaced by NADW, the increased efficiency of the soft-tissue pump would drive a 13–20 ppm decline in atmospheric CO_2 (see **Section 8.18.2.2**).

The geochemical mechanism behind the ventilation volume hypothesis, as outlined above, has been established theoretically (Ito and Follows, 2005; Primeau, 2005), and its effectiveness has been demonstrated in ocean models (Hain et al., 2010; Marinov et al., 2008). However, there is strong evidence that during the last ice age, the deepest ocean was dominantly filled from the South, not from the North Atlantic (e.g., Curry and Oppo, 2005; Duplessy et al., 1988; Lynch-Stieglitz et al., 2007; Marchitto et al., 2002). Taken at face value, this evidence would seem to suggest that NADW volume was replaced with AABW volume – the opposite direction of that needed to strengthen the soft-tissue pump and to reduce atmospheric CO_2.

One way out of this bind is to propose that AABW of the last ice age is actually largely composed of water last ventilated in the North Atlantic. The main water mass in the modern deep ocean, AABW, is indeed a mixture of waters last ventilated in the Southern Ocean and the North Atlantic surface (e.g., Broecker et al., 1998; DeVries and Primeau, 2011; Gebbie and Huybers, 2010; Primeau, 2005). In the ice age ocean, a smaller portion of newly forming AABW may have been derived from the Antarctic surface, with an equivalently greater portion of its volume being composed of North Atlantic-derived water that was entrained into the abyss within the ocean interior (Hain et al., 2010, 2011; Kwon et al., 2012). This hypothetical scenario is consistent with the deep carbon isotope data from the LGM (Hain et al., 2010, 2011; Kwon et al., 2012; see **Section 8.18.3.2.1**). Alternatively, the surface processes that produce new deep water in the Antarctic may not have allowed the waters to exchange CO_2 before sinking into the interior, for example, if there was pervasive sea ice cover preventing gas exchange (Stephens and Keeling, 2000). In both cases – more entrainment of NADW or less gas exchange (i.e., ventilation) in the Antarctic surface – physical processes exert a control on atmospheric CO_2 via their effect on the biological pump.

It appears that an expansion of North Atlantic ocean ventilation, at the expense of Southern Ocean ventilation, acts to increase the sequestration of regenerated alkalinity at depth (Hain et al., 2010; Kwon et al., 2011). Biological productivity in the low-latitude surface ocean is associated with $CaCO_3$ export (i.e., coccolithophores and foraminifera), whereas Southern Ocean productivity is dominated by diatoms, which use dissolved silicic acid to build their opal shells. Given this difference, alkalinity is only sequestered by the action of the low-latitude/North Atlantic overturning loop (e.g., Brzezinski et al., 2002, 2003; Sarmiento et al., 2004; **Figure 7(b)**). Conversely, the ocean overturning in the Southern Ocean releases sequestered alkalinity from the ocean interior without causing significant $CaCO_3$ rain, converting regenerated alkalinity to preformed alkalinity (**Figure 7(b)**). As a result, a shift in ocean ventilation from Southern Ocean to North Atlantic dominated would tend to strengthen the carbonate pump (i.e., increase the deep sequestration of regenerated alkalinity) and thereby counter a portion of the decline in atmospheric CO_2 due to the simultaneous strengthening of the soft-tissue pump (**Figure 7**, North Atlantic loop). This appears to be an important constraint on the total CO_2 drawdown that can be driven by ocean ventilation changes alone (Hain et al., 2010; Kwon et al., 2011).

8.18.3 Tools

We have discussed the biological pump as a global phenomenon, the efficiency of which is set by regional processes and their relative impacts on the DIC and ALK sequestered in the global ocean interior. In our introduction to the tools used to reconstruct the biological pump, we begin with local surface biogeochemical conditions and then proceed to regional ocean interior processes, finishing with geochemical parameters that speak to global characteristics of the biological pump at a given time in Earth history. While one might argue that the last is most fundamental, a mechanistic understanding of changes in the ocean's biological pump requires information on each of these scales.

8.18.3.1 Surface Ocean Biogeochemistry

While there are many aspects of surface ocean biogeochemical change that one might hope to reconstruct through time, the nutrient status of the high-latitude surface ocean is the most critical because it sets the concentration of unused, preformed nutrients for most of the ocean's volume and it can be used to quantitatively derive the CO_2 effect of the soft-tissue pump (see **Sections 8.18.2.2–8.18.2.3**). Surface ocean productivity is less of a controlling variable – the biological pump can be more efficient even when productivity is lower – but is critically important to develop a mechanistic understanding of why surface nutrient changes may have occurred. In this regard, we must note that we are using the term 'productivity' loosely; our geochemical tools typically reconstruct export production rather than net primary production, and it is the former that most directly relates to the soft-tissue pump.

In regions where a deviation from major nutrient limitation is highly unlikely, in particular, the tropical and subtropical ocean characterized by perennial low nutrient status, export production is the major regional constraint that local paleoceanographic data can provide. In these regions, while reconstruction of export production is valuable for understanding

oceanographic change, it does not appreciably affect the soft-tissue pump, except in the case that global nutrient reservoirs have changed (Sigman and Haug, 2003). In contrast, the low-latitude export rate of $CaCO_3$ can affect the net effect of the biological pump because it drives the carbonate pump (e.g., Hain et al., 2010) and it affects the oceanic input/output budget of $CaCO_3$ (e.g., Sigman et al., 1998); in both cases, greater $CaCO_3$ rain raises atmospheric CO_2 (see **Sections 8.18.2.1–8.18.2.3**). Similarly, the rate of opal rain is of interest because export production of organic matter associated with opal represents a foregone opportunity for the carbonate pump to sequester alkalinity at depth.

Finally, we limit ourselves to tools that are largely based on geochemical measurement. We refer the interested reader to Fischer and Wefer (1999) for additional information and references.

8.18.3.1.1 Nutrient status

The measurable geochemical parameters currently available for addressing the nutrient status of the surface ocean include (1) the cadmium/calcium (Cd/Ca) ratio (Boyle, 1988a) and $^{13}C/^{12}C$ of planktonic (surface-dwelling) foraminiferal carbonate (Shackleton et al., 1983), which are intended to record the concentration of Cd and the $^{13}C/^{12}C$ of DIC in surface water; (2) the nitrogen isotopic composition of bulk sedimentary organic matter (Altabet and Francois, 1994a) and microfossil-bound organic matter (Ren et al., 2009; Shemesh et al., 1993; Sigman et al., 1999b), which may record the degree of nitrate utilization by phytoplankton in surface water; (3) the silicon isotopic composition (De La Rocha et al., 1997, 1998) and germanium/silicon ratio (Froelich and Andreae, 1981) of diatom microfossils, which may record the degree of silicate utilization in surface water; and (4) the carbon isotopic composition of organic matter in sediments (Rau et al., 1989) and diatom microfossils (Rosenthal et al., 2000a; Shemesh et al., 1993), which may record the aqueous CO_2 of surface water and/or the carbon uptake rate by phytoplankton.

The concentration of dissolved Cd is strongly correlated with the major nutrients (i.e., phosphate) throughout the global deep ocean, and the Cd/Ca ratio of benthic (seafloor-dwelling) foraminifera shells records the Cd concentration of seawater (Boyle, 1988a). As a result, benthic foraminiferal Cd/Ca measurements allow for the reconstruction of deep-ocean nutrient concentration gradients over glacial/interglacial cycles. Planktonic foraminiferal Cd/Ca measurements in surface waters provide an analogous approach to reconstruct surface ocean nutrient concentration, although this application has been less intensively used and studied.

A number of factors appear to complicate the link between planktonic foraminiferal Cd/Ca and surface nutrient concentrations in specific regions. First, temperature may have a major effect on the Cd/Ca ratio of planktonic foraminifera (Elderfield and Rickaby, 2000; Rickaby and Elderfield, 1999). Second, planktonic foraminiferal shell growth continues below the surface layer and probably integrates the Cd/Ca ratio of surface and shallow subsurface waters (Bauch et al., 1997; Kohfeld et al., 1996). This is of greatest concern in polar regions such as the Antarctic, where there are very sharp vertical gradients within the depth zone in which planktonic foraminiferal calcification occurs. Third, carbonate geochemistry on the deep seafloor may affect the Cd/Ca ratio of foraminifera preserved in deep-sea sediments (McCorkle et al., 1995; Van Geen et al., 1995). Fourth, the link between Cd and phosphate concentration in surface waters is not as tight as it is in deeper waters (Frew and Hunter, 1992).

Because of isotopic fractionation during carbon uptake by phytoplankton, there is a strong correlation between the $^{13}C/^{12}C$ of DIC and regenerated nutrient concentration in the global deep ocean; as a result, the $^{13}C/^{12}C$ of benthic foraminiferal fossils is a central tool in paleoceanography. The $^{13}C/^{12}C$ of planktonic foraminiferal calcite can also be useful in the surface ocean, as a tool to study the strength of the biological pump (Shackleton et al., 1983). However, the exchange of CO_2 with the atmosphere leads to a complicated relationship between the $^{13}C/^{12}C$ of DIC and the nutrient concentration in surface waters (Broecker and Maier-Reimer, 1992; Lynch-Stieglitz et al., 1995), such that even a perfect reconstruction of surface water $^{13}C/^{12}C$ would not provide direct information of surface ocean nutrient status. In addition, the $^{13}C/^{12}C$ of planktonic foraminiferal fossils found in surface sediments appears to be an imperfect recorder of the $^{13}C/^{12}C$ of DIC in modern surface waters, for a variety of reasons (Spero and Lea, 1993; Spero and Williams, 1988; Spero et al., 1997). Finally, the same concerns about the calcification depth noted for Cd/Ca also apply to carbon isotopes or, for that matter, any geochemical signal involving the precipitation of planktonic foraminiferal calcite.

During nitrate assimilation, phytoplankton preferentially consume ^{14}N-nitrate relative to ^{15}N-nitrate (Granger et al., 2010; Needoba and Harrison, 2004; Needoba et al., 2004; Waser et al., 1998a,b), leaving the surface nitrate pool enriched in ^{15}N (DiFiore et al., 2006, 2009). This results in a correlation between the $^{15}N/^{14}N$ ratio of organic N and the degree of nitrate utilization by phytoplankton in surface waters (Altabet and Francois, 1994a,b). There are uncertainties in the use of this correlation as the basis for paleoceanographic reconstruction of nutrient status, which include (1) the isotopic composition of deep-ocean nitrate through time (Kienast, 2000; Ren et al., 2012a), (2) temporal variations in the relationship between nitrate utilization and the nitrogen isotopes in the surface ocean (i.e., the 'isotope effect' of nitrate assimilation) (DiFiore et al., 2010), (3) the survival of the isotope signal of sinking organic matter into the sedimentary record (Lourey et al., 2003; Robinson et al., 2012), and (4) the potential for allochtonous N-bearing compounds to dilute/perturb/conceal the isotopic signature of organic N sinking from the surface (Kienast et al., 2005) . The nitrogen isotope analysis of microfossil-bound organic matter (Brunelle et al., 2007; Ren et al., 2009; Robinson and Sigman, 2008; Sigman et al., 1999b) and of specific compound classes such as chlorophyll degradation products (Higgins et al., 2009, 2010; Sachs and Repeta, 1999) circumvents the effect of diagenesis (Robinson et al., 2005b, 2012) and the problem of allochtonous N inputs (Meckler et al., 2011). However, more work is needed to test the linkage of selective N pools such as microfossil-bound N to the nitrogen isotope ratio of the nitrate consumed in surface waters, the parameter that relates most directly to the degree of nitrate utilization in surface waters (Altabet and Francois, 1994a; Galbraith et al., 2008a,b; Horn et al., 2011; Ren et al., 2012b).

The isotopic composition of silicon in diatom opal has been investigated as a proxy for the degree of silicate utilization by diatoms, based on the fact that diatoms fractionate the Si isotopes (^{30}Si and ^{28}Si) during uptake (e.g., Beucher et al., 2007; Cardinal et al., 2005; De La Rocha et al., 1997, 1998; Fripiat et al., 2011b). This application is analogous to the use of N isotopes to study nitrate utilization (e.g., De La Rocha, 2006), with important differences. On the one hand, the upper ocean cycle is arguably simpler for silica than bioavailable N (Reynolds et al., 2006), which bodes well for the silicon isotope system. On the other hand, there are very few regions of the surface ocean that maintain high dissolved silicate concentrations (**Figure 6(c)**). As a result, in regions of strong vertical silicate gradients, the link between silicate utilization and silicon isotopic composition is affected by mixing processes in surface and shallow subsurface waters (Fripiat et al., 2011a). In addition, isotope fractionation occurs during opal dissolution (Demarest et al., 2009) and this can affect the silicon isotopic composition of diatom opal and its preserved fraction in seafloor sediments (e.g., Fripiat et al., 2011b). An exciting new application of the silicon isotopes involves the use of sponge spicules to reconstruct silicate concentration (see Hendry et al., 2010, 2011; Wille et al., 2010), but this tool has not yet been applied to the nutrient conditions of the surface ocean.

The carbon isotopic composition of sedimentary organic matter was originally developed as a paleoceanographic proxy for the aqueous CO_2 concentration of Southern Ocean surface waters (Rau et al., 1989). The aqueous CO_2 concentration is a nearly ideal constraint for understanding a region's effect on the biological pump, as it would provide an indication of its tendency to release or absorb carbon dioxide. However, it has become clear that growth rate and related parameters are as important as the concentration of aqueous CO_2 for setting the $^{13}C/^{12}C$ of phytoplankton biomass and the sinking organic matter that it yields (Popp et al., 1998). In addition, the method of carbon acquisition by phytoplankton is also probably important for phytoplankton $^{13}C/^{12}C$ in at least some environments (Keller and Morel, 1999). Thus, the $^{13}C/^{12}C$ of organic carbon is a useful paleoceanographic constraint on nutrient status (Rosenthal et al., 2000a) but one that is currently difficult to interpret in isolation.

8.18.3.1.2 Export production

Export production, as defined earlier, is the flux of organic carbon (C_{org}) that sinks (or is mixed) out of the surface ocean and into the deep sea. While it is extremely difficult to imagine how paleoceanographic measurements can provide direct constraints on this highly specific parameter, approaches exist for the reconstruction of the flux of biogenic debris to the seafloor. To the degree that sinking biogenic debris has a predictable chemical composition and that its export out of the surface ocean is correlated with its rain rate to the seafloor, these approaches can provide insight into export production variations (Mueller and Suess, 1979; Ruhlemann et al., 1999; Sarnthein et al., 1988; but see Abelmann et al., 2006).

Only a very small fraction of the organic carbon exported out of the surface ocean accumulates in deep-sea sediments, with loss occurring both in the water column and at the seafloor. Moreover, various environmental conditions may influence the fraction of export production preserved in the sedimentary record. The mineral components of the biogenic rain (calcium carbonate, $CaCO_3$; opal, SiO_2) do not represent a source of chemical energy to benthic organisms and thus may be preserved in a more predictable fashion in deep-sea sediments. Thus, paleoceanographers sometimes hope to reconstruct export production (the flux of C_{org} out of the surface ocean) from the biogenic rain of opal or carbonate to the seafloor (Ruhlemann et al., 1999). We know that systematic variations in the ratio of SiO_2 or $CaCO_3$ to C_{org} in export production do occur; so there are many cases where changes in the mineral flux can be interpreted either as a change in the rate of export production or as a change in the composition of biogenic rain. Despite these limitations, we are better off with this information than without it.

The most basic strategy to reconstruct the biogenic rain to the seafloor is to measure accumulation rate in the sediments. This approach is appropriate for materials that accumulate without loss in the sediments or that are preserved to a constant or predictable degree. For the biogenic components of interest, C_{org}, SiO_2, and $CaCO_3$, the degree of preservation varies with diverse environmental variables, detracting from the usefulness of accumulation rate for the reconstruction of their rain to the seafloor. Nevertheless, because the environmental variables controlling preservation in the sediments can be linked to rain rate to the seafloor, accumulation rate can sometimes be a sound basis for at least the qualitative reconstruction of changes in some components of the biogenic rain. For instance, the fraction of the opal rain that is preserved in the sediment appears to be higher in opal-rich environments (Broecker and Peng, 1982). As a result, an observed increase in sedimentary opal accumulation rate may have been partially due to an increase in preservation. However, an increase in opal rain (and thus diatom-driven export) would typically have been needed to increase the sedimentary opal content in the first place.

If an age model can be developed for a deep-sea sediment core, then the accumulation histories of the various sediment components can be reconstructed. Assuming that the age model is correct, the main uncertainty in the reconstruction is then the potential for lateral sediment transport. Sediments, especially material such as clays, opal, and organic matter associated with the sediment fine fraction, can be winnowed from or focused to a given site on the seafloor, leading the sedimentary accumulation at that site to be less or greater than the rain of material through the water column to seafloor.

The geochemistry of radiogenic thorium provides a way to evaluate the effect of lateral sediment transport and related processes (Bacon, 1984; Bacon and Anderson, 1982; Bacon and Rosholt, 1982; Francois et al., 1990, 2004; Suman and Bacon, 1989; see **Chapter 8.12**). Thorium-230 (^{230}Th) is produced at a constant, well-known rate throughout the oceanic water column by the decay of dissolved uranium-234 (Chen et al., 1986). As ^{230}Th is produced, it is almost completely scavenged onto particles at the site of its production (Anderson et al., 1983; Bacon and Anderson, 1982; Nozaki et al., 1987). As a result, the accumulation rate of ^{230}Th in deep-sea sediments should match its integrated production in the overlying water column (Henderson and Anderson, 2003; Henderson et al., 1999; Siddall et al., 2008). If the

accumulation of ^{230}Th over a time period, as defined by a sediment age model, is more or less than should have been produced in the overlying water column during that period, then sediment is being focused or winnowed, respectively.

^{230}Th is also of great use as an independent constraint on the flux of biogenic material to the seafloor (Bacon, 1984; DeMasters, 2002; Francois et al., 2004; Suman and Bacon, 1989). Because the production rate of ^{230}Th in the water column is essentially constant over space and time, its concentration in sinking particles is diluted in environments with a large biogenic flux to the seafloor, yielding lower sedimentary concentrations of ^{230}Th in these environments.

The ^{230}Th 'constant flux tracer' has become a broadly used tool in paleoceanography (Francois et al., 2004); however, the underlying assumption of immediate scavenging onto sinking particles continues to be questioned (Broecker, 2008; Lyle et al., 2005; Mangini and Diester-Haass, 1983; Scholten et al., 1990; Thomas et al., 2000; Walter et al., 2001). These authors argue that ^{230}Th scavenging is incomplete in regions of low particle rain or strong currents, thereby allowing for some amount of lateral transport in solution to sites with greater biogenic rain. Another recently invigorated concern is that ^{230}Th focusing overestimates lateral sediment transport because it is partitioned preferentially into the small size-class fraction of the sediments, which are most easily winnowed away and focused elsewhere (Chase et al., 2002; Geibert and Usbeck, 2004; Kretschmer et al., 2010, 2011; Singh et al., 2011; Thomson et al., 1993). However, this problem may be suppressed by the cohesive behavior of fine particles in marine settings (McGee et al., 2010). Overall, this continuing evaluation of the ^{230}Th 'constant flux tracer' is a good illustration for how the quantitative interpretation of broadly used geochemical proxies is still being improved. A major international survey of trace elements and isotopes in the ocean currently underway (http://www.geotraces.org; Henderson et al., 2007) should help to resolve some of the outstanding questions.

One limitation on the use of ^{230}Th is the radioactive decay of this isotope, which has a half-life of 75 000 years. With corrections for terrestrial sources, it is possible to measure the accumulation rate of the stable isotope ^{3}He derived from interplanetary dust (Marcantonio et al., 1995). It appears that the ^{3}He flux from space has been roughly constant since the last ice age (e.g., Winckler and Fischer, 2006). If so, deviations of ^{3}He burial from this constant extraterrestrial ^{3}He flux would be interpreted in terms of sediment focusing versus winnowing, much as with ^{230}Th (Higgins et al., 2002; Marcantonio et al., 1996, 2001; McGee et al., 2010) but without an age limitation due to decay.

The flux of barium (Ba) to the seafloor is strongly related to the rain of organic matter out of the surface ocean (Dehairs et al., 1980, 1991; Dymond and Collier, 1996; Dymond et al., 1992; Francois et al., 1995; Hernandez-Sanchez et al., 2011; Paytan and Griffith, 2007; Paytan et al., 1996; Pfeifer et al., 2001; Pollard et al., 2009). Apparently, the oxidation of organic sulfur is the dominant process that produces microsites within sinking particles and living organisms that become supersaturated with respect to the mineral barite ($BaSO_4$) (see Hernandez-Sanchez et al., 2011 and references therein). On this basis, Ba accumulation has been investigated and applied as a measure of export production in the past, representing a more durable sedimentary signal of the C_{org} sinking flux than sedimentary C_{org} itself (Bains et al., 2000; Bonn et al., 1998; Dean et al., 1997; Dymond et al., 1992; Francois et al., 1995; Gingele et al., 1999; Nurnberg et al., 1997; Paytan et al., 1996; Rutsch et al., 1995). While debates continue on aspects of the biogenic Ba flux, some problems with preservation are broadly recognized. In sedimentary environments with low bottom water O_2 and/or high C_{org} rain rates, active sulfate reduction in the shallow sediments can cause barite to dissolve (Dymond et al., 1992; Eagle et al., 2003; Paytan and Kastner, 1996). In addition, there is some low level of barite dissolution under all conditions (Paytan and Kastner, 1996); if the biogenic barium flux is low, a large fraction of it can dissolve at the seafloor. Thus, Ba accumulation studies appear to be most applicable to environments of intermediate productivity.

The rapidly growing field of organic geochemistry promises new approaches for the study of biological productivity in the past. By studying specific chemical components – biomarkers – of the organic matter found in marine sediments, uncertainties associated with carbon source can be removed, and a richer understanding of past surface conditions can be developed (e.g., Hinrichs et al., 1999; Martinez et al., 1996). For example, alkenone lipids produced by haptophyte algae (Conte et al., 1994a,b; Marlowe et al., 1984) are relatively resistant to biodegradation and sedimentary diagenesis (Cleaveland and Herbert, 2009; Rechka and Maxwell, 1988; Sun and Wakeham, 1994), and thus their rate of accumulation on the seafloor may track the productivity of these organisms in the surface (see **Chapter 8.15**). There are a growing number of reconstructions of ocean productivity changes over the recent ice age cycles and beyond using these compounds (Bolton et al., 2010, 2011; Caissie et al., 2010; Lawrence et al., 2006; Liu and Herbert, 2004; Martinez-Garcia et al., 2009; McClymont et al., 2005).

8.18.3.2 Ocean Ventilation

Different high-latitude ocean regions impose different concentrations of preformed nutrients on the ocean interior, and thus changes in their relative volumetric importance in ventilating the ocean interior affect CO_2 through the soft-tissue pump (see **Section 8.18.2.4**). Therefore, reconstructions of changes in ocean overturning and mixing also attest to the efficiency of the global soft-tissue pump. The major water masses in the modern ocean are mixtures of water last ventilated mostly in the Southern Ocean and the North Atlantic. The 'ventilation volumes' for these two surface ocean regions are thus arguably the most critical to the efficiency of the soft-tissue pump. At the same time, we need to know the absolute rates of ocean overturning to develop a mechanistic understanding for both biogeochemical changes at the surface and ventilation volume changes at depth. In addition, the rate of deep-ocean ventilation (i.e., the age of deep waters) directly affects the strength of the carbonate pump (see **Section 8.18.2.3**). Below, we briefly describe approaches that have been developed to reconstruct specifically where the ocean was last ventilated and the rates of ocean overturning during the ice age.

8.18.3.2.1 Water mass distribution

The distribution of the main water masses at the LGM appears to be reflected in the distribution of carbon isotopes, but the C isotopes are not a conservative tracer of interior water masses,

as described below. During the LGM, the DIC associated with NADW was more enriched in ^{13}C over ^{12}C (high $\delta^{13}C$) relative to AABW (low $\delta^{13}C$) (e.g., Curry and Oppo, 2005; Duplessy et al., 1988; Lynch-Stieglitz et al., 2007). This isotopic contrast has been reconstructed from the $CaCO_3$ shells of benthic foraminifera. Based on a large body of such data, it is accepted that the volume of AABW expanded to dominate the global abyssal ocean while NADW was displaced upward in the water column so as not directly to fill the deepest ocean. The isotopic contrast between the upper ocean and the abyss records in itself the biological sequestration of ^{13}C-depleted C_{org} at depth. Hence, as newly ventilated water descends from the surface, its $\delta^{13}C$ is being continuously modified by the respiration of organic matter that adds low $\delta^{13}C$ carbon to the DIC pool. In that sense, as North Atlantic-ventilated water ages in the ocean interior, its $\delta^{13}C$ declines toward the $\delta^{13}C$ of AABW, such that the information as to where the water was last ventilated is eventually lost. Indeed, one plausible interpretation of the glacial Atlantic $\delta^{13}C$ data is that more of the interior of the ice age ocean was ventilated from the North Atlantic than occurs at present (Kwon et al., 2012).

The Cd/Ca ratio also recorded in the shells of benthic foraminifera has the potential to correct for the effect of respiration on foraminiferal $\delta^{13}C$. As described in **Section 8.18.3.1.1**, Cd is correlated with the distribution of phosphate in the modern ocean, which is also released during respiration (Boyle, 1988a; but also see Elderfield and Rickaby, 2000). Thus, foraminiferal Cd/Ca can be used to constrain the amount of respiration that a given water parcel had experienced and correct the measured $\delta^{13}C$ for the low-$\delta^{13}C$ respired carbon (Broecker and Maier-Reimer, 1992; Charles et al., 1993; Lynch-Stieglitz et al., 1995). The notion is that this regeneration-corrected $\delta^{13}C$ (e.g., '$\delta^{13}C_{as}$,' Lynch-Stieglitz et al., 1995) does not change after water descends from the surface into the ocean interior, making it suitable for reconstructing the mixing of North Atlantic-ventilated and Southern Ocean-ventilated water in the ocean interior. However, the end-member $\delta^{13}C_{as}$ of Southern Ocean surface water during the LGM that is needed to calculate southern versus northern ventilation is poorly constrained (e.g., Marchitto and Broecker, 2006) because of a lack of foraminifera in Antarctic sediments, and because seafloor respiration in highly productive regions may also decouple the benthic foraminiferal $\delta^{13}C$ from the $\delta^{13}C$ of the DIC of the overlying bottom water (Mackensen et al., 1993).

The distribution of neodymium isotopes (^{143}Nd, ^{144}Nd) in the ocean, as recorded in Fe–Mn coatings that develop on particle surfaces in the ocean interior, presents a powerful tool for reconstructing the basin-to-basin ocean overturning in the past (Albarede and Goldstein, 1992; Albarede et al., 1997; Piotrowski et al., 2004, 2008; Rutberg et al., 2000). The weathering of young volcanic rocks along the active continental margins of the Pacific imposes a high $^{143}Nd/^{144}Nd$ ratio on Pacific waters, while weathering of the old cratons straddling the passive continental margins of the Atlantic imposes a low $^{143}Nd/^{144}Nd$ ratio on Atlantic waters. Hence, changes in the $^{143}Nd/^{144}Nd$ distribution track the exchange and mixing of waters among these basins (see **Chapter 8.17**). However, since these source signals do not derive from the regions of surface ventilation, it is unlikely that changes in ocean ventilation can be constrained by reconstructing $^{143}Nd/^{144}Nd$ changes.

Temperature and salinity of water are not significantly affected by chemical processes in the interior ocean and can thus be used to infer surface source regions and the mixing of ocean interior waters. The $\delta^{18}O$ of benthic foraminiferal calcite is closely related to both temperature and salinity of the water from which it was precipitated, such that downcore records in some regions speak directly to the density of that water (Lynch-Stieglitz et al., 1999a,b). The $\delta^{18}O$–density relationship is temperature dependent and varies among different water masses (Zahn and Mix, 1991), but even if not taken as a density tracer, the foraminiferal $\delta^{18}O$ can still be used to trace the mixing of water masses in the interior (e.g., Herguera et al., 1992; Kallel et al., 1988; Lund et al., 2011). However, it is not clear yet whether it is feasible to quantify the relative importance of northern versus southern ventilatiation of the ice age ocean based on foraminiferal $\delta^{18}O$, mainly because this parameter cannot distinguish between warm/salty versus cold/fresh waters (e.g., Dansgaar and Tauber, 1969; Fairbanks and Matthews, 1978; Shackleton, 1967). Efforts to independently reconstruct these fundamental physical parameters, either through deep pore waters (Adkins and Schrag, 2001; Adkins et al., 2002; Paul et al., 2001; Schrag and DePaolo, 1993; Schrag et al., 1996, 2002) or through the Mg/Ca of benthic foraminiferal calcite (e.g., Elderfield and Ganssen, 2000; Lea et al., 2000; Rosenthal et al., 2000b), may thus be required to deconvolve the ocean ventilation signal.

8.18.3.2.2 Rates of ocean overturning and ventilation

The rate of ocean overturning is a critical control on the rate of gross nutrient supply from the subsurface to the surface ocean, and the local efficiency of the soft-tissue pump directly corresponds to the fraction of the gross nutrient supply that is converted to organic matter and exported to depth. Reconstructing the rates of ice age ocean circulation and mixing is thus central to explaining the history of atmospheric CO_2. Below, we briefly discuss two geochemical proxies that are used to address the dynamics of ocean overturning during the ice ages.

The radioactive isotope ^{14}C is produced by cosmic ray spallation in the atmosphere, mixes with the stable carbon isotopes, and decays with a half-life of 5730 years. The vast majority of ^{14}C resides in the ocean's DIC pool, with only $\sim$10% in the atmosphere and terrestrial biosphere, such that $\sim$90% of the ^{14}C decay occurs in the ocean (ignoring the recent addition of ^{14}C from nuclear activities). Because the ocean hosts only ^{14}C decay, the $^{14}C/C$ of the ocean is less than that of the atmosphere, and the relative depletion of the ocean is a measure for the rate of bulk ocean ventilation. Reconstructions of atmospheric $^{14}C/C$ exist for the last 50 000 years (Reimer et al., 2009 and references therein), well into the last ice age, whereas independent reconstructions of the global ^{14}C production rate only agree for the last 20 000 years (Frank et al., 1997; Laj et al., 2002; Muscheler et al., 2004), leaving substantial uncertainty regarding the global ^{14}C inventory (and thus the whole ocean $^{14}C/C$) before about 10 000 years ago (e.g., Broecker and Barker, 2007). The $^{14}C/C$ of $CaCO_3$ records the DIC $^{14}C/C$ of the water the carbonate was precipitated from, but most of the initial ^{14}C of ice age carbonate samples has decayed. In order to correct for this decay, an independent constraint on the age of the sample is needed. In practice, this is done by comparing the $^{14}C/C$ of benthic and planktonic

foraminifera from the same stratigraphic level (a proxy for the ^{14}C depletion of bottom waters versus surface waters) or by combined $^{14}C/C$ measurement and uranium–thorium dating on fossil deep-sea corals (e.g., Robinson et al., 2005a). Taking into account a number of corrections and additional considerations (Adkins and Boyle, 1997; Stuiver and Polach, 1977), the initial $^{14}C/C$ depletion of DIC relative to the contemporaneous atmosphere (or surface ocean) can be interpreted as the average time that has passed as the water was last at the surface – the apparent ^{14}C ventilation age. The modern deep ocean is characterized by apparent ventilation ages of a few 100 years in the Atlantic to almost 2000 years in the North Pacific, recording mainly the path and rate of ocean overturning (e.g., Broecker et al., 1988; Duplessy et al., 1989, 1991; Shackleton et al., 1988). However, surface water is also depleted in $^{14}C/C$ relative to the atmosphere because the exchange of carbon isotopes across the air–sea interface is slow (see Butzin et al., 2005; Fairbanks et al., 2005; Stuiver and Braziunas, 1993). This 'reservoir age' of surface waters can range between a few hundred years in the low-latitude surface and the North Atlantic to significantly more than 1000 years in the Southern Ocean surface. The deconvolution of inherent surface reservoir age and ^{14}C decay that occurred since the water left the surface is the main challenge for interpreting apparent ventilation ages; a greater fractional $^{14}C/C$ depletion of ocean interior water can result from more sluggish circulation and/or a greater surface reservoir age (e.g., Schmittner, 2003).

In recent years, the $^{231}Pa/^{230}Th$ ratio of marine sediments has received attention as a recorder of deepwater flow (e.g., Gherardi et al., 2005, 2009; McManus et al., 2004; Negre et al., 2010; but see also Anderson et al., 2009b). This approach is based on the different potentials for ^{231}Pa and ^{230}Th to be carried by ocean circulation before being scavenged by sinking particles and delivered to the sediments. As the central example in the modern ocean, North Atlantic sediments have a low $^{231}Pa/^{230}Th$ ratio, apparently because NADW carries ^{231}Pa (but not the rapidly scavenged ^{230}Th) southward out of the basin (Yu et al., 1996). A comprehensive treatment is provided by Anderson in this volume (see **Chapter 8.9**).

8.18.3.3 Integrative Constraints on the Biological Pump

If our goal is to explain the global net effect of ocean biology on the carbon cycle, we must also search for more integrative constraints on the biological pump. This is possible because the atmosphere, surface ocean, and deep ocean, while being distinct from one another, are each relatively homogeneous geochemical reservoirs. There are a number of global-scale geochemical parameters that may provide important constraints on the biological pump; we describe several of these below.

8.18.3.3.1 Carbon isotope distribution of the ocean and atmosphere

As described earlier, the biological pump tends to sequester ^{12}C-rich carbon in the ocean interior. All else being equal, the stronger the global biological pump, the higher will be the $^{13}C/^{12}C$ of DIC in the surface ocean and of carbon dioxide in the atmosphere. Broecker (1982a,b) and Shackleton et al. (1983) compared sediment core records of the $^{13}C/^{12}C$ of calcite precipitated by planktonic and benthic foraminifera, the goal being to reconstruct the $^{13}C/^{12}C$ difference in DIC between the surface and deep oceans, a measure of the strength of the global ocean's biological pump. Indeed, this work was the first suggestion that the biological pump was stronger during ice ages, thus potentially explaining the lower CO_2 levels of glacial times. Our view of these results is now more complicated (e.g., Spero et al., 1997); however, the basic inference remains defensible (Hofmann et al., 1999). Complementary records of the $^{13}C/^{12}C$ ratio of atmospheric CO_2, mainly based on air trapped in Antarctic ice cores, have been developed back into the last ice age and across the penultimate deglaciation (Elsig et al., 2009; Francey et al., 1999; Indermühle et al., 1999; Leuenberger et al., 1992; Lourantou et al., 2010a,b; Marino and McElroy, 1991; Smith et al., 1999). There are a number of additional modifiers of the $^{13}C/^{12}C$ of atmospheric CO_2, such as the temperature of gas exchange, and all of the ocean/atmosphere inorganic carbon would respond to changes in the sequestration of carbon by the terrestrial biosphere (Curry et al., 1988; Shackleton, 1977). Nevertheless, the reconstructed decline of $^{13}C/^{12}C$ of atmospheric CO_2 during deglacial CO_2 rise is consistent with the biological pump hypothesis for glacial/interglacial CO_2 change (Lourantou et al., 2010a,b; Smith et al., 1999).

8.18.3.3.2 Deep-ocean oxygen content

The atmosphere/ocean partitioning of diatomic oxygen (O_2) is a potentially important constraint on the strength of the biological pump. The rain of organic matter from the surface drives respiration at depth, thereby consuming O_2 in a stoichiometric proportion relative to the sequestration of carbon. Surface waters are near O_2 saturation with respect to the large (and therefore relatively stable) atmospheric O_2 reservoir. Thus, the concentration of O_2 in the ocean interior is equal to the initial O_2 concentration that the water carried when leaving the surface (which can be estimated from water temperature) minus the amount of O_2 consumed by respiration in the water since it left the surface. Because regenerated nutrients are also released during this respiration, the amount of O_2 consumed in an ocean interior water parcel is proportional to its concentration of regenerated nutrients, which we have already identified as a fundamental metric of the soft-tissue pump. A decrease in atmospheric CO_2 due to enhanced carbon sequestration by the soft-tissue pump should, therefore, be accompanied by a decrease in the O_2 content of the ocean interior.

The concentration of dissolved O_2 in the ocean interior has long been a target for paleoceanographic reconstruction, while the change in atmospheric O_2 content would be minute and thus difficult to measure. Sediments underlying waters with nearly no O_2 tend to lack burrowing organisms, so that sediments in these regions are undisturbed by bioturbation and can be laminated; this is perhaps our most reliable paleoceanographic indicator of deepwater anoxia (i.e., lack of O_2). Arguments have been made for surface area normalized sedimentary organic carbon content as an index of O_2 content in some settings (Keil and Cowie, 1999). It remains to be seen whether this is complicated by the potential for changes in the rain rate of organic matter to the sediments. There are a number of redox-sensitive metals, the accumulation of which gives information on the O_2 content of the pore water in shallow

sediments (Anderson et al., 1989; Crusius and Thomson, 2000; Crusius et al., 1996). The most widely used of these is uranium, the sedimentary concentration of which rises as bottom-water O_2 declines (Anderson, 1987; see also Boiteau et al., 2012 for a technique based on uranium in foraminiferal coatings). Unfortunately, the O_2 content of the sediment pore waters can vary due to organic matter supply to the sediments as well as the O_2 content of the bottom water bathing the seafloor (McManus et al., 2005, 2006), so that these two parameters can be difficult to separate (a situation that is analogous to that for sedimentary organic carbon content). Nevertheless, in a number of studies based on authigenic uranium, ice age increases in uranium content were observed despite the lack of substantial productivity change or in the face of productivity declines (Bradtmiller et al., 2010; Francois et al., 1997; Galbraith et al., 2007; Jaccard et al., 2009). These cases make a strong argument for reduced O_2 in much of the deep ocean during the last ice age, consistent with a role for soft-tissue pump changes in glacial/interglacial CO_2 change (Jaccard and Galbraith, 2012). While interesting data and arguments have been put forward in support of various approaches (Hastings et al., 1996; Russell et al., 1996), a globally integrative measure of ocean dissolved O_2 content is lacking.

In the Arabian Sea and the eastern Pacific, where water column suboxia (i.e., severe oxygen depletion but not complete anoxia) is reached today, the nitrogen isotopes have been used to diagnose changes in upper ocean O_2 concentration. Suboxic zones in the upper water column host denitrification, a biological process that preferentially removes ^{14}N-rich nitrate, leaving the residual nitrate of the shallow subsurface water column elevated in $^{15}N/^{14}N$ (Liu and Kaplan, 1989). When this nitrate is upwelled or mixed into the overlying surface ocean, it yields biomass and sinking N with a high $^{15}N/^{14}N$, which is subsequently buried in the sediments (Altabet et al., 1999a). Partly based on this approach, it appears that during the last ice age, oxygen levels were higher in the upper water column in regions where oxygen is low today, such that each of the major ocean suboxic zones became more oxygenated during the last ice age (Altabet et al., 1995, 1999b, 2002; De Pol-Holz et al., 2006, 2009, 2010; Galbraith et al., 2004; Ganeshram et al., 1995, 2002). As these suboxic zones are found at mid-depth, these data have led to the view that the ocean's oxygen deficit due to respiration shifted into the deeper ocean during the last ice age (e.g., Sigman and Boyle, 2000).

Initial model results (e.g., Knox and McElroy, 1984; Sarmiento et al., 1988; Toggweiler and Sarmiento, 1985) suggested that a biological pump mechanism for the glacial/interglacial CO_2 change would have rendered the ocean subsurface so O_2 deficient as to prevent the presence of burrowing organisms and oxic respiration over large expanses of the seafloor, which should leave some tell-tale signs in the sediment record. However, these models did not consider the potential of depth changes in the burden of regenerated carbon (Boyle, 1988c; Jaccard et al., 2009) or the potential of changes in $CaCO_3$ to magnify the CO_2 effect of the soft-tissue pump (e.g., Hain et al., 2010). A recent synthesis of the ocean's O_2 changes from the LGM through the deglaciation (Jaccard and Galbraith, 2012) concluded that (1) the deglacial oxygenation of the deep-ocean tracks the release of sequestered carbon and (2) the apparent deglacial expansion of suboxic zones in the upper ocean was related to an overall shoaling of the ocean's nutrient inventory that helped partition respired carbon, and thus respiration-driven oxygen depletion, from the deep ocean to the upper ocean. Indeed, this scenario is consistent with conclusions reached based on the $\delta^{13}C$ and Cd/Ca of benthic foraminifera (Berger and Lange, 1998; Boyle, 1988c; Herguera et al., 1992; Marchitto et al., 1998). In that sense, the glacial deepening of nutrients may have helped to prevent upper ocean anoxia by focusing carbon sequestration in deep waters which are currently relatively rich in O_2 (Boyle, 1988c).

8.18.3.3.3 Carbon chemistry and boron

As outlined earlier, the fidelity of atmospheric CO_2 fluctuations on millennial timescales (e.g., Ahn and Brook, 2008; Indermühle et al., 2000; Neftel et al., 1988) and the rapidity of deglacial CO_2 rise (e.g., Monnin et al., 2001) are strong evidence that much of the CO_2 change was driven by carbon redistributions within the atmosphere/ocean/terrestrial biosphere system. Therefore, perhaps the most direct evidence for the role of the biological pump in controlling these CO_2 changes may arise from reconstructions of ocean carbon chemistry. The classical approach involves the assessment of sedimentary $CaCO_3$ preservation versus dissolution (referring to either bulk sediment $CaCO_3$ or individual shells of specific organisms), which is influenced by the $CaCO_3$ saturation state of the overlying bottom water (e.g., Archer, 1991; Archer et al., 1989; Emerson and Archer, 1990; Emerson and Bender, 1981; Jahnke et al., 1994; see **Section 8.18.2.1**). In this section, we briefly outline more recently developed methods – based on the incorporation of boron into the carbonate shells of foraminifera – to reconstruct ocean carbon chemistry.

Appreciable concentrations of boron (^{10}B, ^{11}B) are dissolved in ocean waters in the form of deprotonated boric acid, mainly $B(OH)_3$ and $B(OH)_4^-$, with their ratio depending on pH. In solution, $B(OH)_4^-$ has a substantially lower $^{11}B/^{10}B$ than $B(OH)_3$ (Kakihana and Kotaka, 1977; Kakihana et al., 1977; Klochko et al., 2006). It has been suggested that only the charged species, $B(OH)_4^-$, is incorporated into foraminiferal $CaCO_3$ such that pH can be calculated from measured foraminiferal $^{11}B/^{10}B$, given knowledge of seawater $^{11}B/^{10}B$ (Hemming and Hanson, 1992; Sanyal et al., 1995, 1996, 2000). There is some concern about this approach due to (1) uncertainties about the magnitude of isotope fractionation among the boron species (Byrne et al., 2006; Klochko et al., 2006; Liu and Tossell, 2005; Pagani et al., 2005; Sanchez-Valle et al., 2005; Zeebe, 2005), (2) the mechanism of boron incorporation into carbonates (Allen et al., 2011a; Hemming and Hanson, 1992; Hemming et al., 1995; Klochko et al., 2009; Rae et al., 2011; Tossell, 2006), and (3) species differences and vital effects (e.g., Honisch and Hemming, 2004; Honisch et al., 2004). However, there is good evidence for its utility to reconstruct ocean pH (e.g., Allen et al., 2011a; Foster, 2008; Honisch et al., 2007; Rae et al., 2011).

Yu and Elderfield (2007) showed that the B/Ca ratio of benthic foraminifera could be used to reconstruct the carbonate ion (CO_3^{2-}) concentration in the ocean interior. This new approach is based on empirical calibrations, and a number of caveats have already been pointed out (Foster, 2008; Rae et al., 2011; Yu and Elderfield, 2007; Yu et al., 2007). Nonetheless,

the direct comparison of the independent $^{11}B/^{10}B$ and B/Ca approaches has yielded striking agreement (Yu et al., 2010a), arguably providing among the strongest support for both of these approaches.

Overall, the boron-based approaches hold the promise to reconstruct the redistribution of carbon and alkalinity over the ice age cycles. While one part of the reconstructed signal can be attributed to changes in the biological pump, another important part is due to temporary imbalances in the $CaCO_3$ budget of the ocean. Upon deglaciation, the release of biologically sequestered carbon from the deep-ocean interior should have raised deep-ocean CO_3^{2-} (eqn [3b]), pH (eqn [3c]), and $CaCO_3$ saturation state (Ω; eqn [4]) so as to promote the sea floor burial of $CaCO_3$ (e.g., Sigman et al., 2010; see **Section 8.18.2.1**). As more $CaCO_3$ was buried than dissolved $CaCO_3$ was supplied by from rivers, the ocean should have lost alkalinity and DIC in a 2:1 ratio, which would have raised atmospheric CO_2 (eqn [3d]) and progressively lowered CO_3^{2-} and Ω until the ocean's $CaCO_3$ was supplied by budget came back into balance. This sequence of events was conceived based on records of $CaCO_3$ preservation/dissolution and carbon cycle modeling (e.g., Broecker, 1982a,b; Broecker and Peng, 1987), and it appears to be borne out by deglacial B/Ca records (Yu et al., 2010b).

8.18.4 Observations

Many specific hypotheses have been put forward for the origin of ice age CO_2 drawdown, variously involving specific phenomena such as sea ice, biological productivity, nutrient availability and utilization, ocean circulation, ocean mixing, shifting winds, carbon sequestration, and whole ocean alkalinity changes. One of the goals of the earlier part of this chapter and the previous version (Sigman and Haug, 2003) was to describe the core geochemical mechanisms for CO_2 drawdown that most of these hypotheses share. In this section, we take a more personal tack and focus on a set of regions and processes that we favor as being involved in the ice age CO_2 drawdown, or part of it: (1) the Polar Antarctic Zone of the Southern Ocean and its ventilation of the deep ocean, (2) the Subantarctic Zone of the Southern Ocean and its biological response to dust fluxes, and (3) the North Atlantic and its impact on the depth and regions of the ocean interior where regenerated carbon is stored. We suggest below that the glacial progression from warm, high-CO_2 interglacial periods to peak glacial conditions with low CO_2 resulted from the superposition of regional changes that have distinct timings, yielding the multiple apparently stable levels of atmospheric CO_2 that have occurred over the last 800 000 years (Hain et al., 2010).

8.18.4.1 800 000 Year Perspective

Atmospheric CO_2 has been reconstructed from ice cores with great fidelity for the last 800 000 years (**Figure 8(a)**; Lüthi et al., 2008 and references therein). The reconstructed CO_2 changes track the progression of global glaciation and cooling (**Figure 8(b)**; Lisiecki and Raymo, 2005). While very similar in its overall temporal pattern, the record of Antarctic air temperature derived from ice cores (**Figure 8(e)**; Jouzel et al., 2007) exhibits the greatest part of the warming and cooling immediately at ice age terminations and initial glacial inceptions, respectively. This distinct timing of Antarctic temperature change appears to be reflected in the sediments deposited in the Polar Antarctic Zone of the Southern Ocean (**Figure 8(f)**; Hodell et al., 2002; see also Kemp et al., 2010), the changes in which suggest high biological productivity during the brief interglacial stages (shaded red in **Figure 8**) and lower productivity otherwise. Taken at face value, Antarctic changes occurred early in the glacial progression associated with the initial decline in atmospheric CO_2 from high interglacial values (Hain et al., 2010). The evidence for low Polar Antarctic productivity during the LGM (e.g., Francois et al., 1997; Frank et al., 2000; Kohfeld et al., 2005; Kumar et al., 1993; Mortlock et al., 1991) in the face of low CO_2 argues for greater fractional utilization of a reduced nutrient supply to the surface (i.e., the 'Antarctic stratification' hypothesis, Francois et al., 1997; see also **Section 8.18.2.3**) and/or expanded sea ice cover that prevents the venting of CO_2 from supersaturated surface waters (i.e., the 'sea ice' hypothesis, Stephens and Keeling, 2000). There is evidence for and against low LGM nutrient concentrations in the Polar Antarctic (Crosta and Shemesh, 2002; De La Rocha et al., 1998; Elderfield and Rickaby, 2000; Francois et al., 1997; Keigwin and Boyle, 1989; Robinson and Sigman, 2008; Robinson et al., 2004; Sigman et al., 1999a,b). There are also hybrid scenarios in which the expansion of sea ice cover and Antarctic density stratification interact on a spatial basis to reduce CO_2 evasion through the Antarctic surface (Sigman and Haug, 2003; Stephens and Keeling, 2000). As the available data set of glacial Southern Ocean sea ice cover grows (e.g., Allen et al., 2011b; CLIMAP, 1981; Collins et al., 2012; Crosta et al., 2004; Gersonde et al., 2003, 2005; Stickley et al., 2005), a more detailed comparison with the CO_2 and temperature records will become possible. In any case, the CO_2 effects of increased Antarctic sea ice cover, reduced Antarctic overturning, and increased nutrient drawdown are not additive, such that the combination of the stratification and sea ice hypotheses is expected to yield only insignificantly more CO_2 drawdown than either mechanism in isolation (Hain et al., 2010).

The subpolar North Pacific experienced changes in productivity and surface nutrient status very similar to those inferred for the Antarctic (e.g., for productivity and/or nutrients, see Brunelle et al., 2007, 2010; Galbraith et al., 2007, 2008a,b; Gebhardt et al., 2008; Haug et al., 2005; Jaccard et al., 2005; Kienast et al., 2004; Okazaki et al., 2005a,b; Seki et al., 2004; e.g., for sea ice, Katsuki and Takahashi, 2005; Sakamoto et al., 2005). Indeed, the North Pacific sediment records, which typically have adequate foraminifera for relative dating by oxygen isotope correlation, may provide an analog for changes in the Antarctic, where the sediments often lack foraminifera and are generally less amenable to paleoceanographic reconstructions (Haug and Sigman, 2009; Sigman et al., 2010). While the similarities are remarkable, they do not extend to the potential of these two regions to affect atmospheric CO_2: unlike the Antarctic, the modern North Pacific ventilates only a modest fraction of the ocean volume (e.g., DeVries and Primeau, 2011; Gebbie and Huybers, 2010) and thus does not possess much leverage on the global soft-tissue pump (Hain et al., 2010; see **Section 8.18.2.4**).

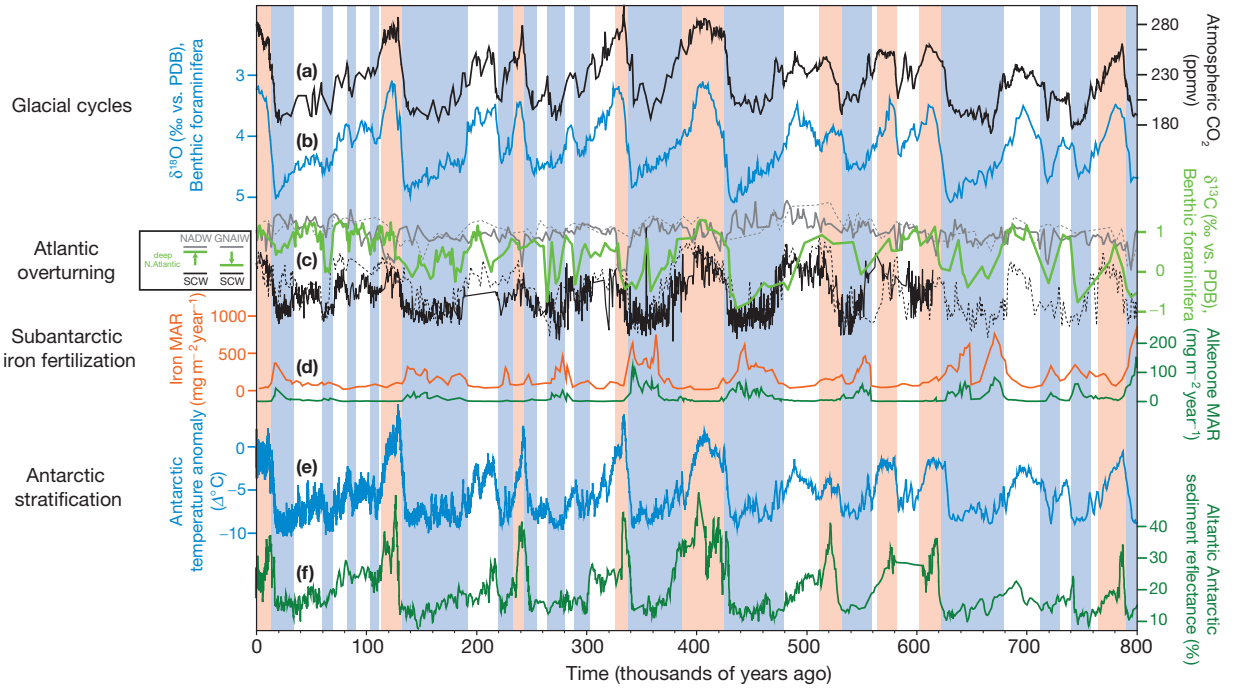

Figure 8 A selection of marine and ice core records that provide a synoptic view of the relationship between ocean overturning and productivity over the late Pleistocene ice age cycles (i.e., the last ~800 000 years). The vertical shaded bars indicate warm interglacial stages (red) and cold stages with lowest atmospheric CO_2 concentration (blue). For a detailed description, see **Section 8.18.4.1**. The sources and particulars of the records are as follows: (a) CO_2: a compilation by Lüthi et al. (2008); (b) benthic foraminiferal $\delta^{18}O$: a global compilation by Lisiecki and Raymo (2005) (higher values correspond to greater volumes of continental ice sheets and colder deep-ocean temperature); (c) benthic foraminiferal $\delta^{13}C$ records (all *Cibicidoides* spp.): (1) shallow northern North Atlantic (solid gray line: ODP Site 982 at 1145 m depth, Venz et al., 1999; dashed gray line: DSDP Site 552 at 2311 m depth, Sarnthein et al., 1994), (2) the deep North Atlantic (solid green line: DSDP Site 607 at 3427 m depth, Ruddiman et al., 1989 compiled from Boyle and Keigwin, 1985; Mix and Fairbanks, 1985 and Raymo et al., 1989), and (3) the abyssal southern South Atlantic (solid black line: ODP Site 1089 at 4620 m depth, Hodell et al., 2003; dashed black line ODP Site 1090 at 3702 m depth, Hodell et al., 2003) – the position of the green curve relative to northern sourced (gray) and southern sourced (black) waters speaks to the geometry of Atlantic overturning through time; (d) Martinez-Garcia et al. (2009) records of Subantarctic iron-bearing dust supply (iron mass accumulation rate, MAR) and haptophyte productivity (alkenone MAR) at ODP Site 1090; (e) Jouzel et al.'s (2007) record of temperature change at the EPICA Dome C ice core drill site; and (f) Hodell et al.'s (2002) record of sediment reflectance (i.e., sediment color) at ODP Site 1094 – a rough metric of Antarctic productivity (bright/reflective layers correspond to greater opal content and thus higher diatom productivity). The age models for DSDP Site 607 and ODP Site 982 were tuned (between 250 and 630 ky) based on comparison of benthic foraminiferal $\delta^{18}O$ to ODP Site 1089 (solid black line in panel (c)) and the global $\delta^{18}O$ stack (panel (b)).

Unlike for the Antarctic, reconstructions from the Subantarctic Zone of the Southern Ocean indicate enhanced productivity along with more complete nutrient utilization during glacial stages (Chase et al., 2001; Kohfeld et al., 2005; Kumar et al., 1995; Martinez-Garcia et al., 2009; Mashiotta et al., 1997; Robinson and Sigman, 2008; Robinson et al., 2005b; Rosenthal et al., 1997, 2000a). These findings agree well with the 'iron fertilization' hypothesis for glacial CO_2 drawdown (Martin, 1990; Martin et al., 1990a,b) because (a) the Subantarctic is located within the westerly wind belt that carries the iron-bearing dust from the southern hemisphere continental dust sources to the ocean and (b) glacial episodes of enhanced dust supply correspond to CO_2 decline, enhanced Subantarctic productivity and greater nutrient drawdown (**Figure 8(d)**; Martinez-Garcia et al., 2009; Robinson et al., 2005b; Watson et al., 2000). The timing of the enhanced wind-borne iron supply and its biological response bear only partial resemblance to the temporal evolution of atmospheric CO_2, the overall progression of the glacial cycles, and the changes in the Antarctic (**Figure 8**). Specifically, it appears that pronounced iron fertilization only occurs during the coldest ice age stages (blue shading **Figure 8**), which also correspond to episodes of greatest CO_2 drawdown (**Figure 8(a)**; Watson et al., 2000).

The volume of the ocean that is ventilated from the Subantarctic surface is modest (e.g., DeVries and Primeau, 2011; Gebbie and Huybers, 2010), such that the direct effect of Subantarctic iron fertilization and surface nutrient decline on the soft-tissue pump may have been rather small. However, the Subantarctic ventilated waters predominantly spread into the mid-depth and shallow subsurface ocean, and nutrients that are left unused in the Subantarctic surface ultimately fuel biological productivity and $CaCO_3$ rain when these shallow interior waters rise to and mix with low-latitude surface waters (Palter et al., 2010; Sarmiento et al., 2004; Toggweiler et al., 1991). Thus, while greater glacial nutrient drawdown in the Subantarctic strengthens the soft-tissue pump, it also indirectly weakens the carbonate pump, both of which act to reduce atmospheric CO_2 and transiently reduce the CO_3^{2-} concentration of the deep ocean (see eqn [3b] in **Section 8.18.2.1**). The decline of deep-ocean CO_3^{2-} concentration causes bottom waters to become more corrosive toward $CaCO_3$, reducing the seafloor preservation of $CaCO_3$, raising ocean alkalinity,

and thus further lowering CO_2 (Hain et al., 2010). Subantarctic iron fertilization also causes a permanent decline in $CaCO_3$ rain, further increasing ocean alkalinity and lowering CO_2 (Hain et al., 2010). Finally, changes in silicate consumption and transport may have further extended the capacity for the Subantarctic to raise ocean alkalinity, through the region's influence on low-latitude $CaCO_3$ export (e.g., Brzezinski et al., 2002; Matsumoto and Sarmiento, 2008). In short, the Subantarctic has a far greater impact on CO_2 than if solely measured from the preformed/regenerated nutrient metric of the soft-tissue pump (see **Section 8.18.2.2**). Overall, model simulations suggest that iron fertilization in the Subantarctic Zone of the Southern Ocean can explain up to 35–40 ppm of the atmospheric CO_2 drawdown during the brief episodes of enhanced dust supply (**Figure 8(d)**), including the less certain downstream effects on low-latitude $CaCO_3$ production and sea floor burial (Hain et al., 2010; Watson et al., 2000).

Finally, a strong case has been made for a major reorganization of water masses in the Atlantic basin between the LGM and the current interglacial (e.g., Curry and Oppo, 2005; Duplessy et al., 1988; Lynch-Stieglitz et al., 2007; Marchitto and Broecker, 2006; Sarnthein et al., 1994). During the LGM, NADW shoaled – prompting the name Glacial North Atlantic Intermediate Water (GNAIW) – while Southern Component Water (SCW) penetrated further northward into the deep North Atlantic. Downcore records of benthic foraminiferal $^{13}C/^{12}C$ ratios (expressed in $\delta^{13}C$ notation) from the deep North Atlantic and its plausible upstream contributors (NADW/GNAIW vs. SCW) clearly show that Atlantic water-mass reorganization has occurred repeatedly over the last 800 000 years (**Figure 8(c)**). For much of the time, the $\delta^{13}C$ of the deep North Atlantic (green in **Figure 8(c)**; Ocean Drilling Program (ODP) Site 607) was essentially identical to the $\delta^{13}C$ of North Atlantic sourced water (gray in **Figure 8(c)**; ODP Site 982 and Deep Sea Drilling Project Site 552), indicating a water-mass distribution similar to the modern ocean. However, during the coldest stages of the ice ages (blue shading in **Figure 8**), deep North Atlantic $\delta^{13}C$ decreased toward that of SCW (black in **Figure 8(c)**; ODP Sites 1089 and 1090), away from the GNAIW $\delta^{13}C$.

This change in deep Atlantic hydrography could either act to raise atmospheric CO_2 during glacials or cause CO_2 drawdown, depending largely on the fraction of SCW that last ventilated in the North Atlantic versus the Polar Antarctic (the 'ventilation volume' hypothesis, see **Section 8.18.2.4**). If the expanded SCW was actually composed of GNAIW that had not been reventilated in the Southern Ocean (e.g., due to Antarctic stratification), then the SCW expansion into the deep North Atlantic would help to explain the coeval decline of atmospheric CO_2 (blue shading in **Figure 8**; Hain et al., 2010; Kwon et al., 2012). In addition to this direct effect on the soft-tissue pump, the shoaling of North Atlantic overturning may have helped to isolate the global deep ocean as a repository for biologically sequestered carbon, as has been reconstructed based on foraminiferal Cd/Ca for the LGM (e.g., Boyle, 1988a). This reconstructed deepening of the respired carbon pool would have reduced $CaCO_3$ burial on the abyssal seafloor, raising whole ocean alkalinity and thereby lowering atmospheric CO_2 (Boyle, 1988b; Sigman and Boyle, 2000; Toggweiler, 1999; Yu et al., 2010b). Moreover, the expansion of corrosive SCW into the Atlantic basin is expected to cause substantial dissolution of $CaCO_3$ from the deep Atlantic seafloor and a permanent shoaling of the Atlantic lysocline, which would also raise whole ocean alkalinity and lower atmospheric CO_2 (Archer and Maier-Reimer, 1994; Hain et al., 2010).

In summary, over the last eight glacial–interglacial cycles, Antarctic temperature and Antarctic opal burial decline most severely upon glacial inception (**Figure 8(e)–8(f)**), suggesting that the 'Antarctic stratification hypothesis' (Francois et al., 1994) may apply to all times other than peak interglacials. In contrast, Subantarctic productivity increases (**Figure 8(d)**) and Atlantic deep water shoaling (**Figure 8(c)**) tends to occur later in the glacial progression, suggesting that the 'iron hypothesis' (Martin, 1990; **Figure 8(d)**) and the 'ventilation volume hypothesis' (Hain et al., 2010; **Figure 8(c)**) apply only to the more extreme conditions of the ice ages. In this view, when all three hypothesized processes are 'inactive' (red vertical shading), atmospheric CO_2 is the highest (similar to the pre-industrial value of ~280 ppmv); and when all three are 'active' (blue vertical shading), atmospheric CO_2 is at a minimum (**Figure 8(a)**). Decoupling of these mechanisms during 'mid-climate states' (suggested for the unshaded intervals) may explain intermediate concentrations of atmospheric CO_2 (Sigman et al., 2010).

8.18.4.2 Deglacial Perspective

The most detailed information on the coupling of the biological pump to the atmospheric CO_2 concentration and climate change arises from the last deglaciation, the transitional period between peak ice age conditions during the LGM (26.5–19 000 years before present (ky BP), see Clark et al., 2009) and the current Holocene interglacial (11.7–0 ky BP). This deglacial transition is further subdivided into Heinrich stadial 1 (HS1; ~17.5–14.6 ky BP), the Bølling-Allerød interstadial (B/A; ~14.6–12.7 ky BP), and the Younger Dryas (YD) stadial (~12.7–11.6 ky BP; see Muscheler et al., 2008). Only the Holocene is a recognized stratigraphic entity (IUGS Subcommission on Quaternary Stratigraphy) whereas the other time intervals are based on the dating of distinct patterns of climate (and ocean) change during the deglacial transition, such that the ages provided in the literature may vary.

During the LGM, cold conditions prevailed in both hemispheres (**Figure 9(a)** and **9(g)**), and atmospheric CO_2 was low and stable (**Figure 9(f)**). As outlined earlier, during the LGM, low $\delta^{13}C$ SCW extended into the deep North Atlantic while a shallow glacial form of North Atlantic Deep Water (GNAIW) occupied the intermediate depths (e.g., Lynch-Stieglitz et al., 2007 and references therein). Low sedimentary $^{231}Pa/^{230}Th$ ratios of North Atlantic LGM age sediments have been interpreted as evidence that the southward flow of GNAIW was vigorous (**Figure 9(b)**; Gherardi et al., 2009; McManus et al., 2004; Robinson and van de Flierdt, 2009; Sigman et al., 2003) but essentially restricted to depths above 3000 m (Marchitto and Broecker, 2006), unlike modern NADW which reaches the bottom of the Atlantic. A 'chemical divide' at 2000–3000 m depth in the LGM Indo-Pacific ocean has also been identified (Boyle et al., 1995; Galbraith et al., 2007; Herguera, 1992; Kallel et al., 1988; Keigwin, 1998; Matsumoto and Lynch-Stieglitz, 1999; Matsumoto et al., 2002),

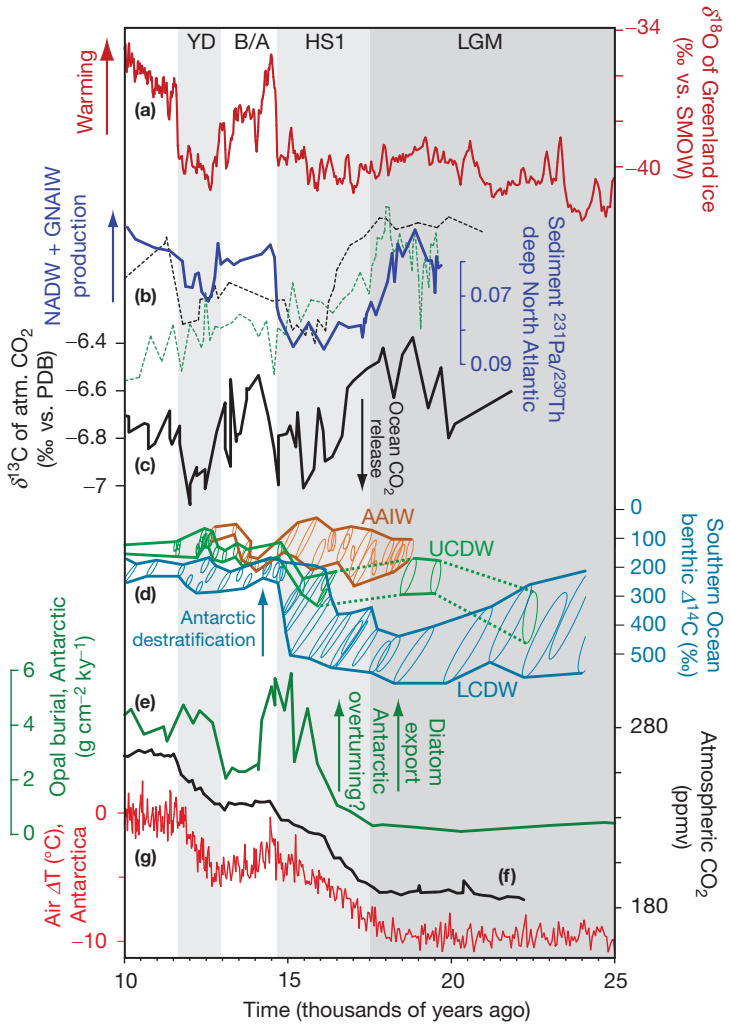

Figure 9 A selection of marine and ice core records that illustrate the ocean and climate change across the deglacial transition from the Last Glacial Maximum (LGM) to the current interglacial. The vertical shaded bars highlight specific time intervals discussed in **Section 8.18.4.2** – the LGM, Heinrich stadial 1 (HS1), the Bølling–Allerød interstadial (B/A), and the Younger Dryas (YD). The records shown here are taken from: (a) Greenland GISP2 record of ice $\delta^{18}O$ (Grootes and Stuiver, 1997) – a measure of local air temperature; (b) sedimentary $^{231}Pa/^{230}Th$ ratios from various sites in the North Atlantic (Gherardi et al., 2009; McManus et al., 2004) – a putative measure for the rate of deep water export from the North Atlantic (values of ~0.09 indicate no export, and lower values indicate greater export of water at depth); (c) ice core reconstruction of the $\delta^{13}C$ of atmospheric CO_2 (Lourantou et al., 2010a) – negative excursions are consistent with the release of biologically sequestered carbon from the ocean; (d) the absolute depletion of deep Southern Ocean waters relative to atmospheric $\Delta^{14}C$ (Burke and Robinson, 2012; Skinner et al., 2010) – greater spread between these records during the LGM suggests less vertical mixing in the ice age Southern Ocean (the acronyms, shown here as assigned by Burke and Robinson (2012), indicate various water masses in the Southern Ocean, with Antarctic Intermediate Water (AAIW) to Upper Circumpolar Deep Water (UCDW) to Lower Circumpolar Deep Water (LCDW) corresponding to increasing depth); (e) opal burial flux in the Atlantic sector of the Antarctic (core site TN057-13-4PC; Anderson et al., 2009a) – greater opal flux indicating greater productivity; (f) atmospheric CO_2 measured from trapped air in an ice core from the Taylor Dome drill site, Antarctica (Monnin et al., 2001); (g) temperature change at the EPICA Dome C ice core drill site reconstructed from ice deuterium-to-hydrogen ratios (Jouzel et al., 2007).

and reconstructions of deep Southern Ocean $^{14}C/C$ depletion from the deep South Atlantic and the Drake Passage suggest that this divide extended into the Southern Ocean (**Figure 9 (d)**; Burke and Robinson, 2012; Skinner et al., 2010). The deep ocean below that divide hosted a substantial amount of biologically sequestered, $^{13}C/^{12}C$-deplete regenerated carbon and thus lower O_2 (e.g., Boyle, 1988a,b,c; Jaccard and Galbraith, 2012; see **Section 8.18.3.3**). The permanent (year-round) LGM Antarctic sea ice cover extended substantially farther northward than today in at least some sectors of the Southern Ocean, especially the Atlantic sector (e.g., Allen et al., 2011b; Gersonde et al., 2003, 2005). Productivity in the Antarctic Zone was lower than modern (Chase et al., 2001, 2003; Frank et al., 2000; Kumar et al., 1993, 1995), but it was higher than modern in at least some parts of the Subantarctic Zone (Kohfeld et al., 2005; Kumar et al., 1995; Martinez-Garcia et al., 2009; Mashiotta et al., 1997; Rosenthal et al., 1997, 2000a). Surface nutrient drawdown appears to have been more complete in

both the Antarctic and Subantarctic zones of the Southern Ocean (e.g., Robinson and Sigman, 2008, and references therein).

HS1 refers to an episode when ice rafted debris accumulated broadly on the northern North Atlantic seafloor during a cold (stadial) phase in northern hemisphere climate (Heinrich, 1988; **Figure 9(a)**). Observations and model simulations of massive North Atlantic freshwater release derived from melting ice indicate that the formation of GNAIW slowed down or even ceased during HS1 (e.g., Gherardi et al., 2009; Hall et al., 2011; Manabe and Stouffer, 1995; Robinson et al., 2005a; Rooth, 1982; Thornalley et al., 2010, 2011a,b; Vidal et al., 1997). The 'chemical divide' at ~2500 m depth persisted during HS1 in the Atlantic basin (Oppo and Curry, 2012; Robinson et al., 2005a), but the vertical $^{14}C/C$ gradient in the Southern Ocean collapsed (**Figure 9(d)**), which implies that the Southern Ocean water column was destratified and began to mix thoroughly (Burke and Robinson, 2012). The destratification of the Southern Ocean apparently yielded a rapid supply of nutrients and biologically sequestered carbon from the deep ocean to the Southern Ocean surface, fueling a deglacial spike in productivity in at least some regions (e.g., Anderson et al., 2009a; **Figure 9(e)**) despite a decline in surface nutrient drawdown (e.g., Francois et al., 1997; Robinson et al., 2004, 2005b; Sigman et al., 1999a,b). That is to say, the efficiency of the biological pump apparently declined in the Southern Ocean, and the release of $^{13}C/^{12}C$-depleted, formerly sequestered CO_2 from the ocean to the atmosphere is supported by a rising concentration (**Figure 9(f)**) and a declining $\delta^{13}C$ (**Figure 9(c)**; Lourantou et al., 2010) of atmospheric CO_2 during HS1.

During HS1, the northern hemisphere experienced cold stadial climate (**Figure 9(a)**), but the southern hemisphere was warming (**Figure 9(g)**), which attests to the meridional transport of heat by both ocean and atmosphere (e.g., Crowley, 1992; Vellinga and Wood, 2002). It has long been suspected that the release of freshwater from melting ice could bring to a halt the formation of deep water in the North Atlantic (Broecker et al., 1989; Kennett and Shackelton, 1975; Rooth, 1982), which reduces ocean heat transport to the north, thereby promoting greater sea ice cover in the North Atlantic and longer seasonal snow cover on the northern hemisphere continents. Under these conditions, monsoonal winds may weaken and the global wind belts may shift southward (e.g., Barnett et al., 1988; Chiang et al., 2003). These wind changes appear to have occurred across the globe during HS1 and previous Heinrich events (e.g., Cheng et al., 2009; Lamy et al., 2007; Lea et al., 2003; Peterson et al., 2000; Wang et al., 2001, 2007, 2008). The shifting of southern hemisphere westerly winds has been suggested to explain the atmospheric CO_2 rise by increasing Southern Ocean overturning (Barker et al., 2009; Broecker, 2006; Toggweiler, 2009; Toggweiler and Samuels, 1995; Toggweiler et al., 2006). If so, the wind-driven upwelling changes must also have increased Antarctic ventilation of the deep ocean (De Boer et al., 2008). Beyond changes in the southern hemisphere westerly winds, alternative and/or complementary physical mechanisms operating through deep-ocean density (Broecker, 1998; Sigman et al., 2007) or changes in the Southern Ocean sea ice dynamics (Keeling and Stephens, 2001) have been invoked to explain the 'bipolar seesaw' of stadial climate in the northern hemisphere and warming in the southern hemisphere during the HS1 CO_2 rise.

At the onset of the Bølling–Allerød (B/A) interstadial, NADW formation reinitiated so as to fill the deep North Atlantic from the North Atlantic surface (Elliot et al., 2002; Gherardi et al., 2009; McManus et al., 2004; Robinson et al., 2005a; Thornalley et al., 2010, 2011a,b). The northward transport of heat associated with NADW formation warmed the northern hemisphere (**Figure 9(a)**), whereas the southern hemisphere experienced either no substantial warming or even a reversal toward colder climate (**Figure 9(g)**). The rise of atmospheric CO_2 halted during B/A (**Figure 9(f)**) and the $\delta^{13}C$ of atmospheric CO_2 increased, suggesting that the ocean carbon release stalled (**Figure 9(c)**). At the end of B/A, however, meltwater apparently once again freshened the North Atlantic surface (e.g., Thornalley et al., 2011b) and North Atlantic overturning slowed and shoaled (**Figure 9(b)**; Gherardi et al., 2009; Robinson et al., 2005a; Thornalley et al., 2011a), giving rise to cold (stadial) northern hemisphere climate and rising temperatures in the southern hemisphere during the YD (**Figure 9(a)** and **9(g)**). In many ways, the YD is very similar to HS1, including changing winds (e.g., Wang et al., 2008), spikes in Southern Ocean productivity (Anderson et al., 2009a; **Figure 9(e)**), rising atmospheric CO_2 (**Figure 9(f)**), and declining atmospheric $\delta^{13}C$ (**Figure 9(c)**). The YD, like HS1, ended abruptly to give rise to the current Holocene interglacial, with high CO_2 and warm climate in both hemispheres.

While significant deviations from the above deglacial narrative may arise from other data, our understanding of the last deglaciation is arguably advanced relative to our view of glaciation. A large body of work demonstrates that, due to coupled changes in ocean circulation and biological activity, the biological pump became less efficient during deglaciation, thereby releasing CO_2 to the atmosphere. However, the specific physical mechanisms for this sequence of events remain unclear. If these can be resolved, we may come to understand the converse problem: why, in the first place, the efficiency of the biological pump rises into ice ages.

References

Abelmann A, Gersonde R, Cortese G, Kuhn G, and Smetacek V (2006) Extensive phytoplankton blooms in the Atlantic sector of the glacial Southern Ocean. *Paleoceanography* 21(1): PA1013.

Adkins JF and Boyle EA (1997) Changing atmospheric $\Delta^{14}C$ and the record of deep water paleoventilation ages. *Paleoceanography* 12(3): 337–344.

Adkins JF, McIntyre K, and Schrag DP (2002) The salinity, temperature, and $\delta^{18}O$ of the glacial deep ocean. *Science* 298(5599): 1769–1773.

Adkins JF and Schrag DP (2001) Pore fluid constraints on deep ocean temperature and salinity during the Last Glacial Maximum. *Geophysical Research Letters* 28(5): 771–774.

Ahn J and Brook EJ (2007) Atmospheric CO_2 and climate from 65 to 30 ka BP. *Geophysical Research Letters* 34(10).

Ahn J and Brook EJ (2008) Atmospheric CO_2 and climate on millennial time scales during the last glacial period. *Science* 322(5898): 83–85.

Albarede F and Goldstein SL (1992) World map of Nd isotopes in sea-floor ferromanganese deposits. *Geology* 20(8): 761–763.

Albarede F, Goldstein SL, and Dautel D (1997) The neodymium isotopic composition of manganese nodules from the Southern and Indian oceans, the global oceanic neodymium budget, and their bearing on deep ocean circulation. *Geochimica et Cosmochimica Acta* 61(6): 1277–1291.

Allen KA, Honisch B, Eggins SM, Yu JM, Spero HJ, and Elderfield H (2011a) Controls on boron incorporation in cultured tests of the planktic foraminifer *Orbulina universa*. *Earth and Planetary Science Letters* 309(3–4): 291–301.

Allen CS, Pike J, and Pudsey CJ (2011b) Last glacial-interglacial sea-ice cover in the SW Atlantic and its potential role in global deglaciation. *Quaternary Science Reviews* 30(19–20): 2446–2458.
Altabet MA and Francois R (1994a) Sedimentary nitrogen isotopic ratio as a recorder for surface ocean nitrate utilization. *Global Biogeochemical Cycles* 8(1): 103–116.
Altabet MA and Francois R (1994b) The use of nitrogen isotopic ratio for reconstruction of past surface ocean nutrient utilization. In: Zahn R, Kaminski M, Laybeyrie L, and Pederson TF (eds.) *Carbon Cycling in the Glacial Ocean: Constraints on the Ocean's Role in Global Change*, pp. 281–306. Berlin, Heidelberg, New York: Springer.
Altabet MA, Francois R, Murray DW, and Prell WL (1995) Climate related variations in denitrification in the Arabian Sea from sediment $^{15}N/^{14}N$ ratios. *Nature* 373(6514): 506–509.
Altabet MA, Murray DW, and Prell WL (1999a) Climatically linked oscillations in Arabian Sea denitrification over the past 1 m.y.: Implications for the marine N cycle. *Paleoceanography* 14(6): 732–743.
Altabet MA, Pilskaln C, Thunell R, et al. (1999b) The nitrogen isotope biogeochemistry of sinking particles from the margin of the Eastern North Pacific. *Deep Sea Research Part I: Oceanographic Research Papers* 46(4): 655–679.
Anderson RF (1987) Redox behavior of uranium in an anoxic marine basin. *Uranium* 3(2–4): 145–164.
Anderson RF, Ali S, Bradtmiller LI, et al. (2009a) Wind-driven upwelling in the Southern Ocean and the deglacial rise in atmospheric CO_2. *Science* 323(5920): 1443–1448.
Anderson RF, Bacon MP, and Brewer PG (1983) Removal of ^{230}Th and ^{231}Pa at ocean margins. *Earth and Planetary Science Letters* 66(1–3): 73–90.
Anderson RF, Chase Z, Fleisher MQ, and Sachs J (2002) The Southern Ocean's biological pump during the Last Glacial Maximum. *Deep Sea Research Part II: Topical Studies in Oceanography* 49(9–10): 1909–1938.
Anderson RF, Lao Y, and Fleisher MQ (2009b) Sedimentary $^{231}Pa/^{230}Th$ ratios are not a proxy for Atlantic meridional overturning circulation. *Geochimica et Cosmochimica Acta* 73(13): A40.
Anderson RF, Lehuray AP, Fleisher MQ, and Murray JW (1989) Uranium deposition in Saanich Inlet sediments, Vancouver Island. *Geochimica et Cosmochimica Acta* 53(9): 2205–2213.
Anderson LA and Sarmiento JL (1994) Redfield ratios of remineralization determined by nutrient data-analysis. *Global Biogeochemical Cycles* 8(1): 65–80.
Archer D (1991) Modeling the calcite lysocline. *Journal of Geophysical Research* 96(C9): 17037–17050.
Archer D, Emerson S, and Reimers C (1989) Dissolution of calcite in deep-sea sediments – pH and O_2 microelectrode results. *Geochimica et Cosmochimica Acta* 53(11): 2831–2845.
Archer DE, Eshel G, Winguth A, et al. (2000) Atmospheric pCO_2 sensitivity to the biological pump in the ocean. *Global Biogeochemical Cycles* 14(4): 1219–1230.
Archer D and Maier-Reimer E (1994) Effect of deep-sea sedimentary calcite preservation on atmospheric CO_2 concentration. *Nature* 367: 260–263.
Armstrong RA, Lee C, Hedges JI, Honjo S, and Wakeham SG (2002) A new, mechanistic model for organic carbon fluxes in the ocean based on the quantitative association of POC with ballast minerals. *Deep Sea Research Part II: Topical Studies in Oceanography* 49(1–3): 219–236.
Bacon MP (1984) Glacial to interglacial changes in carbonate and clay sedimentation in the Atlantic Ocean estimated from ^{230}Th measurements. *Isotope Geoscience* 2(2): 97–111.
Bacon MP and Anderson RF (1982) Distribution of thorium isotopes between dissolved and particulate forms in the deep sea. *Journal of Geophysical Research* 87(C3): 2045–2056.
Bacon MP and Rosholt JN (1982) Accumulation rates of ^{230}Th, ^{231}Pa and some transition metals on the Bermuda Rise. *Geochimica et Cosmochimica Acta* 46(4): 651–666.
Bains S, Norris RD, Corfield RM, and Faul KL (2000) Termination of global warmth at the Palaeocene/Eocene boundary through productivity feedback. *Nature* 407(6801): 171–174.
Bareille G, Labracherie M, Mortlock RA, Maier-Reimer E, and Froelich PN (1998) A test of $Ge/Si_{(opal)}$ as a paleorecorder of $Ge/Si_{(seawater)}$. *Geology* 26(2): 179–182.
Barker S, Diz P, Vautravers MJ, et al. (2009) Interhemispheric Atlantic seesaw response during the last deglaciation. *Nature* 457(7233): 1097–1102.
Barker S, Knorr G, Edwards RL, et al. (2011) 800,000 years of abrupt climate variability. *Science* 334: 347–351.
Barnett TP, Dumenil L, Schlese U, and Roeckner E (1988) The effect of Eurasian snow cover on global climate. *Science* 239: 504–507.
Barnola JM, Pimienta P, Raynaud D, and Korotkevich YS (1991) CO_2-climate relationship as deduced from the Vostok ice core – A reexamination based on new measurements and on a re-evaluation of the air dating. *Tellus Series B: Chemical and Physical Meteorology* 43(2): 83–90.
Bauch D, Carstens J, and Wefer G (1997) Oxygen isotope composition of living *Neogloboquadrina pachyderma* (sin) in the Arctic Ocean. *Earth and Planetary Science Letters* 146(1–2): 47–58.
Bender ML (2002) Orbital tuning chronology for the Vostok climate record supported by trapped gas composition. *Earth and Planetary Science Letters* 204(1–2): 275–289.
Bender M, Sowers T, Dickson ML, et al. (1994) Climate correlations between Greenland and Antarctica during the past 100,000 years. *Nature* 372(6507): 663–666.
Bereiter B, Lüthi D, Siegrist M, Schüpbach S, Stocker TF, and Fischer H (2012) Mode change of millennial CO_2 variability during the last glacial cycle associated with a bipolar marine carbon seesaw. *Proceedings of the National Academy of Sciences of the United States of America* 109: 9755–9760.
Berelson WM (2001) The flux of particulate organic carbon into the ocean interior: A comparison of four U.S. JGOFS regional studies. *Oceanography* 14(4): 59–67.
Berger A (1978a) Long-term variations of caloric insolation resulting from the Earth's orbital elements. *Quaternary Research* 9: 139–167.
Berger A (1978b) Long-term variations of daily insolation and Quaternary climatic changes. *Journal of the Atmospheric Sciences* 35: 2362–2367.
Berger A (1988) Milankovitch theory and climate. *Reviews of Geophysics* 26(4): 624–657.
Berger WH and Lange CB (1998) Silica depletion in the thermocline of the glacial North Pacific: Corollaries and implications. *Deep Sea Research Part II: Topical Studies in Oceanography* 45(8–9): 1885–1904.
Berner W, Stauffer B, and Oeschger H (1978) Past atmospheric composition and climate, gas parameters measured on ice cores. *Nature* 276(5683): 53–55.
Beucher CP, Brzezinski MA, and Crosta X (2007) Silicic acid dynamics in the glacial sub-Antarctic: Implications for the silicic acid leakage hypothesis. *Global Biogeochemical Cycles* 21(3): GB3015.
Blunier T and Brook EJ (2001) Timing of millennial-scale climate change in Antarctica and Greenland during the last glacial period. *Science* 291(5501): 109–112.
Boiteau R, Greaves M, and Elderfield H (2012) Authigenic uranium in foraminiferal coatings: A proxy for ocean redox chemistry. *Paleoceanography* 27: PA3227.
Bolton CT, Lawrence KT, Gibbs SJ, Wilson PA, Cleaveland LC, and Herbert TD (2010) Glacial–interglacial productivity changes recorded by alkenones and microfossils in late Pliocene eastern equatorial Pacific and Atlantic upwelling zones. *Earth and Planetary Science Letters* 295(3–4): 401–411.
Bolton CT, Lawrence KT, Gibbs SJ, Wilson PA, and Herbert TD (2011) Biotic and geochemical evidence for a global latitudinal shift in ocean biogeochemistry and export productivity during the late Pliocene. *Earth and Planetary Science Letters* 308(1–2): 200–210.
Bonn WJ, Gingele FX, Grobe H, Mackensen A, and Futterer DK (1998) Palaeoproductivity at the Antarctic continental margin: Opal and barium records for the last 400 ka. *Palaeogeography, Palaeoclimatology, Palaeoecology* 139(3–4): 195–211.
Boyle EA (1988a) Vertical oceanic nutrient fractionation and glacial interglacial CO_2 cycles. *Nature* 331(6151): 55–56.
Boyle EA (1988b) The role of vertical chemical fractionation in controlling late Quaternary atmospheric carbon-dioxide. *Journal of Geophysical Research* 93(C12): 15701–15714.
Boyle EA (1988c) Cadmium chemical tracer of deepwater paleoceanography. *Paleoceanography* 3(4): 471–489.
Boyle EA and Keigwin LD (1985) Comparison of Atlantic and Pacific paleochemical records of the last 215,000 years – Changes in deep ocean circulation and chemical inventories. *Earth and Planetary Science Letters* 76(1–2): 135–150.
Boyle EA, Labeyrie L, and Duplessy JC (1995) Calcitic foraminiferal data confirmed by cadmium in aragonitic *Hoeglundina* – Application to the Last Glacial Maximum in the northern Indian Ocean. *Paleoceanography* 10(5): 881–900.
Bradtmiller LI, Anderson RF, Sachs JP, and Fleisher MQ (2010) A deeper respired carbon pool in the glacial equatorial Pacific Ocean. *Earth and Planetary Science Letters* 299(3–4): 417–425.
Broecker WS (1982a) Glacial to interglacial changes in ocean chemistry. *Progress in Oceanography* 11(2): 151–197.
Broecker WS (1982b) Ocean chemistry during glacial time. *Geochimica et Cosmochimica Acta* 46(10): 1689–1705.
Broecker WS (1998) Paleocean circulation during the last deglaciation: A bipolar seesaw? *Paleoceanography* 13(2): 119–121.
Broecker WS (2006) Abrupt climate change revisited. *Global and Planetary Change* 54: 211–215.
Broecker W (2008) Excess sediment ^{230}Th: Transport along the sea floor or enhanced water column scavenging? *Global Biogeochemical Cycles* 22(1): GB1006.
Broecker W and Barker S (2007) A 190% drop in atmosphere's $\Delta^{14}C$ during the 'Mystery Interval' (17.5 to 14.5 kyr). *Earth and Planetary Science Letters* 256(1–2): 90–99.

Broecker WS and Henderson GM (1998) The sequence of events surrounding Termination II and their implications for the cause of glacial–interglacial CO_2 changes. *Paleoceanography* 13(4): 352–364.

Broecker W, Klas M, Ragano-Beavan N, et al. (1988) Accelerator mass spectrometry radiocarbon measurements on marine carbonate samples from deep-sea cores and sediment traps. *Radiocarbon* 30(3): 261–295.

Broecker WS, Kennett JP, Flower BP, et al. (1989) Routing of meltwater from the Laurentide ice-sheet during the Younger Dryas cold episode. *Nature* 341: 318–321.

Broecker WS and Maier-Reimer E (1992) The influence of air and sea exchange on the carbon isotope distribution in the sea. *Global Biogeochemical Cycles* 6(3): 315–320.

Broecker WS, Peacock SL, Walker S, et al. (1998) How much deep water is formed in the Southern Ocean? *Journal of Geophysical Research* 103(C8): 15833–15843.

Broecker WS and Peng T-H (1987) The role of $CaCO_3$ compensation in the glacial to interglacial atmospheric CO_2 change. *Global Biogeochemical Cycles* 1: 15–29.

Broecker WS and Peng T-H (1982) *Tracers in the Sea*. Palisades, NY: Lamont-Doherty Geological Observatory.

Broecker WS and Takahashi T (1978) Relationship between lysocline depth and carbonate ion concentration. *Deep Sea Research* 25(1): 65–95.

Broecker WS and Takahashi T (1985) Sources and flow patterns of deep-ocean waters as deduced from potential temperature, salinity, and initial phosphate concentrations. *Journal of Geophysical Research* 90(C4): 6925–6939.

Brunelle BG, Sigman DM, Cook MS, et al. (2007) Evidence from diatom-bound nitrogen isotopes for subarctic Pacific stratification during the last ice age and a link to North Pacific denitrification changes. *Paleoceanography* 22(1): PA1215.

Brunelle BG, Sigman DM, Jaccard SL, et al. (2010) Glacial/interglacial changes in nutrient supply and stratification in the western subarctic North Pacific since the penultimate glacial maximum. *Quaternary Science Reviews* 29(19–20): 2579–2590.

Brzezinski MA (1985) The Si-C-N ratio of marine diatoms – Interspecific variability and the effect of some environmental variables. *Journal of Phycology* 21(3): 347–357.

Brzezinski MA, Dickson ML, Nelson DM, and Sambrotto R (2003) Ratios of Si, C and N uptake by microplankton in the Southern Ocean. *Deep Sea Research Part II: Topical Studies in Oceanography* 50(3–4): 619–633.

Brzezinski MA, Pride CJ, Franck VM, et al. (2002) A switch from $Si(OH)_4$ to NO_3^- depletion in the glacial Southern Ocean. *Geophysical Research Letters* 29(12): 1564.

Burke A and Robinson LF (2012) The Southern Ocean's role in carbon exchange during the last deglaciation. *Science* 335(6068): 557–561.

Butzin M, Prange M, and Lohmann G (2005) Radiocarbon simulations for the glacial ocean: The effects of wind stress, Southern Ocean sea ice and Heinrich events. *Earth and Planetary Science Letters* 235(1–2): 45–61.

Byrne RH, Yao WS, Klochko K, Tossell JA, and Kaufman AJ (2006) Experimental evaluation of the isotopic exchange equilibrium $^{10}B(OH)_3 + {}^{11}B(OH)_4^- = {}^{11}B(OH)_3 + {}^{10}B(OH)_4^-$ in aqueous solution. *Deep Sea Research Part I: Oceanographic Research Papers* 53(4): 684–688.

Cai W and Cowan T (2007) Trends in Southern Hemisphere circulation in IPCC AR4 models over 1950–99: Ozone depletion versus greenhouse forcing. *Journal of Climate* 20(4): 681–693.

Caissie BE, Brigham-Grette J, Lawrence KT, Herbert TD, and Cook MS (2010) Last Glacial Maximum to Holocene sea surface conditions at Umnak Plateau, Bering Sea, as inferred from diatom, alkenone, and stable isotope records. *Paleoceanography* 25: PA1206.

Cardinal D, Alleman LY, Dehairs F, Savoye N, Trull TW, and Andre L (2005) Relevance of silicon isotopes to Si-nutrient utilization and Si-source assessment in Antarctic. *Global Biogeochemical Cycles* 19(2): GB2007.

Charles CD, Wright JD, and Fairbanks RG (1993) Thermodynamic influences on the marine carbon-isotope record. *Paleoceanography* 8(6): 691–697.

Chase Z, Anderson RF, and Fleisher MQ (2001) Evidence from authigenic uranium for increased productivity of the glacial Subantarctic Ocean. *Paleoceanography* 16(5): 468–478.

Chase Z, Anderson RF, Fleisher MQ, and Kubik PW (2002) The influence of particle composition and particle flux on scavenging of Th, Pa and Be in the ocean. *Earth and Planetary Science Letters* 204(1–2): 215–229.

Chase Z, Anderson RF, Fleisher MQ, and Kubik PW (2003) Accumulation of biogenic and lithogenic material in the Pacific sector of the Southern Ocean during the past 40,000 years. *Deep Sea Research Part II: Topical Studies in Oceanography* 50(3–4): 799–832.

Chen JH, Wasserburg GJ, Von Damm KL, and Edmond JM (1986) The U-Th-Pb systematics in hot springs on the East Pacific Rise at 21° N and Guaymas-basin. *Geochimica et Cosmochimica Acta* 50(11): 2467–2479.

Cheng H, Edwards RL, Broecker WS, et al. (2009) Ice age terminations. *Science* 326(5950): 248–252.

Chiang JCH, Biasutti M, and Battisti DS (2003) Sensitivity of the Atlantic Intertropical Convergence Zone to Last Glacial Maximum boundary conditions. *Paleoceanography* 18(4): 1094.

Chung SN, Lee K, Feely RA, et al. (2003) Calcium carbonate budget in the Atlantic Ocean based on water column inorganic carbon chemistry. *Global Biogeochemical Cycles* 17(4): 16.

Clark PU, Dyke AS, Shakun JD, et al. (2009) The Last Glacial Maximum. *Science* 325(5941): 710–714.

Cleaveland LC and Herbert TD (2009) Preservation of the alkenone paleotemperature proxy in uplifted marine sequences: A test from the Vrica outcrop, Crotone, Italy. *Geology* 37(2): 179–182.

CLIMAP Project Members (1981) Seasonal reconstruction of the Earth's surface at the Last Glacial Maximum. In: *Map and Chart Series MC-36*, NOAA/NCDC Paleoclimatology Program, Geological Society of America.

Collins LG, Pike J, Allen CS, and Hodgson DA (2012) High-resolution reconstruction of southwest Atlantic sea-ice and its role in the carbon cycle during marine isotope stages 3 and 2. Paleoceanography 27: PA3217.

Conte MH, Thompson A, and Eglinton G (1994a) Primary production of lipid biomarker compounds by *Emiliania huxleyi*. Results from an experimental mesocosm study in fjords of southwestern Norway. *Sarsia* 79: 319–331.

Conte MH, Volkman JK, and Eglinton G (1994b) Lipid biomarkers of the Haptophyta. In: Green JC and Leadbeater BSC (eds.) *The Haptophyte Algae, Systematics Association Special Volume Series*. No. 51.: pp. 351–377. Oxford: Clarendon Press.

Crosta X and Shemesh A (2002) Reconciling down core anticorrelation of diatom carbon and nitrogen isotopic ratios from the Southern Ocean. *Paleoceanography* 17(1): 1010.

Crosta X, Sturm A, Armand L, and Pichon JJ (2004) Late Quaternary sea ice history in the Indian sector of the Southern Ocean as recorded by diatom assemblages. *Marine Micropaleontology* 50(3–4): 209–223.

Crowley TJ (1992) North Atlantic Deep Water cools the southern hemisphere. *Paleoceanography* 7(4): 489–497.

Crusius J, Calvert S, Pedersen T, and Sage D (1996) Rhenium and molybdenum enrichments in sediments as indicators of oxic, suboxic and sulfidic conditions of deposition. *Earth and Planetary Science Letters* 145(1–4): 65–78.

Crusius J and Thomson J (2000) Comparative behavior of authigenic Re, U, and Mo during reoxidation and subsequent long-term burial in marine sediments. *Geochimica et Cosmochimica Acta* 64(13): 2233–2242.

Curry WB, Duplessy JC, Labeyrie LD, and Shackleton NJ (1988) Changes in the distribution of $\delta^{13}C$ of deep water ΣCO_2 between the last glaciation and the Holocene. *Paleoceanography* 3: 317–342.

Curry WB and Oppo DW (2005) Glacial water mass geometry and the distribution of $\delta^{13}C$ of ΣCO_2 in the western Atlantic Ocean. *Paleoceanography* 20: PA1017.

Dansgaar W and Tauber H (1969) Glacier oxygen-18 content and Pleistocene ocean temperatures. *Science* 166(3904): 499–502.

De Boer AM, Toggweiler JR, and Sigman DM (2008) Atlantic dominance of the meridional overturning circulation. *Journal of Physical Oceanography* 38: 435–450.

De La Rocha CL (2006) Opal-based isotopic proxies of paleoenvironmental conditions. *Global Biogeochemical Cycles* 20(4): GB4S09.

De La Rocha CL, Brzezinski MA, and DeNiro MJ (1997) Fractionation of silicon isotopes by marine diatoms during biogenic silica formation. *Geochimica et Cosmochimica Acta* 61(23): 5051–5056.

De La Rocha CL, Brzezinski MA, DeNiro MJ, and Shemesh A (1998) Silicon-isotope composition of diatoms as an indicator of past oceanic change. *Nature* 395(6703): 680–683.

De Pol-Holz R, Keigwin L, Southon J, Hebbeln D, and Mohtadi M (2010) No signature of abyssal carbon in intermediate waters off Chile during deglaciation. *Nature Geoscience* 3: 192–195.

De Pol-Holz R, Robinson RS, Hebbeln D, Sigman DM, and Ulloa O (2009) Controls on sedimentary nitrogen isotopes along the Chile margin. *Deep Sea Research Part II: Topical Studies in Oceanography* 56(16): 1100–1112.

De Pol-Holz R, Ulloa O, Dezileau L, Kaiser J, Lamy F, and Hebbeln D (2006) Melting of the Patagonian Ice Sheet and deglacial perturbations of the nitrogen cycle in the eastern South Pacific. *Geophysical Research Letters* 33(4): L04704.

De Pol-Holz R, Ulloa O, Lamy F, Dezileau L, Sabatier P, and Hebbeln D (2007) Late Quaternary variability of sedimentary nitrogen isotopes in the eastern South Pacific Ocean. *Paleoceanography* 22(2).

Dean WE, Gardner JV, and Piper DZ (1997) Inorganic geochemical indicators of glacial–interglacial changes in productivity and anoxia on the California continental margin. *Geochimica et Cosmochimica Acta* 61(21): 4507–4518.

Dehairs F, Chesselet R, and Jedwab J (1980) Discrete suspended particles of barite and the barium cycle in the open ocean. *Earth and Planetary Science Letters* 49(2): 528–550.

Dehairs F, Stroobants N, and Goeyens L (1991) Suspended barite as a tracer of biological activity in the Southern Ocean. *Marine Chemistry* 35: 399–410.

Delmas RJ, Ascencio JM, and Legrand M (1980) Polar ice evidence that atmospheric CO_2 20,000-yr BP was 50 percent of present. *Nature* 284(5752): 155–157.
Demarest MS, Brzezinski MA, and Beucher CP (2009) Fractionation of silicon isotopes during biogenic silica dissolution. *Geochimica et Cosmochimica Acta* 73: 5572–5583.
DeMaster DJ (2002) The accumulation and cycling of biogenic silica in the Southern Ocean: Revisiting the marine silica budget. *Deep Sea Research Part II: Topical Studies in Oceanography* 49(16): 3155–3167.
Deutsch C, Sarmiento JL, Sigman DM, Gruber N, and Dunne JP (2007) Spatial coupling of nitrogen inputs and losses in the ocean. *Nature* 445(7124): 163–167.
Deutsch C and Weber T (2012) Nutrient ratios as a tracer and driver of Ocean biogeochemistry. *Annual Review of Marine Science* 4: 113–141.
DeVries T and Primeau F (2011) Dynamically and observationally constrained estimates of water-mass distributions and ages in the Global Ocean. *Journal of Physical Oceanography* 41(12): 2381–2401.
DeVries T, Primeau F, and Deutsch C (2012) The sequestration efficiency of the biological pump. *Geophysical Research Letters* 39: L13601.
DiFiore PJ, Sigman DM, and Dunbar RB (2009) Upper ocean nitrogen fluxes in the Polar Antarctic Zone: Constraints from the nitrogen and oxygen isotopes of nitrate. *Geochemistry, Geophysics, Geosystems* 10: Q11016.
DiFiore PJ, Sigman DM, Karsh KL, Trull TW, Dunbar RB, and Robinson RS (2010) Poleward decrease in the isotope effect of nitrate assimilation across the Southern Ocean. *Geophysical Research Letters* 37: L17601.
DiFiore PJ, Sigman DM, Trull TW, et al. (2006) Nitrogen isotope constraints on subantarctic biogeochemistry. *Journal of Geophysical Research* 111: C08016.
Duplessy JC, Arnold M, Bard E, Juilletleclerc A, Kallel N, and Labeyrie L (1989) AMS ^{14}C study of transient events and of the ventilation rate of the Pacific intermediate water during the last deglaciation. *Radiocarbon* 31(3): 493–502.
Duplessy JC, Bard E, Arnold M, Shackleton NJ, Duprat J, and Labeyrie L (1991) How fast did the Ocean-Atmosphere system run during the last deglaciation. *Earth and Planetary Science Letters* 103(1–4): 27–40.
Duplessy JC, Shackleton NJ, Fairbanks RG, Labeyrie L, Oppo D, and Kallel N (1988) Deepwater source variations during the last climatic cycle and their impact on the global deepwater circulation. *Paleoceanography* 3(3): 343–360.
Duplessy JC, Shackleton NJ, Matthews RK, et al. (1984) ^{13}C record of benthic foraminifera in the last interglacial ocean: Implications for the carbon cycle and the global deep water circulation. *Quaternary Research* 21(2): 225–243.
Dymond J, Suess E, and Lyle M (1992) Barium in deep-sea sediment: A geochemical proxy for paleoproductivity. *Paleoceanography* 7(2): 163–181.
Dymond J and Collier R (1996) Particulate barium fluxes and their relationships to biological productivity. *Deep Sea Research Part II: Topical Studies in Oceanography* 43(4–6): 1283–1308.
Eagle M, Paytan A, Arrigo KR, van Dijken G, and Murray RW (2003) A comparison between excess barium and barite as indicators of carbon export. *Paleoceanography* 18(1): 13.
Egge JK and Aksnes DL (1992) Silicate as regulating nutrient in phytoplankton competition. *Marine Ecology Progress Series* 83(2–3): 281–289.
Elderfield H and Ganssen G (2000) Past temperature and $\delta^{18}O$ of surface ocean waters inferred from foraminiferal Mg/Ca ratios. *Nature* 405(6785): 442–445.
Elderfield H and Rickaby REM (2000) Oceanic Cd/P ratio and nutrient utilization in the glacial Southern Ocean. *Nature* 405(6784): 305–310.
Elliot M, Labeyrie L, and Duplessy JC (2002) Changes in North Atlantic deep-water formation associated with the Dansgaard–Oeschger temperature oscillations (60–10 ka). *Quaternary Science Reviews* 21(10): 1153–1165.
Elsig J, Schmitt J, Leuenberger D, et al. (2009) Stable isotope constraints on Holocene carbon cycle changes from an Antarctic ice core. *Nature* 461(7263): 507–510.
Emerson SR and Archer D (1990) Calcium carbonate preservation in the ocean. *Philosophical Transactions of the Royal Society, Series A* 331(1616): 29–40.
Emerson S and Bender M (1981) Carbon fluxes at the sediment–water interface of the deep sea – Calcium carbonate preservation. *Journal of Marine Research* 39(1): 139–162.
EPICA Community Members (2004) Eight glacial cycles from an Antarctic ice core. *Nature* 429(6992): 623–628.
Fairbanks RG and Matthews RK (1978) Marine oxygen isotope record in Pleistocene coral, Barbados, West-Indies. *Quaternary Research* 10(2): 181–196.
Fairbanks RG, Mortlock RA, Chiu TC, et al. (2005) Radiocarbon calibration curve spanning 0 to 50,000 years BP based on paired $^{230}Th/^{234}U/^{238}U$ and ^{14}C dates on pristine corals. *Quaternary Science Reviews* 24(16–17): 1781–1796.
Feely RA, Sabine CL, Lee K, et al. (2002) In situ calcium carbonate dissolution in the Pacific Ocean. *Global Biogeochemical Cycles* 16(4): 1144.
Fischer H, Schmitt J, Luthi D, et al. (2010) The role of Southern Ocean processes in orbital and millennial CO_2 variations – A synthesis. *Quaternary Science Reviews* 29(1–2): 193–205.
Fischer G and Wefer G (eds.) (1999) *Use of Proxies in Paleoceanography: Examples from the South Atlantic*. Berlin: Springer.
Foster GL (2008) Seawater pH, pCO_2 and CO_3^{2-} variations in the Caribbean Sea over the last 130 kyr: A boron isotope and B/Ca study of planktic forminifera. *Earth and Planetary Science Letters* 271(1–4): 254–266.
Francey RJ, Allison CE, Etheridge DM, et al. (1999) A 1000-year high precision record of $\delta^{13}C$ in atmospheric CO_2. *Tellus Series B: Chemical and Physical Meteorology* 51(2): 170–193.
Francois R, Altabet MA, Yu EF, et al. (1997) Contribution of Southern Ocean surface-water stratification to low atmospheric CO_2 concentrations during the last glacial period. *Nature* 389(6654): 929–935.
Francois R, Bacon MP, and Suman DO (1990) Thorium 230 profiling in deep-sea sediments: High-resolution records of flux and dissolution of carbonate in the equatorial Atlantic during the last 24,000 years. *Paleoceanography* 5(5): 761–787.
Francois R, Frank M, van der Loeff MMR, and Bacon MP (2004) ^{230}Th normalization: An essential tool for interpreting sedimentary fluxes during the late Quaternary. *Paleoceanography* 19(1): PA1018.
Francois R, Honjo S, Manganini SJ, and Ravizza GE (1995) Biogenic barium fluxes to the deep sea: Implications for paleoproductivity reconstructions. *Global Biogeochemical Cycles* 9(2): 289–303.
Frank M, Gersonde R, van der Loeff MR, et al. (2000) Similar glacial and interglacial export bioproductivity in the Atlantic sector of the Southern Ocean: Multiproxy evidence and implications for glacial atmospheric CO_2. *Paleoceanography* 15(6): 642–658.
Frank M, Schwarz B, Baumann S, Kubik PW, Suter M, and Mangini A (1997) A 200 kyr record of cosmogenic radionuclide production rate and geomagnetic field intensity from ^{10}Be in globally stacked deep-sea sediments. *Earth and Planetary Science Letters* 149(1–4): 121–129.
Frew RD and Hunter KA (1992) Influence of Southern Ocean waters on the cadmium phosphate properties of the global ocean. *Nature* 360(6400): 144–146.
Fripiat F, Cavagna A-J, Dehairs F, De Brauwere A, André L, and Cardinal D (2011a) Processes controlling the Si-isotopic composition in the Southern Ocean and application for paleoceanography. *Biogeosciences Discussions* 8(5): 10155–10185.
Fripiat F, Cavagna AJ, Dehairs F, Speich S, Andre L, and Cardinal D (2011b) Silicon pool dynamics and biogenic silica export in the Southern Ocean inferred from Si-isotopes. *Ocean Science* 7(5): 533–547.
Froelich PN and Andreae MO (1981) The marine geochemistry of germanium: Ekasilicon. *Science* 213(4504): 205–207.
Galbraith ED, Jaccard SL, Pedersen TF, et al. (2007) Carbon dioxide release from the North Pacific abyss during the last deglaciation. *Nature* 449: 890–893.
Galbraith ED, Kienast M, Jaccard SL, et al. (2008a) Consistent relationship between global climate and surface nitrate utilization in the western subarctic Pacific throughout the last 500 ka. *Paleoceanography* 23: PA2212.
Galbraith ED, Kienast M, Pedersen TF, and Calvert SE (2004) Glacial-interglacial modulation of the marine nitrogen cycle by high-latitude O_2 supply to the global thermocline. *Paleoceanography* 19: PA4007.
Galbraith ED, Sigman DM, Robinson RS, and Pederson TF (2008b) Nitrogen in past marine environments. In: Capone D, Bronk D, Mulholland M, and Carpenter E (eds.) *Nitrogen in the Marine Environment*, 2nd edn., ch. 34, pp. 1497–1535. Amsterdam: Academic Press.
Ganeshram RS, Pedersen TF, Calvert SE, and Francois R (2002) Reduced nitrogen fixation in the glacial ocean inferred from changes in marine nitrogen and phosphorus inventories. *Nature* 415(6868): 156–159.
Ganeshram RS, Pedersen TF, Calvert SE, and Murray JW (1995) Large changes in ocean nutrient inventories from glacial to interglacial periods. *Nature* 376(6543): 755–758.
Garcia HE, Locarnini RA, Boyer TP, et al. (2009) World Ocean Atlas 2009: Nutrients (phosphate, nitrate, and silicate). In: Levitus S (ed.) *NOAA Atlas–ESDIS 71*. Washington, DC: US Government Printing Office.
Gebbie G and Huybers P (2010) Total matrix intercomparison: A method for determining the geometry of water-mass pathways. *Journal of Physical Oceanography* 40(8): 1710–1728.
Gebhardt H, Sarnthein M, Grootes PM, et al. (2008) Paleonutrient and productivity records from the subarctic North Pacific for Pleistocene glacial terminations I to V. *Paleoceanography* 23: PA4212.
Geibert W and Usbeck R (2004) Adsorption of thorium and protactinium onto different particle types: Experimental findings. *Geochimica et Cosmochimica Acta* 68(7): 1489–1501.
Gersonde R, Abelmann A, Brathauer U, et al. (2003) Last glacial sea surface temperatures and sea-ice extent in the Southern Ocean (Atlantic-Indian sector): A multiproxy approach. *Paleoceanography* 18(3): 1061.

Gersonde R, Crosta X, Abelmann A, and Armand L (2005) Sea-surface temperature and sea lee distribution of the Southern Ocean at the EPILOG Last Glacial Maximum – A circum-Antarctic view based on siliceous microfossil records. *Quaternary Science Reviews* 24(7–9): 869–896.

Gherardi JM, Labeyrie L, McManus JF, Francois R, Skinner LC, and Cortijo E (2005) Evidence from the Northeastern Atlantic basin for variability in the rate of the meridional overturning circulation through the last deglaciation. *Earth and Planetary Science Letters* 240(3–4): 710–723.

Gherardi JM, Labeyrie L, Nave S, Francois R, McManus JF, and Cortijo E (2009) Glacial–interglacial circulation changes inferred from $^{231}Pa/^{230}Th$ sedimentary record in the North Atlantic region. *Paleoceanography* 24: PA2204.

Gingele FX, Abel M, Kasten S, Bonn WJ, and Nürnberg CC (1999) Biogenic barium as a proxy for paleoproductivity: Methods and limitations of application. In: Fischer G and Wefer G (eds.) *Use of Proxies in Paleoceanography: Examples from the South Atlantic*, pp. 345–364. Berlin: Springer.

Granger J, Sigman DM, Rohde MM, Maldonado MT, and Tortell PD (2010) N and O isotope effects during nitrate assimilation by unicellular prokaryotic and eukaryotic plankton cultures. *Geochimica et Cosmochimica Acta* 74(3): 1030–1040.

Grootes PM and Stuiver M (1997) Oxygen 18/16 variability in Greenland snow and ice with 10^{-3}- to 10^{5}-year time resolution. *Journal of Geophysical Research* 102(C12): 26455–26470.

Hain MP, Sigman DM, and Haug GH (2010) Carbon dioxide effects of Antarctic stratification, North Atlantic Intermediate Water formation, and subantarctic nutrient drawdown during the last ice age: Diagnosis and synthesis in a geochemical box model. *Global Biogeochemical Cycles* 24: GB4023.

Hain MP, Sigman DM, and Haug GH (2011) Shortcomings of the isolated abyssal reservoir model for deglacial radiocarbon changes in the mid-depth Indo-Pacific Ocean. *Geophysical Research Letters* 38: L04604.

Hall IR, Evans HK, and Thornalley DJR (2011) Deep water flow speed and surface ocean changes in the subtropical North Atlantic during the last deglaciation. *Global and Planetary Change* 79(3–4): 255–263.

Hastings DW, Emerson SR, and Mix AC (1996) Vanadium in foraminiferal calcite as a tracer for changes in the areal extent of reducing sediments. *Paleoceanography* 11(6): 665–678.

Haug GH, Pedersen TF, Sigman DM, Calvert SE, Nielsen B, and Peterson LC (1998) Glacial/interglacial variations in production and nitrogen fixation in the Cariaco Basin during the last 580 kyr. *Paleoceanography* 13(5): 427–432.

Haug GH and Sigman DM (2009) Polar twins. *Nature Geoscience* 2(2): 91–92.

Haug GH, Ganopolski A, Sigman DM, et al. (2005) North Pacific seasonality and the glaciation of North America 2.7 million years ago. *Nature* 433(7028): 821–825.

Hays JD, Imbrie J, and Shackleton NJ (1976) Variations in Earth's orbit – Pacemakers of ice ages. *Science* 194(4270): 1121–1132.

Headly MA and Severinghaus JP (2007) A method to measure Kr/N_2 ratios in air bubbles trapped in ice cores and its application in reconstructing past mean ocean temperature. *Journal of Geophysical Research* 112: D19105.

Heinrich H (1988) Origin and consequences of cyclic ice rafting in the northeast Atlantic-Ocean during the past 130,000 years. *Quaternary Research* 29(2): 142–152.

Hemming NG and Hanson GN (1992) Boron isotopic composition and concentration in modern marine carbonates. *Geochimica et Cosmochimica Acta* 56(1): 537–543.

Hemming NG, Reeder RJ, and Hanson GN (1995) Mineral-fluid partitioning and isotopic fractionation of boron in synthetic calcium carbonate. *Geochimica et Cosmochimica Acta* 59(2): 371–379.

Henderson GM and Anderson RF (2003) The U-series toolbox for paleoceanography. *Uranium-Series Geochemistry* 52: 493–531.

Henderson GM, Heinze C, Anderson RF, and Winguth AME (1999) Global distribution of the ^{230}Th flux to ocean sediments constrained by GCM modelling. *Deep Sea Research Part I: Oceanographic Research Papers* 46(11): 1861–1893.

Henderson GM, Anderson R, Adkins J, et al. (2007) GEOTRACES – An international study of the global marine biogeochemical cycles of trace elements and their isotopes. *Chemie der Erde – Geochemistry* 67(2): 85–131.

Hendry KR, Georg RB, Rickaby REM, Robinson LF, and Halliday AN (2010) Deep ocean nutrients during the Last Glacial Maximum deduced from sponge silicon isotopic compositions. *Earth and Planetary Science Letters* 292: 290–300.

Hendry KR, Leng MJ, Robinson LF, et al. (2011) Silicon isotopes in Antarctic sponges: An interlaboratory comparison. *Antarctic Science* 23(1): 34–42.

Henson SA, Sanders R, and Madsen E (2012) Global patterns in efficiency of particulate organic carbon export and transfer to the deep ocean. *Global Biogeochemical Cycles* 26: GB1028.

Herguera JC (1992) Deep-sea benthic foraminifera and biogenic opal – Glacial to postglacial productivity in the western equatorial Pacific. *Marine Micropaleontology* 19(1–2): 79–98.

Herguera JC, Jansen E, and Berger WH (1992) Evidence for a bathyal front at 2000-m depth in the glacial Pacific, based on a depth transect on Ontong Java plateau. *Paleoceanography* 7: 273–288.

Hernandez-Sanchez MT, Mills RA, Planquette H, et al. (2011) Quantifying export production in the Southern Ocean: Implications for the Ba_{xs} proxy. *Paleoceanography* 26: PA4222.

Higgins SM, Anderson RF, Marcantonio F, Schlosser P, and Stute M (2002) Sediment focusing creates 100-ka cycles in interplanetary dust accumulation on the Ontong Java Plateau. *Earth and Planetary Science Letters* 203(1): 383–397.

Higgins MB, Robinson RS, Carter SJ, and Pearson A (2010) Evidence from chlorin nitrogen isotopes for alternating nutrient regimes in the Eastern Mediterranean Sea. *Earth and Planetary Science Letters* 290(1–2): 102–107.

Higgins MB, Robinson RS, Casciotti KL, McIlvin MR, and Pearson A (2009) A method for determining the nitrogen isotopic composition of porphyrins. *Analytical Chemistry* 81(1): 184–192.

Hinrichs KU, Schneider RR, Muller PJ, and Rullkotter J (1999) A biomarker perspective on paleoproductivity variations in two Late Quaternary sediment sections from the Southeast Atlantic Ocean. *Organic Geochemistry* 30(5): 341–366.

Hodell DA, Gersonde R, and Blum P (2002) Leg 177 synthesis: Insights into Southern Ocean paleoceanography on tectonic to millennial timescales. *Proceedings of the Ocean Drilling Program, Scientific Results* 177: 1–54.

Hodell DA, Venz KA, Charles CD, and Ninnemann US (2003) Pleistocene vertical carbon isotope and carbonate gradients in the South Atlantic sector of the Southern Ocean. *Geochemistry, Geophysics, Geosystems* 4: 1004.

Hofmann M, Broecker WS, and Lynch-Stieglitz J (1999) Influence of a CO_2(aq) dependent biological C-isotope fractionation on glacial $^{13}C/^{12}C$ ratios in the ocean. *Global Biogeochemical Cycles* 13(4): 873–883.

Holmen K (1992) The global carbon cycle. *International Geophysics Series: Global Biogeochemical Cycles* 50: 239–262.

Honisch B, Bijma J, Russell AD, et al. (2003) The influence of symbiont photosynthesis on the boron isotopic composition of foraminifera shells. *Marine Micropaleontology* 49(1–2): 87–96.

Honisch B and Hemming NG (2004) Ground-truthing the boron isotope-paleo-pH proxy in planktonic foraminifera shells: Partial dissolution and shell size effects. *Paleoceanography* 19: PA4010.

Honisch B, Hemming NG, Grottoli AG, Amat A, Hanson GN, and Buma J (2004) Assessing scleractinian corals as recorders for paleo-pH: Empirical calibration and vital effects. *Geochimica et Cosmochimica Acta* 68(18): 3675–3685.

Honisch B, Hemming NG, and Loose B (2007) Comment on "A critical evaluation of the boron isotope-pH proxy: The accuracy of ancient ocean pH estimates" by M. Pagani, D. Lemarchand, A. Spivack J Gaillardet. *Geochimica et Cosmochimica Acta* 71(6): 1636–1641.

Huybers P (2007) Glacial variability over the last two million years: An extended depth-derived agemodel, continuous obliquity pacing, and the Pleistocene progression. *Quaternary Science Reviews* 26(1–2): 37–55.

Huybers P (2011) Combined obliquity and precession pacing of late Pleistocene deglaciations. *Nature* 480(7376): 229–232.

Huybers P and Wunsch C (2005) Obliquity pacing of the late Pleistocene glacial terminations. *Nature* 434(7032): 491–494.

Indermühle A, Monnin E, Stauffer B, Stocker TF, and Wahlen M (2000) Atmospheric CO_2 concentration from 60 to 20 kyr BP from the Taylor Dome ice core, Antarctica. *Geophysical Research Letters* 27(5): 735–738.

Indermühle A, Stocker TF, Joos F, et al. (1999) Holocene carbon-cycle dynamics based on CO_2 trapped in ice at Taylor Dome, Antarctica. *Nature* 398(6723): 121–126.

Ito T and Follows MJ (2005) Preformed phosphate, soft tissue pump and atmospheric CO_2. *Journal of Marine Research* 63(4): 813–839.

Iudicone D, Speich S, Madec G, and Blanke B (2008) The global conveyor belt from a Southern Ocean perspective. *Journal of Physical Oceanography* 38(7): 1401–1425.

Jaccard SL and Galbraith ED (2012) Large climate-driven changes of oceanic oxygen concentrations during the last deglaciation. *Nature Geoscience* 5(2): 151–156.

Jaccard SL, Galbraith ED, Sigman DM, et al. (2009) Subarctic Pacific evidence for a glacial deepening of the oceanic respired carbon pool. *Earth and Planetary Science Letters* 277(1–2): 156–165.

Jaccard SL, Haug GH, Sigman DM, Pedersen TF, Thierstein HR, and Rohl U (2005) Glacial/interglacial changes in subarctic North Pacific stratification. *Science* 308(5724): 1003–1006.

Jahnke RA, Craven DB, and Gaillard JF (1994) The influence of organic-matter diagenesis on $CaCO_3$ dissolution at the deep-sea floor. *Geochimica et Cosmochimica Acta* 58(13): 2799–2809.

Jouzel J, Barkov NI, Barnola JM, et al. (1993) Extending the Vostok ice-core record of paleoclimate to the penultimate glacial period. *Nature* 364(6436): 407–412.

Jouzel J, Masson-Delmotte V, Cattani O, et al. (2007) Orbital and millennial Antarctic climate variability over the past 800,000 years. *Science* 317(5839): 793–796.

Kakihana H and Kotaka M (1977) Equilibrium constants for boron isotope-exchange reactions. *Bulletin of the Research Laboratory for Nuclear Reactors* 2: 1–12.
Kakihana H, Kotaka M, Satoh S, Nomura M, and Okamoto M (1977) Fundamental studies on ion-exchange separation of boron isotopes. *Bulletin of the Chemical Society of Japan* 50(1): 158–163.
Kallel N, Labeyrie LD, Juilletleclerc A, and Duplessy JC (1988) A deep hydrological front between intermediate and deep-water masses in the glacial Indian-Ocean. *Nature* 333(6174): 651–655.
Karsh KL, Trull TW, Lourey AJ, and Sigman DM (2003) Relationship of nitrogen isotope fractionation to phytoplankton size and iron availability during the Southern Ocean Iron RElease Experiment (SOIREE). *Limnology and Oceanography* 48(3): 1058–1068.
Katsuki K and Takahashi K (2005) Diatoms as paleoenvironmental proxies for seasonal productivity, sea-ice and surface circulation in the Bering Sea during the late Quaternary. *Deep Sea Research Part II: Topical Studies in Oceanography* 52(16–18): 2110–2130.
Kawamura K, Parrenin F, Lisiecki L, et al. (2007) Northern Hemisphere forcing of climatic cycles in Antarctica over the past 360,000 years. *Nature* 448(7156): 912–914.
Keeling RF and Stephens BB (2001) Antarctic sea ice and the control of Pleistocene climate instability. *Paleoceanography* 16(1): 112–131.
Keigwin LD (1998) Glacial-age hydrography of the far northwest Pacific Ocean. *Paleoceanography* 13(4): 323–339.
Keigwin LD and Boyle EA (1989) Late Quaternary paleochemistry of high-latitude surface waters. *Palaeogeography, Palaeoclimatology, Palaeoecology* 73(1–2): 85–106.
Keil RG and Cowie GL (1999) Organic matter preservation through the oxygen-deficient zone of the NE Arabian Sea as discerned by organic carbon: Mineral surface area ratios. *Marine Geology* 161(1): 13–22.
Keller K and Morel FMM (1999) A model of carbon isotopic fractionation and active carbon uptake in phytoplankton. *Marine Ecology Progress Series* 182: 295–298.
Kemp AES, Grigorov I, Pearce RB, and Garabato ACN (2010) Migration of the Antarctic Polar Front through the mid-Pleistocene transition: Evidence and climatic implications. *Quaternary Science Reviews* 29: 1993–2009.
Kennett JP and Shackleton NJ (1975) Laurentide ice sheet meltwater recorded in Gulf of Mexico deep-sea cores. *Science* 188: 147–150.
Kienast M (2000) Unchanged nitrogen isotopic composition of organic matter in the South China Sea during the last climatic cycle: Global implications. *Paleoceanography* 15(2): 244–253.
Kienast M, Higginson MJ, Mollenhauer G, Eglinton TI, Chen MT, and Calvert SE (2005) On the sedimentological origin of down-core variations of bulk sedimentary nitrogen isotope ratios. *Paleoceanography* 20(2): PA2009.
Kienast SS, Hendy IL, Crusius J, Pedersen TF, and Calvert SE (2004) Export production in the subarctic North Pacific over the last 800 kyrs: No evidence for iron fertilization? *Journal of Oceanography* 60(1): 189–203.
Klochko K, Cody GD, Tossell JA, Dera P, and Kaufman AJ (2009) Re-evaluating boron speciation in biogenic calcite and aragonite using ^{11}B MAS NMR. *Geochimica et Cosmochimica Acta* 73(7): 1890–1900.
Klochko K, Kaufman AJ, Yao WS, Byrne RH, and Tossell JA (2006) Experimental measurement of boron isotope fractionation in seawater. *Earth and Planetary Science Letters* 248(1–2): 276–285.
Knox F and McElroy MB (1984) Changes in atmospheric CO_2: Influence of the marine biota at high-latitude. *Journal of Geophysical Research* 89(D3): 4629–4637.
Kohfeld KE, Fairbanks RG, Smith SL, and Walsh ID (1996) *Neogloboquadrina pachyderma* (sinistral coiling) as paleoceanographic tracers in polar oceans: Evidence from northeast water polynya plankton tows, sediment traps, and surface sediments. *Paleoceanography* 11(6): 679–699.
Kohfeld KE, Le Quere C, Harrison SP, and Anderson RF (2005) Role of marine biology in glacial–interglacial CO_2 cycles. *Science* 308(5718): 74–78.
Kornilova O and Rosell-Mele A (2003) Application of microwave-assisted extraction to the analysis of biomarker climate proxies in marine sediments. *Organic Geochemistry* 34(11): 1517–1523.
Kretschmer S, Geibert W, van der Loeff MMR, and Mollenhauer G (2010) Grain size effects on $^{230}Th_{xs}$ inventories in opal-rich and carbonate-rich marine sediments. *Earth and Planetary Science Letters* 294(1–2): 131–142.
Kretschmer S, Geibert W, van der Loeff MMR, Schnabel C, Xu S, and Mollenhauer G (2011) Fractionation of ^{230}Th, ^{231}Pa, and ^{10}Be induced by particle size and composition within an opal-rich sediment of the Atlantic Southern Ocean. *Geochimica et Cosmochimica Acta* 75(22): 6971–6987.
Kuhlbrodt T, Griesel A, Montoya M, Levermann A, Hofmann M, and Rahmstorf S (2007) On the driving processes of the Atlantic meridional overturning circulation. *Reviews of Geophysics* 45(1): RG2001.
Kumar N, Anderson RF, Mortlock RA, et al. (1995) Increased biological productivity and export production in the glacial Southern Ocean. *Nature* 378(6558): 675–680.
Kumar N, Gwiazda R, Anderson RF, and Froelich PN (1993) ^{231}Pa /^{230}Th ratios in sediments as a proxy for past changes in Southern Ocean productivity. *Nature* 362(6415): 45–48.
Kwon EY, Hain MP, Sigman DM, Galbraith ED, Sarmiento JL, and Toggweiler JR (2012) North Atlantic ventilation of "southern-sourced" deep water in the glacial ocean, *Paleoceanography* 27: PA2208.
Kwon EY, Sarmiento JL, Toggweiler JR, and DeVries T (2011) The control of atmospheric pCO_2 by ocean ventilation change: The effect of the oceanic storage of biogenic carbon. *Global Biogeochemical Cycles* 25: GB2036.
Laj C, Kissel C, Mazaud A, Michel E, Muscheler R, and Beer J (2002) Geomagnetic field intensity, North Atlantic Deep Water circulation and atmospheric Δ^{14}C during the last 50 kyr. *Earth and Planetary Science Letters* 200(1–2): 177–190.
Lamy F, Kaiser J, Arz HW, et al. (2007) Modulation of the bipolar seesaw in the southeast pacific during Termination 1. *Earth and Planetary Science Letters* 259(3–4): 400–413.
Lawrence KT, Liu ZH, and Herbert TD (2006) Evolution of the eastern tropical Pacific through Plio–Pleistocene glaciation. *Science* 312(5770): 79–83.
Le Quere C, Rodenbeck C, Buitenhuis ET, et al. (2007) Saturation of the Southern Ocean CO_2 sink due to recent climate change. *Science* 316(5832): 1735–1738.
Lea DW, Pak DK, Peterson LC, and Hughen KA (2003) Synchroneity of tropical and high-latitude Atlantic temperatures over the last glacial termination. *Science* 301: 1361–1364.
Lea DW, Pak DK, and Spero HJ (2000) Climate impact of late quaternary equatorial Pacific sea surface temperature variations. *Science* 289(5485): 1719–1724.
Lemieux-Dudon B, Blayo E, Petit J-R, et al. (2010) Consistent dating for Antarctic and Greenland ice cores. *Quaternary Science Reviews* 29: 8–20.
Leuenberger M, Siegenthaler U, and Langway CC (1992) Carbon isotope composition of atmospheric CO_2 during the last ice-age from an Antarctic ice core. *Nature* 357(6378): 488–490.
Lisiecki LE and Raymo ME (2005) A Pliocene–Pleistocene stack of 57 globally distributed benthic δ^{18}O records. *Paleoceanography* 20(1): 17.
Liu ZH and Herbert TD (2004) High-latitude influence on the eastern equatorial Pacific climate in the early Pleistocene epoch. *Nature* 427(6976): 720–723.
Liu KK and Kaplan IR (1989) The eastern tropical Pacific as a source of ^{15}N-enriched nitrate in seawater off southern-California. *Limnology and Oceanography* 34(5): 820–830.
Liu Y and Tossell JA (2005) Ab initio molecular orbital calculations for boron isotope fractionations on boric acids and borates. *Geochimica et Cosmochimica Acta* 69(16): 3995–4006.
Lourantou A, Chappellaz J, Barnola JM, Masson-Delmotte V, and Raynaud D (2010a) Changes in atmospheric CO_2 and its carbon isotopic ratio during the penultimate deglaciation. *Quaternary Science Reviews* 29(17–18): 1983–1992.
Lourantou A, Lavric JV, Koehler P, et al. (2010b) Constraint of the CO_2 rise by new atmospheric carbon isotopic measurements during the last deglaciation. *Global Biogeochemical Cycles* 24: GB2015.
Lourey MJ, Trull TW, and Sigman DM (2003) Sensitivity of δ^{15}N of nitrate, surface suspended and deep sinking particulate nitrogen to seasonal nitrate depletion in the Southern Ocean. *Global Biogeochemical Cycles* 17(3): 1081.
Lund DC, Adkins JF, and Ferrari R (2011) Abyssal Atlantic circulation during the Last Glacial Maximum: Constraining the ratio between transport and vertical mixing. *Paleoceanography* 26: PA1213.
Lüthi D, Le Floch B, Bereiter B, et al. (2008) High-resolution carbon dioxide concentration record 650,000–800,000 years before present. *Nature* 453: 379–382.
Lyle M, Mitchell N, Pisias N, Mix A, Martinez JI, and Paytan A (2005) Do geochemical estimates of sediment focusing pass the sediment test in the equatorial Pacific? *Paleoceanography* 20(1): PA1005.
Lynch-Stieglitz J, Adkins JF, Curry WB, et al. (2007) Atlantic meridional overturning circulation during the Last Glacial Maximum. *Science* 316(5821): 66–69.
Lynch-Stieglitz J, Curry WB, and Slowey N (1999a) A geostrophic transport estimate for the Florida Current from the oxygen isotope composition of benthic foraminifera. *Paleoceanography* 14(3): 360–373.
Lynch-Stieglitz J, Curry WB, and Slowey N (1999b) Weaker Gulf Stream in the Florida Straits during the Last Glacial Maximum. *Nature* 402(6762): 644–648.
Lynch-Stieglitz J, Stocker TF, Broecker WS, and Fairbanks RG (1995) The influence of air-sea exchange on the isotopic composition of oceanic carbon – Observations and modeling. *Global Biogeochemical Cycles* 9(4): 653–665.
Mackensen A, Hubberten HW, Bickert T, Fischer G, and Futterer DK (1993) The δ^{13}C in benthic foraminiferal tests of *Fontbotia wuellerstorfi* (Schwager) relative to the δ^{13}C of dissolved inorganic carbon in Southern Ocean Deep Water: Implications for glacial ocean circulation models. *Paleoceanography* 8(5): 587–610.

Manabe S and Stouffer RJ (1995) Simulation of abrupt climate change induced by freshwater input to the North Atlantic Ocean. *Nature* 378(6553): 165–167.

Mangini A and Diester-Haass L (1983) Excess ^{230}Th in sediments off NW Africa traces upwelling in the past. In: Suess E and Thiede J (eds.) *Coastal Upwelling: Its Sediment Record. Part A: Responses of the Sedimentary Regime to Present Coastal Upwelling*, pp. 455–466. New York: Plenum.

Marcantonio F, Anderson RF, Higgins S, Stute M, Schlosser P, and Kubik P (2001) Sediment focusing in the central equatorial Pacific Ocean. *Paleoceanography* 16(3): 260–267.

Marcantonio F, Anderson RF, Stute M, Kumar N, Schlosser P, and Mix A (1996) Extraterrestrial ^{3}He as a tracer of marine sediment transport and accumulation. *Nature* 383: 705–707.

Marcantonio F, Kumar N, Stute M, et al. (1995) Comparative study of accumulation rates derived by He and Th isotope analysis of marine sediments. *Earth and Planetary Science Letters* 133(3–4): 549–555.

Marchitto TM and Broecker WS (2006) Deep water mass geometry in the glacial Atlantic Ocean: A review of constraints from the paleonutrient proxy Cd/Ca. *Geochemistry, Geophysics, Geosystems* 7: Q12003.

Marchitto TM, Curry WB, and Oppo DW (1998) Millennial-scale changes in North Atlantic circulation since the last glaciation. *Nature* 393(6685): 557–561.

Marchitto TM, Oppo DW, and Curry WB (2002) Paired benthic foraminiferal Cd/Ca and Zn/Ca evidence for a greatly increased presence of Southern Ocean Water in the glacial North Atlantic. *Paleoceanography* 17(3): 1038.

Marino BD and McElroy MB (1991) Isotopic composition of atmospheric CO_2 inferred from carbon in C4 plant cellulose. *Nature* 349(6305): 127–131.

Marinov I, Gnanadesikan A, Sarmiento JL, Toggweiler JR, Follows M, and Mignone BK (2008) Impact of oceanic circulation on biological carbon storage in the ocean and atmospheric pCO_2. *Global Biogeochemical Cycles* 22(3): GB3007.

Marinov I, Gnanadesikan A, Toggweiler JR, and Sarmiento JL (2006) The Southern Ocean biogeochemical divide. *Nature* 441(7096): 964–967.

Marlowe IT, Green JC, Neal AC, Brassell SC, Eglinton G, and Course PA (1984) Long chain (n-C_{37}–C_{39}) alkenones in the Prymnesiophyceae. Distribution of alkenones and other lipids and their taxonomic significance. *British Phycological Journal* 19(3): 203–216.

Martin JH (1990) Glacial–interglacial CO_2 change: The iron hypothesis. *Paleoceanography* 5(1): 1–13.

Martin JH, Broenkow WW, Fitzwater SE, and Gordon RM (1990a) Does iron really limit phytoplankton in the offshore Sub-Arctic Pacific – Yes, it does – A reply. *Limnology and Oceanography* 35(3): 775–777.

Martin JH, Gordon RM, and Fitzwater SE (1990b) Iron in Antarctic waters. *Nature* 345(6271): 156–158.

Martin JH, Knauer GA, Karl DM, and Broenkow WW (1987) VERTEX – Carbon cycling in the northeast Pacific. *Deep Sea Research Part A – Oceanographic Research Papers* 34(2): 267–285.

Martinez P, Bertrand P, Bouloubassi I, et al. (1996) An integrated view of inorganic and organic biogeochemical indicators of palaeoproductivity changes in a coastal upwelling area. *Organic Geochemistry* 24(4): 411–420.

Martinez-Garcia A, Rosell-Mele A, Geibert W, et al. (2009) Links between iron supply, marine productivity, sea surface temperature, and CO_2 over the last 1.1 Ma. *Paleoceanography* 24: PA1207.

Martinez-Garcia A, Rosell-Mele A, Jaccard SL, Geibert W, Sigman DM, and Haug GH (2011) Southern Ocean dust–climate coupling over the past four million years. *Nature* 476(7360): 312–315.

Mashiotta TA, Lea DW, and Spero HJ (1997) Experimental determination of cadmium uptake in shells of the planktonic foraminifera *Orbulina universa* and *Globigerina bulloides*: Implications for surface water paleoreconstructions. *Geochimica et Cosmochimica Acta* 61(19): 4053–4065.

Matsumoto K and Lynch-Stieglitz J (1999) Similar glacial and Holocene deep water circulation inferred from southeast Pacific benthic foraminiferal carbon isotope composition. *Paleoceanography* 14(2): 149–163.

Matsumoto K, Oba T, Lynch-Stieglitz J, and Yamamoto H (2002) Interior hydrography and circulation of the glacial Pacific Ocean. *Quaternary Science Reviews* 21(14–15): 1693–1704.

Matsumoto K and Sarmiento JL (2008) A corollary to the silicic acid leakage hypothesis. *Paleoceanography* 23(2): PA2203.

McClymont EL, Rosell-Mele A, Giraudeau J, Pierre C, and Lloyd JM (2005) Alkenone and coccolith records of the mid-Pleistocene in the south-east Atlantic: Implications for the $U^{K'}_{37}$ index and South African climate. *Quaternary Science Reviews* 24(14–15): 1559–1572.

McCorkle DC, Martin PA, Lea DW, and Klinkhammer GP (1995) Evidence of a dissolution effect on benthic foraminiferal shell chemistry: δ^{13}C, Cd/Ca, Ba/Ca and Sr/Ca results from the Ontong Java Plateau. *Paleoceanography* 10(4): 699–714.

McGee D, Marcantonio F, McManus JF, and Winckler G (2010) The response of excess ^{230}Th and extraterrestrial ^{3}He to sediment redistribution at the Blake Ridge, western North Atlantic. *Earth and Planetary Science Letters* 299(1–2): 138–149.

McManus J, Berelson WM, Klinkhammer GP, Hammond DE, and Holm C (2005) Authigenic uranium: Relationship to oxygen penetration depth and organic carbon rain. *Geochimica et Cosmochimica Acta* 69(1): 95–108.

McManus J, Berelson WM, Severmann S, et al. (2006) Molybdenum and uranium geochemistry in continental margin sediments: Paleoproxy potential. *Geochimica et Cosmochimica Acta* 70(18): 4643–4662.

McManus JF, Francois R, Gherardi JM, Keigwin LD, and Brown-Leger S (2004) Collapse and rapid resumption of Atlantic meridional circulation linked to deglacial climate changes. *Nature* 428(6985): 834–837.

Meckler AN, Ren H, Sigman DM, et al. (2011) Deglacial nitrogen isotope changes in the Gulf of Mexico: Evidence from bulk sedimentary and foraminifera-bound nitrogen in Orca Basin sediments. *Paleoceanography* 26: PA4216.

Mills MM and Arrigo KR (2010) Magnitude of oceanic nitrogen fixation influenced by the nutrient uptake ratio of phytoplankton. *Nature Geoscience* 3(6): 412–416.

Mix AC and Fairbanks RG (1985) North-Atlantic surface-ocean control of Pleistocene deep-ocean circulation. *Earth and Planetary Science Letters* 73(2–4): 231–243.

Monnin E, Indermühle A, Dallenbach A, et al. (2001) Atmospheric CO_2 concentrations over the last glacial termination. *Science* 291(5501): 112–114.

Montoya JP and McCarthy JJ (1995) Isotopic fractionation during nitrate uptake by phytoplankton grown in continuous culture. *Journal of Plankton Research* 17(3): 439–464.

Morel FMM (1987) Kinetics of nutrient uptake and growth in phytoplankton. *Journal of Phycology* 23(1): 137–150.

Mortlock RA, Charles CD, Froelich PN, et al. (1991) Evidence for lower productivity in the Antarctic Ocean during the last glaciation. *Nature* 351(6323): 220–223.

Mueller PJ and Suess E (1979) Productivity, sedimentation rate and sedimentary organic matter in the oceans: 1. Organic carbon preservation. *Deep Sea Research Part A. Oceanographic Research Papers* 26(12A): 1347–1362.

Muscheler R, Beer J, Wagner G, et al. (2004) Changes in the carbon cycle during the last deglaciation as indicated by the comparison of ^{10}Be and ^{14}C records. *Earth and Planetary Science Letters* 219(3–4): 325–340.

Muscheler R, Kromer B, Bjorck S, et al. (2008) Tree rings and ice cores reveal ^{14}C calibration uncertainties during the Younger Dryas. *Nature Geoscience* 1(4): 263–267.

Needoba JA and Harrison PJ (2004) Influence of low light and a light: Dark cycle on NO_3^- uptake, intracellular NO_3^-, and nitrogen isotope fractionation by marine phytoplankton. *Journal of Phycology* 40(3): 505–516.

Needoba JA, Sigman DM, and Harrison PJ (2004) The mechanism of isotope fractionation during algal nitrate assimilation as illuminated by the ^{15}N/^{14}N of intracellular nitrate. *Journal of Phycology* 40(3): 517–522.

Neftel A, Oeschger H, Schwander J, Stauffer B, and Zumbrunn R (1982) Ice core sample measurements give atmospheric CO_2 content during the past 40,000 yr. *Nature* 295(5846): 220–223.

Neftel A, Oeschger H, Staffelbach T, and Stauffer B (1988) CO_2 record in the Byrd ice core 50,000-5,000 years BP. *Nature* 331(6157): 609–611.

Negre C, Zahn R, Thomas AL, et al. (2010) Reversed flow of Atlantic deep water during the Last Glacial Maximum. *Nature* 468(7320): 84–88.

Nozaki Y, Yang HS, and Yamada M (1987) Scavenging of thorium in the ocean. *Journal of Geophysical Research* 92(C1): 772–778.

Nurnberg CC, Bohrmann G, Schluter M, and Frank M (1997) Barium accumulation in the Atlantic sector of the Southern Ocean: Results from 190,000-year records. *Paleoceanography* 12(4): 594–603.

Officer CB and Ryther JH (1980) The possible importance of silicon in marine eutrophication. *Marine Ecology Progress Series* 3(1): 83–91.

Okazaki Y, Takahashi K, Asahi H, et al. (2005a) Productivity changes in the Bering Sea during the late Quaternary. *Deep Sea Research Part II: Topical Studies in Oceanography* 52(16–18): 2150–2162.

Okazaki Y, Takahashi K, Katsuki K, et al. (2005b) Late Quaternary paleoceanographic changes in the southwestern Okhotsk Sea: Evidence from geochemical, radiolarian, and diatom records. *Deep Sea Research Part II: Topical Studies in Oceanography* 52(16–18): 2332–2350.

Oppo DW and Curry WB (2012) Deep Atlantic circulation during the Last Glacial Maximum and deglaciation. *Nature Education Knowledge* 3(10): 1.

Orsi AH, Johnson GC, and Bullister JL (1999) Circulation, mixing, and production of Antarctic Bottom Water. *Progress in Oceanography* 43(1): 55–109.

Pagani M, Lemarchand D, Spivack A, and Gaillardet J (2005) A critical evaluation of the boron isotope-pH proxy: The accuracy of ancient ocean pH estimates. *Geochimica et Cosmochimica Acta* 69(4): 953–961.

Palter JB, Sarmiento JL, Gnanadesikan A, Simeon J, and Slater RD (2010) Fueling export production: Nutrient return pathways from the deep ocean and their dependence on the Meridional Overturning Circulation. *Biogeosciences* 7(11): 3549–3568.
Paul HA, Bernasconi SM, Schmid DW, and McKenzie JA (2001) Oxygen isotopic composition of the Mediterranean Sea since the Last Glacial Maximum: Constraints from pore water analyses. *Earth and Planetary Science Letters* 192(1): 1–14.
Paytan A and Griffith EM (2007) Marine barite: Recorder of variations in ocean export productivity. *Deep Sea Research Part II: Topical Studies in Oceanography* 54(5–7): 687–705.
Paytan A and Kastner M (1996) Benthic Ba fluxes in the central Equatorial Pacific, implications for the oceanic Ba cycle. *Earth and Planetary Science Letters* 142(3–4): 439–450.
Paytan A, Kastner M, and Chavez FP (1996) Glacial to interglacial fluctuations in productivity in the equatorial Pacific as indicated by marine barite. *Science* 274(5291): 1355–1357.
Peacock S, Lane E, and Restrepo JM (2006) A possible sequence of events for the generalized glacial-interglacial cycle. *Global Biogeochemical Cycles* 20(2): GB2010.
Pepin L, Raynaud D, Barnola JM, and Loutre MF (2001) Hemispheric roles of climate forcings during glacial-interglacial transitions as deduced from the Vostok record and LLN-2D model experiments. *Journal of Geophysical Research* 106(D23): 31885–31892.
Peterson LC, Haug GH, Hughen KA, and Rohl U (2000) Rapid changes in the hydrologic cycle of the tropical Atlantic during the last glacial. *Science* 290(5498): 1947–1951.
Petit JR, Jouzel J, Raynaud D, et al. (1999) Climate and atmospheric history of the past 420,000 years from the Vostok ice core, Antarctica. *Nature* 399(6735): 429–436.
Pfeifer K, Kasten S, Hensen C, and Schulz HD (2001) Reconstruction of primary productivity from the barium contents in surface sediments of the South Atlantic Ocean. *Marine Geology* 177(1–2): 13–24.
Piotrowski AM, Goldstein SL, Hemming SR, and Fairbanks RG (2004) Intensification and variability of ocean thermohaline circulation through the last deglaciation. *Earth and Planetary Science Letters* 225(1–2): 205–220.
Piotrowski AM, Goldstein SL, Hemming SR, Fairbanks RG, and Zylberberg DR (2008) Oscillating glacial northern and southern deep water formation from combined neodymium and carbon isotopes. *Earth and Planetary Science Letters* 272(1–2): 394–405.
Pollard RT, Salter I, Sanders RJ, et al. (2009) Southern Ocean deep-water carbon export enhanced by natural iron fertilization. *Nature* 457(7229): 577–580.
Popp BN, Laws EA, Bidigare RR, Dore JE, Hanson KL, and Wakeham SG (1998) Effect of phytoplankton cell geometry on carbon isotopic fractionation. *Geochimica et Cosmochimica Acta* 62(1): 69–77.
Price JF and Baringer MO (1994) Outflows and deep-water production by marginal seas. *Progress in Oceanography* 33(3): 161–200.
Primeau F (2005) Characterizing transport between the surface mixed layer and the ocean interior with a forward and adjoint global ocean transport model. *Journal of Physical Oceanography* 35(4): 545–564.
Rae JWB, Foster GL, Schmidt DN, and Elliott T (2011) Boron isotopes and B/Ca in benthic foraminifera: Proxies for the deep ocean carbonate system. *Earth and Planetary Science Letters* 302(3–4): 403–413.
Rau GH, Takahashi T, and Marais DJD (1989) Latitudinal variations in planktonic $\delta^{13}C$ – Implications for CO_2 and productivity in past oceans. *Nature* 341(6242): 516–518.
Raymo ME, Ruddiman WF, Backman J, Clement BM, and Martinson DG (1989) Late Pliocene variation in northern hemisphere ice sheets and North Atlantic deep water circulation. *Paleoceanography* 4(4): 413–446.
Raynaud D, Barnola JM, Souchez R, et al. (2005) Palaeoclimatology – The record for marine isotopic stage 11. *Nature* 436(7047): 39–40.
Rechka JA and Maxwell JR (1988) Characterization of alkenone temperature indicators in sediments and organics. *Organic Geochemistry* 13(4–6): 727–734.
Redfield AC (1934) On the proportions of organic derivations in seawater and their relation to the composition of plankton. In: Danie RJ (ed.) *James Johnstone Memorial Volume*, pp. 177–192. Liverpool: University Press of Liverpool.
Redfield AC (1958) The biological control of chemical factors in the environment. *American Scientist* 46(3): 205–221, 230A.
Reimer PJ, Baillie MGL, Bard E, et al. (2009) IntCal09 and Marine09 radiocarbon age calibration curves, 0–50,000 years cal BP. *Radiocarbon* 51(4): 1111–1150.
Ren H, Sigman DM, Chen M-T, and Kao S-J (2012a) Elevated foraminifera-bound nitrogen isotopic composition during the last ice age in the South China Sea and its global and regional implications. *Global Biogeochemical Cycles* 26: GB1031.
Ren H, Sigman DM, Meckler AN, et al. (2009) Foraminiferal isotope evidence of reduced nitrogen fixation in the ice age Atlantic Ocean. *Science* 323(5911): 244–248.
Ren H, Sigman DM, Thunell RC, and Prokopenko MG (2012b) Nitrogen isotopic composition of planktonic foraminifera from the modern ocean and recent sediments. *Limnology and Oceanography* 57(4): 1011–1024.
Reynolds BC, Frank M, and Halliday AN (2006) Silicon isotope fractionation during nutrient utilization in the North Pacific. *Earth and Planetary Science Letters* 244(1–2): 431–443.
Rickaby REM and Elderfield H (1999) Planktonic foraminiferal Cd/Ca: Paleonutrients or paleotemperature? *Paleoceanography* 14(3): 293–303.
Robinson LF, Adkins JF, Keigwin LD, et al. (2005a) Radiocarbon variability in the western North Atlantic during the last deglaciation. *Science* 310(5753): 1469–1473.
Robinson LF and van de Flierdt T (2009) Southern Ocean evidence for reduced export of North Atlantic Deep Water during Heinrich event 1. *Geology* 37(3): 195–198.
Robinson RS, Brunelle BG, and Sigman DM (2004) Revisiting nutrient utilization in the glacial Antarctic: Evidence from a new method for diatom-bound N isotopic analysis. *Paleoceanography* 19(3): PA3001.
Robinson RS, Kienast M, Albuquerque AS, et al. (2012) A review of nitrogen isotopic alteration in marine sediments. *Paleoceanography* 27: PA4203.
Robinson RS and Sigman DM (2008) Nitrogen isotopic evidence for a poleward decrease in surface nitrate within the ice age Antarctic. *Quaternary Science Reviews* 27(9–10): 1076–1090.
Robinson RS, Sigman DM, DiFiore PJ, Rohde MM, Mashiotta TA, and Lea DW (2005b) Diatom-bound $^{15}N/^{14}N$: New support for enhanced nutrient consumption in the ice age subantarctic. *Paleoceanography* 20(3): PA3003.
Rooth C (1982) Hydrology and ocean circulation. *Progress in Oceanography* 11(2): 131–149.
Rosenthal Y, Boyle EA, and Labeyrie L (1997) Last Glacial Maximum paleochemistry and deepwater circulation in the Southern Ocean: Evidence from foraminiferal cadmium. *Paleoceanography* 12(6): 787–796.
Rosenthal Y, Dahan M, and Shemesh A (2000a) Southern Ocean contributions to glacial–interglacial changes of atmospheric pCO_2: An assessment of carbon isotope records in diatoms. *Paleoceanography* 15(1): 65–75.
Rosenthal Y, Lohmann GP, Lohmann KC, and Sherrell RM (2000b) Incorporation and preservation of Mg in *Globigerinoides sacculifer*: Implications for reconstructing the temperature and $^{18}O/^{16}O$ of seawater. *Paleoceanography* 15(1): 135–145.
Ruddiman WF, Raymo ME, Martinson DG, Clement BM, and Backman J (1989) Pleistocene evolution: Northern Hemisphere ice sheets and North Atlantic Ocean. *Paleoceanography* 4(4): 353–412.
Ruhlemann C, Müller PJ, and Schneider RR (1999) Organic carbon and carbonate as paleoproductivity proxies: Examples from high and low productivity areas of the tropical Atlantic. In: Fischer G and Wefer G (eds.) *Use of Proxies in Paleoceanography: Examples from the South Atlantic*, pp. 315–344. Berlin: Springer.
Russell JL, Dixon KW, Gnanadesikan A, Stouffer RJ, and Toggweiler JR (2006) The Southern Hemisphere westerlies in a warming world: Propping open the door to the deep ocean. *Journal of Climate* 19(24): 6382–6390.
Russell AD, Emerson S, Mix AC, and Peterson LC (1996) The use of foraminiferal uranium/calcium ratios as an indicator of changes in seawater uranium content. *Paleoceanography* 11(6): 649–663.
Rutberg RL, Hemming SR, and Goldstein SL (2000) Reduced North Atlantic Deep Water flux to the glacial Southern Ocean inferred from neodymium isotope ratios. *Nature* 405(6789): 935–938.
Rutsch HJ, Mangini A, Bonani G, et al. (1995) ^{10}Be and Ba concentrations in west-African sediments trace productivity in the past. *Earth and Planetary Science Letters* 133(1–2): 129–143.
Sabine CL, Key RM, Feely RA, and Greeley D (2002) Inorganic carbon in the Indian Ocean: Distribution and dissolution processes. *Global Biogeochemical Cycles* 16(4): 1067.
Sachs JP and Repeta DJ (1999) Oligotrophy and nitrogen fixation during eastern Mediterranean sapropel events. *Science* 286(5449): 2485–2488.
Sakamoto T, Ikehara M, Aoki K, et al. (2005) Ice-rafted debris (IRD)-based sea-ice expansion events during the past 100 kyrs in the Okhotsk Sea. *Deep Sea Research Part II: Topical Studies in Oceanography* 52(16–18): 2275–2301.
Sanchez-Valle C, Reynard B, Daniel I, Lecuyer C, Martinez I, and Chervin JC (2005) Boron isotopic fractionation between minerals and fluids: New insights from in situ high pressure-high temperature vibrational spectroscopic data. *Geochimica et Cosmochimica Acta* 69(17): 4301–4313.
Sanyal A, Hemming NG, Broecker WS, Lea DW, Spero HJ, and Hanson GN (1996) Oceanic pH control on the boron isotopic composition of foraminifera: Evidence from culture experiments. *Paleoceanography* 11(5): 513–517.
Sanyal A, Hemming NG, Hanson GN, and Broecker WS (1995) Evidence for a higher pH in the glacial ocean from boron isotopes in foraminifera. *Nature* 373(6511): 234–236.
Sanyal A, Nugent M, Reeder RJ, and Buma J (2000) Seawater pH control on the boron isotopic composition of calcite: Evidence from inorganic calcite precipitation experiments. *Geochimica et Cosmochimica Acta* 64(9): 1551–1555.

Sarmiento JL, Gruber N, Brzezinski MA, and Dunne JP (2004) High-latitude controls of thermocline nutrients and low latitude biological productivity. *Nature* 427(6969): 56–60.

Sarmiento JL, Hughes TMC, Stouffer RJ, and Manabe S (1998) Simulated response of the ocean carbon cycle to anthropogenic climate warming. *Nature* 393: 245–249.

Sarmiento JL and Toggweiler JR (1984) A new model for the role of the ocean in determining atmospheric pCO_2. *Nature* 308(5960): 621–624.

Sarmiento JL, Toggweiler JR, and Najjar R (1988) Ocean carbon-cycle dynamics and atmospheric pCO_2. *Philosophical Transactions of the Royal Society, Series A* 325(1583): 3–21.

Sarnthein M, Winn K, Duplessy J-C, and Fontugne MR (1988) Global variations of surface ocean productivity in low and mid latitudes: Influence on CO_2 reservoirs of the deep ocean and atmosphere during the last 21,000 years. *Paleoceanography* 3(3): 361–399.

Sarnthein M, Winn K, Jung SJA, et al. (1994) Changes in East Atlantic Deepwater Circulation over the last 30,000 years: Eight time slice reconstructions. *Paleoceanography* 9(2): 209–267.

Schmittner A (2003) Southern Ocean sea ice and radiocarbon ages of glacial bottom waters. *Earth and Planetary Science Letters* 213(1–2): 53–62.

Scholten JC, Botz R, Mangini A, Paetsch H, Stoffers P, and Vogelsang E (1990) High-resolution $^{230}Th_{ex}$ stratigraphy of sediments from high-latitude areas (Norwegian Sea, Fram Straight). *Earth and Planetary Science Letters* 101(1): 54–62.

Schrag DP, Adkins JF, McIntyre K, et al. (2002) The oxygen isotopic composition of seawater during the Last Glacial Maximum. *Quaternary Science Reviews* 21(1–3): 331–342.

Schrag DP and Depaolo DJ (1993) Determination of $\delta^{18}O$ of seawater in the deep ocean during the Last Glacial Maximum. *Paleoceanography* 8(1): 1–6.

Schrag DP, Hampt G, and Murray DW (1996) Pore fluid constraints on the temperature and oxygen isotopic composition of the glacial ocean. *Science* 272(5270): 1930–1932.

Seki O, Ikehara M, Kawamura K, et al. (2004) Reconstruction of paleoproductivity in the Sea of Okhotsk over the last 30 kyr. *Paleoceanography* 19(1): 18.

Severinghaus JP, Sowers T, Brook EJ, Alley RB, and Bender ML (1998) Timing of abrupt climate change at the end of the Younger Dryas interval from thermally fractionated gases in polar ice. *Nature* 391(6663): 141–146.

Shackleton N (1967) Oxygen isotope analyses and Pleistocene temperatures re-assessed. *Nature* 215(5096): 15–17.

Shackleton NJ (1977) Carbon-13 in *Uvigerina*: Tropical rain forest history and the equatorial Pacific carbonate dissolution cycles. In: Anderson NR and Malahoff A (eds.) *The Fate of Fossil Fuel CO_2 in the Ocean*, pp. 401–428. New York: Plenum.

Shackleton NJ, Duplessy JC, Arnold M, Maurice P, Hall MA, and Cartlidge J (1988) Radiocarbon age of last glacial Pacific deep water. *Nature* 335(6192): 708–711.

Shackleton NJ, Hall MA, Line J, and Shuxi C (1983) Carbon isotope data in core V19-30 confirm reduced carbon dioxide concentration in the ice age atmosphere. *Nature* 306(5941): 319–322.

Shemesh A, Macko SA, Charles CD, and Rau GH (1993) Isotopic evidence for reduced productivity in the glacial Southern Ocean. *Science* 262(5132): 407–410.

Siddall M, Anderson RF, Winckler G, et al. (2008) Modeling the particle flux effect on distribution of ^{230}Th in the equatorial Pacific. *Paleoceanography* 23(2): PA2208.

Siegenthaler U, Stocker TF, Monnin E, et al. (2005) Stable carbon cycle-climate relationship during the late Pleistocene. *Science* 310: 1313–1317.

Siegenthaler U and Wenk T (1984) Rapid atmospheric CO_2 variations and ocean circulation. *Nature* 308(5960): 624–626.

Sigman DM, Altabet MA, Francois R, McCorkle DC, and Gaillard JF (1999a) The isotopic composition of diatom-bound nitrogen in Southern Ocean sediments. *Paleoceanography* 14(2): 118–134.

Sigman DM, Altabet MA, McCorkle DC, Francois R, and Fischer G (1999b) The $\delta^{15}N$ of nitrate in the Southern Ocean: Consumption of nitrate in surface waters. *Global Biogeochemical Cycles* 13(4): 1149–1166.

Sigman DM and Boyle EA (2000) Glacial/interglacial variations in atmospheric carbon dioxide. *Nature* 407(6806): 859–869.

Sigman DM, De Boer AM, and Haug GH (2007) Antarctic stratification, atmospheric water vapor, and Heinrich Events: A hypothesis for late Pleistocene deglaciations. In: Schmittner A, Chiang JCH, and Hemming SR (eds.) *Ocean Circulation: Mechanisms and Impacts*, *Geophysical Monograph Series*, vol. 173, pp. 335–349. Washington, DC: American Geophysical Union.

Sigman DM, Hain MP, and Haug GH (2010) The polar ocean and glacial cycles in atmospheric CO_2 concentration. *Nature* 466(7302): 47–55.

Sigman DM and Haug GH (2003) The biological pump in the past. In: Elderfield H (ed.) *Treatise on Geochemistry*. *The Oceans and Marine Geochemistry*, vol. 6, pp. 491–528. Oxford: Elsevier-Pergamon.

Sigman DM, Lehman SJ, and Oppo DW (2003) Evaluating mechanisms of nutrient depletion and ^{13}C enrichment in the intermediate-depth Atlantic during the last ice age. *Paleoceanography* 18(3): 1072.

Sigman DM, McCorkle DC, and Martin WR (1998) The calcite lysocline as a constraint on glacial/interglacial low-latitude production changes. *Global Biogeochemical Cycles* 12(3): 409–427.

Singh AK, Marcantonio F, and Lyle M (2011) Sediment focusing in the Panama Basin, Eastern Equatorial Pacific Ocean. *Earth and Planetary Science Letters* 309(1–2): 33–44.

Skinner LC, Fallon S, Waelbroeck C, Michel E, and Barker S (2010) Ventilation of the deep Southern Ocean and deglacial CO_2 rise. *Science* 328(5982): 1147–1151.

Smith HJ, Fischer H, Wahlen M, Mastroianni D, and Deck B (1999) Dual modes of the carbon cycle since the Last Glacial Maximum. *Nature* 400(6741): 248–250.

Sowers T and Bender M (1995) Climate records covering the last deglaciation. *Science* 269(5221): 210–214.

Sowers T, Bender M, Labeyrie L, et al. (1993) A 135,000 year Vostok-SPECMAP common temporal framework. *Paleoceanography* 8(6): 737–766.

Sowers T, Bender M, and Raynaud D (1989) Elemental and isotopic composition of occluded O_2 and N_2 in polar ice. *Journal of Geophysical Research* 94(D4): 5137–5150.

Spero HJ, Bijma J, Lea DW, and Bemis BE (1997) Effect of seawater carbonate concentration on foraminiferal carbon and oxygen isotopes. *Nature* 390(6659): 497–500.

Spero HJ and Lea DW (1993) Intraspecific stable-isotope variability in the planktic foraminifera *Globigerinoides sacculifer* – Results from laboratory experiments. *Marine Micropaleontology* 22(3): 221–234.

Spero HJ and Williams DF (1988) Extracting environmental information from planktonic foraminiferal $\delta^{13}C$ data. *Nature* 335(6192): 717–719.

Stephens BB and Keeling RF (2000) The influence of Antarctic sea ice on glacial–interglacial CO_2 variations. *Nature* 404(6774): 171–174.

Stickley CE, Pike J, Leventer A, et al. (2005) Deglacial ocean and climate seasonality in laminated diatom sediments, Mac. Robertson Shelf, Antarctica. *Palaeogeography, Palaeoclimatology, Palaeoecology* 227(4): 290–310.

Stuiver M and Braziunas TF (1993) Modeling atmospheric ^{14}C influences and ^{14}C ages of marine samples to 10,000 BC. *Radiocarbon* 35(1): 137–189.

Stuiver M and Polach HA (1977) Reporting of ^{14}C data – Discussion. *Radiocarbon* 19(3): 355–363.

Stumm W and Morgan JJ (1981) *Aquatic Chemistry*. New York: Wiley.

Suman DO and Bacon MP (1989) Variations in Holocene sedimentation in the North-American basin determined from ^{230}Th measurements. *Deep Sea Research Part A. Oceanographic Research Papers* 36(6): 869–878.

Sun MY and Wakeham SG (1994) Molecular evidence for degradation and preservation of organic matter in the anoxic Black Sea basin. *Geochimica et Cosmochimica Acta* 58(16): 3395–3406.

Takahashi T, Broecker WS, and Langer S (1985) Redfield ratio based on chemical data from isopycnal surfaces. *Journal of Geophysical Research* 90(C4): 6907–6924.

Thomas E, Turekian KK, and Wei KY (2000) Productivity control of fine particle transport to equatorial Pacific sediment. *Global Biogeochemical Cycles* 14(3): 945–955.

Thomson J, Colley S, Anderson R, Cook GT, Mackenzie AB, and Harkness DD (1993) Holocene sediment fluxes in the northeast Atlantic from ^{230}Th (excess) an radiocarbon measurements. *Paleoceanography* 8(5): 631–650.

Thornalley DJR, Barker S, Broecker WS, Elderfield H, and McCave IN (2011a) The deglacial evolution of North Atlantic deep convection. *Science* 331(6014): 202–205.

Thornalley DJR, Elderfield H, and McCave IN (2009) Holocene oscillations in temperature and salinity of the surface subpolar North Atlantic. *Nature* 457(7230): 711–714.

Thornalley DJR, Elderfield H, and McCave IN (2011b) Reconstructing North Atlantic deglacial surface hydrography and its link to the Atlantic overturning circulation. *Global and Planetary Change* 79(3–4): 163–175.

Thornalley DJR, McCave IN, and Elderfield H (2010) Freshwater input and abrupt deglacial climate change in the North Atlantic. *Paleoceanography* 25: 1201.

Toggweiler JR (1999) Variation of atmospheric CO_2 by ventilation of the ocean's deepest water. *Paleoceanography* 14(5): 571–588.

Toggweiler JR (2009) Shifting westerlies. *Science* 323(5920): 1434–1435.

Toggweiler JR, Dixon K, and Broecker WS (1991) The Peru upwelling and the ventilation of the South-Pacific thermocline. *Journal of Geophysical Research* 96(C11): 20467–20497.

Toggweiler JR, Gnanadesikan A, Carson S, Murnane R, and Sarmiento JL (2003a) Representation of the carbon cycle in box models and GCMs: 1. Solubility pump. *Global Biogeochemical Cycles* 17(1): 1026.

Toggweiler JR, Murnane R, Carson S, Gnanadesikan A, and Sarmiento JL (2003b) Representation of the carbon cycle in box models and GCMs – 2. Organic pump. *Global Biogeochemical Cycles* 17(1): 1027.

Toggweiler JR, Russell JL, and Carson SR (2006) Midlatitude westerlies, atmospheric CO_2, and climate change during the ice ages. *Paleoceanography* 21: PA2005.

Toggweiler JR and Samuels B (1995) Effect of Drake Passage on the global thermohaline circulation. *Deep Sea Research Part I: Oceanographic Research Papers* 42(4): 477–500.

Toggweiler JR and Sarmiento JL (1985) Glacial to interglacial changes in atmospheric carbon dioxide: The critical role of ocean surface water in high latitudes. In: Sundquist ET and Broecker WS (eds.) *The Carbon Cycle and Atmospheric CO_2: Natural Variations Archean to Present, Geophysical Monograph Series*, vol. 32, pp. 163–184. Washington, DC: American Geophysical Union.

Tossell JA (2006) Boric acid adsorption on humic acids: Ab initio calculation of structures, stabilities, ^{11}B NMR and ^{11}B, ^{10}B isotopic fractionations of surface complexes. *Geochimica et Cosmochimica Acta* 70(20): 5089–5103.

Tyrrell T (1999) The relative influences of nitrogen and phosphorus on oceanic primary production. *Nature* 400(6744): 525–531.

Van Geen A, McCorkle DC, and Klinkhammer GP (1995) Sensitivity of the phosphate-cadmium-carbon isotope relation in the ocean to cadmium removal by suboxic sediments. *Paleoceanography* 10(2): 159–169.

Vellinga M and Wood RA (2002) Global climatic impacts of a collapse of the Atlantic thermohaline circulation. *Climatic Change* 54: 251–267.

Venz KA, Hodell DA, Stanton C, and Warnke DA (1999) A 1.0 Myr record of glacial North Atlantic intermediate water variability from ODP site 982 in the northeast Atlantic. *Paleoceanography* 14(1): 42–52.

Vidal L, Labeyrie L, Cortijo E, et al. (1997) Evidence for changes in the North Atlantic Deep Water linked to meltwater surges during the Heinrich events. *Earth and Planetary Science Letters* 146(1–2): 13–27.

Volk T and Hoffert MI (1985) Ocean carbon pumps: Analysis of relative strengths and efficiencies in ocean-driven atmospheric CO_2 changes. In: Sundquist ET and Broecker WS (eds.) *The Carbon Cycle and Atmospheric CO_2: Natural Variations Archean to Present*, *Geophysical Monograph Series*, vol. 32, pp. 99–110. Washington, DC: American Geophysical Union.

Waelbroeck C, Skinner LC, Labeyrie L, et al. (2011) The timing of deglacial circulation changes in the Atlantic. *Paleoceanography* 26: PA3213.

Walter HJ, Geibert W, van der Loeff MMR, Fischer G, and Bathmann U (2001) Shallow vs. deep-water scavenging of ^{231}Pa and ^{230}Th in radionuclide enriched waters of the Atlantic sector of the Southern Ocean. *Deep Sea Research Part I: Oceanographic Research Papers* 48(2): 471–493.

Wang XF, Auler AS, Edwards RL, et al. (2007) Millennial-scale precipitation changes in southern Brazil over the past 90,000 years. *Geophysical Research Letters* 34(23): 5.

Wang YJ, Cheng H, Edwards RL, et al. (2001) A high-resolution absolute-dated Late Pleistocene monsoon record from Hulu Cave, China. *Science* 294(5550): 2345–2348.

Wang YJ, Cheng H, Edwards RL, et al. (2008) Millennial- and orbital-scale changes in the East Asian monsoon over the past 224,000 years. *Nature* 451(7182): 1090–1093.

Waser NAD, Harrison PJ, Nielsen B, Calvert SE, and Turpin DH (1998a) Nitrogen isotope fractionation during the uptake and assimilation of nitrate, nitrite, ammonium, and urea by a marine diatom. *Limnology and Oceanography* 43(2): 215–224.

Waser NA, Yin KD, Yu ZM, et al. (1998b) Nitrogen isotope fractionation during nitrate, ammonium and urea uptake by marine diatoms and coccolithophores under various conditions of N availability. *Marine Ecology Progress Series* 169: 29–41.

Watson AJ, Bakker DCE, Ridgwell AJ, Boyd PW, and Law CS (2000) Effect of iron supply on Southern Ocean CO_2 uptake and implications for glacial atmospheric CO_2. *Nature* 407(6805): 730–733.

Weaver AJ, Eby M, Augustus FF, and Wiebe EC (1998) Simulated influence of carbon dioxide, orbital forcing and ice sheets on the climate of the Last Glacial Maximum. *Nature* 394(6696): 847–853.

Webb RS, Rind DH, Lehman SJ, Healy RJ, and Sigman D (1997) Influence of ocean heat transport on the climate of the Last Glacial Maximum. *Nature* 385(6618): 695–699.

Weber TS and Deutsch C (2010) Ocean nutrient ratios governed by plankton biogeography. *Nature* 467(7315): 550–554.

Wille M, Sutton J, Ellwood MJ, et al. (2010) Silicon isotopic fractionation in marine sponges: A new model for understanding silicon isotopic variations in sponges. *Earth and Planetary Science Letters* 292(3–4): 281–289.

Winckler G and Fischer H (2006) 30,000 years of cosmic dust in Antarctic ice. *Science* 313(5786): 491.

Yu JM, Broecker WS, Elderfield H, Jin ZD, McManus J, and Zhang F (2010a) Loss of carbon from the deep sea since the Last Glacial Maximum. *Science* 330(6007): 1084–1087.

Yu JM and Elderfield H (2007) Benthic foraminiferal B/Ca ratios reflect deep water carbonate saturation state. *Earth and Planetary Science Letters* 258(1–2): 73–86.

Yu JM, Elderfield H, and Honisch B (2007) B/Ca in planktonic foraminifera as a proxy for surface seawater pH. *Paleoceanography* 22: PA2202.

Yu J, Foster GL, Elderfield H, Broecker WS, and Clark E (2010b) An evaluation of benthic foraminiferal B/Ca and δ^{11}B for deep ocean carbonate ion and pH reconstructions. *Earth and Planetary Science Letters* 293(1–2): 114–120.

Yu EF, Francois R, and Bacon MP (1996) Similar rates of modern and last-glacial ocean thermohaline circulation inferred from radiochemical data. *Nature* 379(6567): 689–694.

Zahn R and Mix AC (1991) Benthic foraminiferal δ^{18}O in the ocean's temperature-salinity-density field: Constraints on ice age thermohaline circulation. *Paleoceanography* 6(1): 1–20.

Zeebe RE (2005) Stable boron isotope fractionation between dissolved $B(OH)_3$ and $B(OH)_4^-$. *Geochimica et Cosmochimica Acta* 69(11): 2753–2766.